

**Stratospheric Chlorine and Nitrogen Chemistry:
Observations and Modeling**

Thesis by
Lyatt Jaeglé

In Partial Fulfillment of the Requirements
for the Degree of
Doctor of Philosophy

California Institute of Technology
Pasadena, California
1996
(Submitted December 14, 1995)

© 1996

Lyatt Jaeglé

All rights Reserved

Un peu d'air,
un peu de hauteur,
et beaucoup de choses
commencent à montrer
le bout de leur nez en souriant...

*...A mes parents,
mon frère,
et mon maître nageur*

Acknowledgments

Many people at Caltech and at JPL have helped in shaping my years as a graduate student around very interesting projects and fruitful discussions. My largest debts are to my advisors, Chris Webster and Yuk Yung. No one could wish for a more sympathetic and sensitive pair of advisors, always listening and encouraging. With boundless humor, Chris showed me the fascinating world of stratospheric chemistry, as seen from up there where it all happens. At the same time, Yuk directed my understanding of science and his fabulous ideas helped in formulating the solutions to some puzzles.

An important part of my formative experience took place in the travels to participate in field campaigns, following the tribulations of the ALIAS experiment on the ER-2 aircraft, from NASA Ames to New Zealand; watching the BLISS instrument go up on a balloon. Being in direct contact with the world of observations while doing modeling work has contributed much to anchor my feet in reality and has given me a deep respect for the ingenuity, knowledge and perseverance required in making atmospheric measurements. I would like to thank everyone in the ALIAS group at JPL, Randy May, Dave Scott, Bob Herman, Matt Tuchscherer and Greg Flesch ... never a dull moment with that team!

I have learned much from many interesting discussions with Stan Sander, trying to pull apart the intricacies of chlorine chemistry. I am grateful to Geoff Toon and Bhaswar Sen, for tolerating and answering my many questions and requests. Mark Allen and Ross Salawitch showed me the tricks of the trade of stratospheric modeling, and were always a source of very helpful advice. I am indebted to the Environmental Engineering Science department, for allowing me to take the route I had chosen, a little bit out of the way, in between JPL and the Geology and Planetary Science Division.

Coming to study in the US, and at Caltech in particular, was a dream that began a long time ago and which my parents helped achieve with their smiling love and support - encouraging me to always go forward and follow my ideas (even the crazy ones about settling in the French Alps to make goat cheese!).

Abstract

In order to predict the effects of anthropogenic perturbations (such as the increase of chlorine) and natural events (such as volcanic eruptions) on the chemical composition of the stratosphere, it is essential to quantitatively test our knowledge of the photochemistry by conducting detailed comparisons between stratospheric observations and models. Through such comparisons, this thesis focuses on explaining sets of simultaneous measurements obtained from balloon (Chapters 3, 4, 5) and ER-2 aircraft (Chapters 2, 6) platforms, with particular emphasis on the basic chemical processes underlying the partitioning of the chlorine and nitrogen families in the stratosphere. Following an introductory first chapter, Chapter 2 tests our knowledge of the photochemical balance between NO_2 and NO . Chapter 3 examines the effects of enhanced heterogeneous chemistry resulting from the eruption of Mt. Pinatubo on the partitioning between NO_2 and HNO_3 . Chapter 4 discusses the factors controlling the distribution of chlorine between its main reservoirs (HCl , ClONO_2) and more reactive (HOCl and ClO) forms. Chapter 5 questions the completeness of our understanding of chlorine chemistry and proposes the existence of a new atmospheric species perchloric acid, HClO_4 . Finally, Chapter 6 focuses on the heterogeneous processes taking place during the Antarctic winter and their effect on the evolution of reactive chlorine and nitrogen species within and outside of the polar vortex.

Table of Contents

	Acknowledgments	iv
	Abstract	v
	List of Figures	vii
	List of Tables	x
Chapter 1	Introduction and Overview.....	A-1
Chapter 2	<i>In Situ</i> Measurements of the NO ₂ /NO Ratio for Testing Atmospheric Photochemical Models	B-1
Chapter 3	Balloon Profiles of NO ₂ and HNO ₃ for Testing the Heterogeneous Hydrolysis of N ₂ O ₅ on Sulfate Aerosols.....	C-1
Chapter 4	Partitioning of Inorganic Chlorine in the Stratosphere: Simultaneous Balloon Profiles of HCl, ClONO ₂ , HOCl and ClO	D-1
Chapter 5	Balloon Observations of Organic and Inorganic Chlorine in the Stratosphere: the role of HClO ₄ Production on Sulfate Aerosols	E-1
Chapter 6	Evolution and Stoichiometry of Heterogeneous Processing in the Antarctic Stratosphere	F-1

List of Figures

Chapter 1:

Figure 1 Stratospheric nitrogen and chlorine species: reaction pathways..... A-4

Figure 2 Diagram of stratospheric processesA-7

Chapter 2:

Figure 1 Comparison of measurements and steady-state predictions of NO_2/NOB-8

Figure 2 ER-2 observations of NO_2 and NO ; modeled JNO_2 used in the steady-state calculations..... B-9

Figure 3 NO_2/NO as a function of ozone:
observations and steady-state calculationsB-12

Figure 4 Daytime NO_2/NO as a function of altitudeB-15

Chapter 3:

Figure 1 BLISS flight spectrumC-8

Figure 2 SAGE measurements of aerosol surface areaC-10

Figure 3 BLISS measurements of NO_2 and HNO_3 ,
comparison to model predictionsC-12

Figure 4 BLISS measurements of NO_2/HNO_3 ,
comparison to model predictionsC-13

Chapter 4:

- Figure 1** Balloon-borne measurements of HCl, ClONO₂, HOCl, and ClOD-9
- Figure 2** Observed and modeled ratios ClONO₂/HCl, HOCl/HCl, and ClO/HCl ...D-10
- Figure 3** Model sensitivity to the ClONO₂ photolysis rateD-13
- Figure 4** Needed JClONO₂ quantum yield to obtain best match to the observations of ClONO₂/HClD-14

Chapter 5:

- Figure 1** MkIV measurements of organic and inorganic chlorine between 5 and 39 kmE-7
- Figure 2** MkIV chlorine deficit and calculated HClO₄ profileE-8
- Figure 3** Time-dependent box model calculation since Mt. Pinatubo's eruptionE-15

Chapter 6:

- Figure 1** Inorganic chlorine partitioning in the unperturbed Antarctic Atmosphere..F-10
- Figure 2** Flight of August 6, 1994F-13
- Figure 3** Time evolution of chlorine species inside the vortex between April and May 1994F-15
- Figure 4** ASHOE/MAESA: Loss of HCl and ClONO₂ as a function of ClO + 2 Cl₂O₂*F-20

Figure 5	AASE-II: Loss of HCl and ClONO ₂ as a function of ClO + 2 Cl ₂ O ₂ *	F-21
Figure 6	Heterogeneous reaction probabilities as a function of temperature on sulfuric acid, NAT, SAT and ice	F-25
Figure 7	Model calculated surface area growth as a function of temperature	F-26
Figure 8a	July 28, 1994: Comparison between model and results from 10-day photochemical trajectory calculation for chlorine species	F-30
Figure 8b	July 28, 1994: Comparison between model and results from 10-day photochemical trajectory calculation for OH, HO ₂ , NO and HOCl*	F-33
Figure 9	Backtrajectory temperatures for end points on July 28 and August 6, 1994	F-34
Figure 10	Evolution of model calculations along trajectory starting July 18, 1994	F-35
Figure 11a	August 6, 1994: Comparison between model and results from 10-day photochemical trajectory calculation for chlorine species	F-41
Figure 11b	August 6, 1994: Comparison between model and results from 10-day photochemical trajectory calculation for OH, HO ₂ , NO and HOCl*	F-42
Figure 12	Evolution of model calculations along trajectory starting July 26, 1994: sulfate aerosols and STS	F-45
Figure 13	Evolution of model calculations along trajectory starting July 26, 1994: sulfate aerosols and PSCs	F-46
Figure 14	Evolution of an idealized air parcel inside the vortex at 20 km between April and November 1994	F-50
Figure 15	HCl/Cl _y , ClONO ₂ /Cl _y , HOCl/Cl _y , Cl _x /Cl _y and O ₃ between April and November 1994: model calculations	F-52

List of Tables

Chapter 2:

Table 1	Uncertainties in the NO ₂ /NO ratio	B-11
----------------	--	------

Chapter 3:

Table 1	BLISS data for the August 26, 1992 balloon flight	C-11
----------------	---	------

Chapter 6:

Table 1	Instruments on board the ER-2	F-8
Table 2	List of heterogeneous reaction probabilities	F-24
Table 3	Chemical loss and production rates for OH and HO ₂	F-38

Chapter 1

Introduction and Overview

Preface

This thesis, “Stratospheric Chlorine and Nitrogen Chemistry: Observations and Modeling,” comprises five papers, two of which have been published in the *Geophysical Research Letters* (Chapters 2 and 3), one has been submitted to that same journal (Chapter 5), and two are now ready for submission to the *Journal of Geophysical Research*. I was the first author on all but one of these papers. Because the theme of my thesis is based on modeling of stratospheric observations, these observations are at the core of my work, and the many co-authors on these papers reflect the highly collaborative nature of work in the field of stratospheric chemistry. In particular, the studies described in Chapters 2 and 6 involved a large number of co-authors with instruments aboard the ER-2 aircraft. I was responsible for the modeling work reported in all of these papers. In addition, I was directly involved in the instrument preparation, laser characterization, field deployment, and data analysis for the balloon flight described in Chapter 3. I also participated in field deployments of the aircraft ER-2 SPADE and ASHOE/MAESA missions (Chapters 2 and 6) out of California, Hawaii, and New Zealand.

Introduction

The last decade has seen great advances in our knowledge of stratospheric chemistry. Two major events have fostered these advances, namely the discovery of the Antarctic ozone hole in 1985 and the eruption of Mt. Pinatubo in the Philippines in 1991. Both events reflect large perturbations to the normal balance of the stratosphere, and have set the stage for an explosion of activity in field measurements, laboratory studies, and computer modeling.

General Background

Most of the chemical functioning of the stratosphere involves substances other than its main constituents, N_2 , O_2 , Ar, H_2O , CO_2 . Among the most important trace gases is ozone, which is responsible for shielding the earth from ultraviolet radiation that is harmful to life. The abundance of ozone (~a few parts per million) is controlled by transport and by photochemistry with other trace constituents in the families of nitrogen oxides, inorganic chlorine, bromine and hydrogen radicals. Understanding the interactions between all these gases is central to being able to predict the impact of anthropogenic activities on the ozone layer. In particular, the possible effects on ozone of NO released from high-flying supersonic aircrafts was first pointed out by Crutzen (1970) and Johnston (1971). A few years later, Molina and Rowland (1974) drew attention to the impact of anthropogenically produced chlorine, via chlorofluorocarbons (CFCs) emissions, on the ozone layer.

Once released in the atmosphere, CFCs are converted to inorganic chlorine by photolysis or reaction with atomic oxygen. Inorganic chlorine takes part in a number of photochemical cycles that maintain a balance between mainly HCl, ClONO₂, ClO, Cl, HOCl and Cl₂O₂ — usually referred to as the Cl_y family. In addition, the concentrations of reactive chlorine species are closely controlled by interactions with active nitrogen ($NO_y = NO + NO_2 + NO_3 + 2 N_2O_5 + HNO_2 + HNO_3 + ClONO_2$) and hydrogen oxides ($HO_x = HO_2 + OH$). NO_y species are produced from stratospheric decomposition of

N_2O , which originates in the troposphere. More than two decades of careful laboratory measurements have elucidated the reactions between all these species and their associated rates (DeMore et al., 1994). The partitioning among these species is affected by changes in temperature, pressure, radiation, as well as by vertical and horizontal transport. Figure 1 summarizes the main reactions linking the members of these families in the stratosphere. Note the particular role of $ClONO_2$ which acts as a long-lived reservoir for both Cl_y and NO_y species.

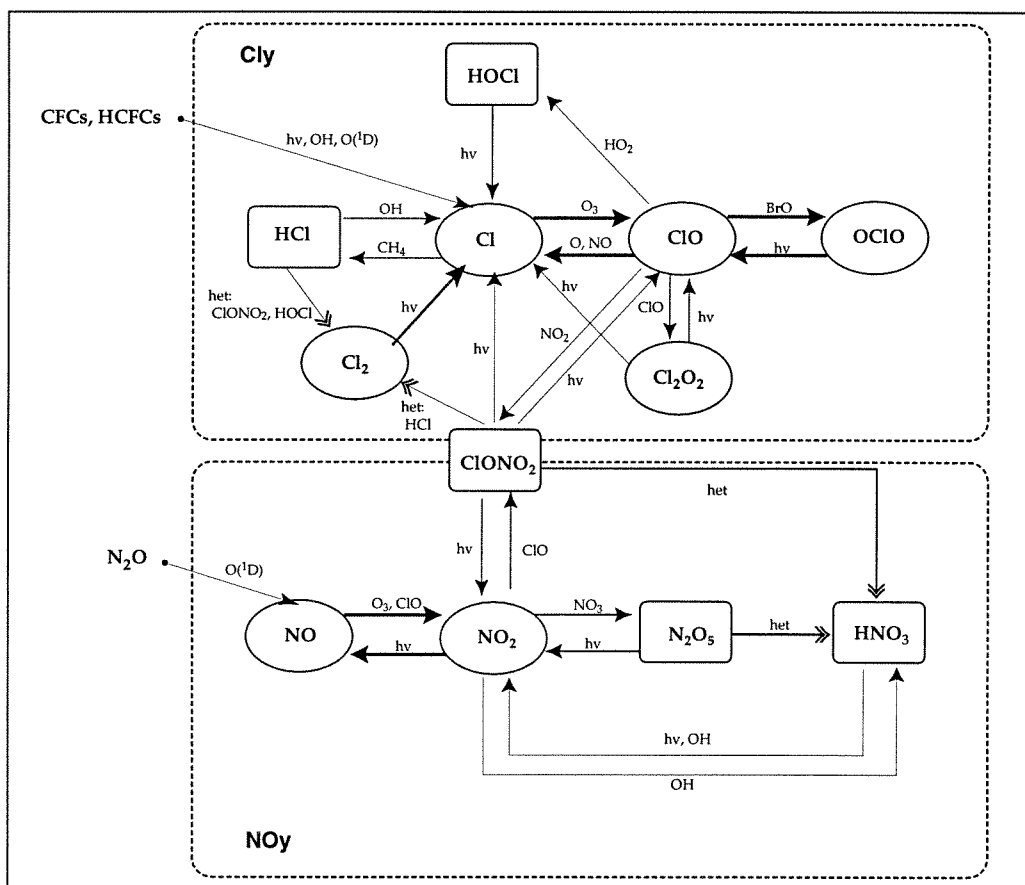
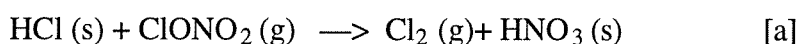


Figure 1: Stratospheric species and reaction pathways. Diagram of the principal species of the NO_y ($= NO + NO_2 + NO_3 + 2 N_2O_5 + HNO_2 + HNO_3 + ClONO_2$) and Cl_y ($= HCl + ClONO_2 + HOCl + ClO + Cl + 2 Cl_2O_2 + 2 Cl_2$) families, as well as their main reaction pathways.

Over the last ten years, the important role of heterogeneous chemistry in transforming chemical species in the atmosphere has become clear. The discovery of the Antarctic ozone hole and the recognition of the role played by reactions on polar stratospheric cloud (PSC) particles have made this field an area of intense research. More recently, and with the scientific opportunity afforded by the eruption of Mt. Pinatubo in 1991, processes on sulfate aerosols (which make up the majority of stratospheric condensed matter in the sub-polar regions) have been recognized.

Polar stratospheric clouds

It has long been known that the extreme cold temperatures of the Antarctic lower stratosphere lead to the formation of polar stratospheric clouds (PSCs) there, and to a lesser degree over the Arctic. Following the discovery of the ozone hole, it was suggested (see review by Solomon, 1990) that heterogeneous reactions such as

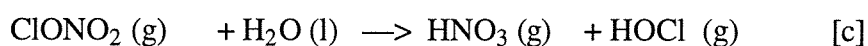
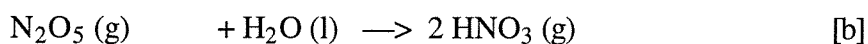


occurring on the surfaces of PSC particles in the dark of the polar winter, could convert chlorine from the rather inactive compounds, HCl and ClONO₂, into more photochemically labile species Cl₂, HOCl, ClNO₂ which readily dissociate in the presence of sunlight to form chlorine radicals which destroy ozone in catalytic cycles during the sunlit period of the spring (Fig. 2).

Observational missions over the Antarctic and the Arctic regions have further elucidated the role of PSCs to produce a clearer picture of the processes important to ozone loss during the polar spring, but many uncertainties still remain.

Heterogeneous chemistry on sulfate aerosols

A layer of liquid sulfuric acid aerosols is present in the stratosphere around the globe year-round between 14 and 25 km. Mt. Pinatubo's eruption in the Philippines in June 1991 injected unprecedented amounts of sulfur compounds in the stratosphere, resulting in high aerosol concentrations that are expected to decrease over the coming 7-9 years before reaching 'pre-Pinatubo' levels (McCormick et al., 1995). This enhancement of aerosol surface area in the stratosphere, and the subsequent inability of purely gas phase models to reproduce observations of reactive species led to the increased consideration of heterogeneous hydrolysis of N_2O_5 (Cadle et al., 1975) and ClONO_2 (Hanson and Ravishankara, 1991) on aerosols:



Both reactions were predicted to form HNO_3 , thereby suppressing the abundance of nitrogen oxides, and indirectly enhancing reactive chlorine.

Thesis work

The work described in this thesis was part of exciting and important developments, and began at a time when the first observations confirming the role of sulfate aerosols were made (Johnston et al., 1992; Fahey et al., 1993) and the first simultaneous measurements of HCl and ClO were being reported from the Northern Hemisphere and the Arctic vortex (Webster et al., 1993; Toohey et al., 1993). In subsequent years, the improved ability of investigators to measure several gases simultaneously provided tighter constraints on the photochemical mechanisms illustrated in Fig. 1, further improving our understanding of both mid-latitude and polar chemistry.

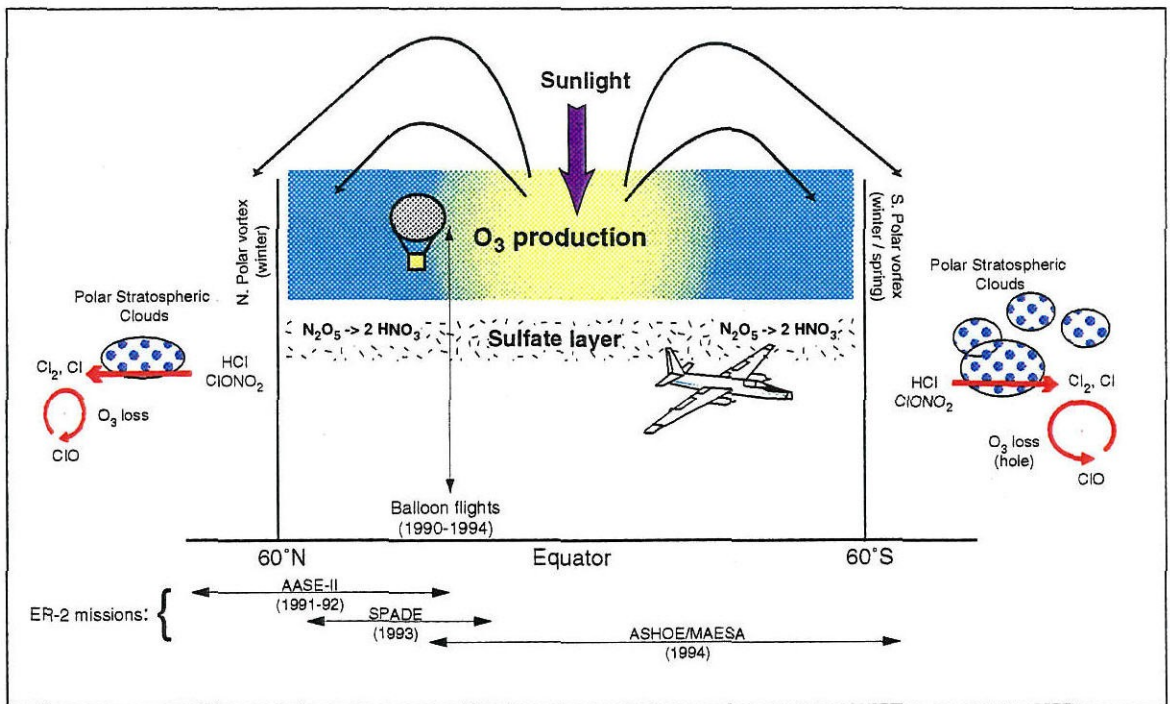


Figure 2: Stratospheric processes. Ozone is produced by sunlight in the tropics and transported to high latitudes where chemical removal occurs. Removal processes are catalyzed by radicals in the nitrogen, hydrogen, and chlorine families. Heterogeneous reactions on the sulfate aerosol layer, and on polar stratospheric clouds can facilitate conversion of NO_x ($=NO_2+NO$) to HNO_3 and of chlorine reservoirs to active chlorine, which destroys ozone. This conversion is particularly efficient in the Antarctic polar vortex. Multi-species observations aboard NASA's high altitude ER-2 aircraft at mid- and high-latitudes, together with balloon-borne experiments, have helped to probe these stratospheric processes [adapted from Rodriguez, 1993].

As part of these new developments, the following chapters detail what has been learned about the stratospheric chlorine and nitrogen chemistry through this thesis work, which is based on multi-species observations aboard NASA's ER-2 high altitude aircraft during 1993 and 1994, as well as on mid-latitude balloon-borne observations between 1991 and 1994 (Fig. 2). Both platforms offer very complementary views of the stratosphere : while the ER-2 samples air from a wide range of latitudes, the balloon instruments reveals its vertical structure.

The second chapter describes how measurements aboard the ER-2 aircraft provided a nearly-complete set of data to critically assess current understanding of the photochemistry governing the partitioning between NO_2 and NO in the stratosphere, and have revealed the need for more accurate laboratory measurements of two important rate constants.

Chapter 3 discusses the impact of the enhanced sulfate aerosol layer resulting from Mt. Pinatubo's eruption on the balance between NO_2 and HNO_3 , and demonstrates the importance of including heterogeneous chemistry on the surfaces provided by these sulfate aerosols even in the absence of major volcanic activity.

The fourth chapter discusses the factors controlling the distribution of chlorine between its main reservoirs (HCl , ClONO_2) and more reactive (HOCl and ClO) forms.

Chapter 5 questions the completeness of our understanding of chlorine chemistry and proposes the existence of a new atmospheric species, perchloric acid (HClO_4).

While the role of heterogeneous processes on both sulfate aerosols and PSCs is now accepted, more quantitative knowledge is needed in order to assess their impact on O_3 depletion in the polar regions. This issue is addressed in Chapter 7, where we examine in detail observations obtained during a recent ER-2 aircraft Antarctic campaign.

This thesis is the fruit of many encounters between theory and experiment; it is a small piece of the fascinating story that atmospheric observations tell us about the stratosphere.

References

Cadle, R.D., P. Crutzen, and D. Ehhalt, Heterogeneous chemical reactions in the stratosphere, *J. Geophys. Res.*, 80, 3381-3385, 1975.

Crutzen, P.J., The influence of nitrogen oxides on the atmospheric ozone content, *Q. J. Met. Soc.*, 96, 320-325, 1970.

DeMore, W.B., S.P. Sander, D.M. Golden, R.F. Hampson, M.J. Kurylo, C.J. Howard, A.R. Ravishankara, C.E. Kolb, and M.J. Molina, Chemical Kinetics and Photochemical Data for Use in Stratospheric Modeling: Evaluation Number 10, *JPL Publication* 94-26, 1994.

Fahey, D.W., S.R. Kawa, E.L. Woodbridge, P. Tin, J.C. Wilson, H.H. Jonsson, J.E. Dye, D. Baumgardner, S. Borrmann, D.W. Toohey, L.M. Avallone, M.H. Proffitt, J. Margitan, M. Loewenstein, J.R. Podolske, R.J. Salawitch, S.C. Wofsy, M.K. W. Ko, D.E. Anderson, M.R. Schoeberl, and K.R. Chan, *In situ* measurements constraining the role of sulphate aerosols in mid-latitude ozone depletion, *Nature*, 363, 509-514, 1993.

Hanson, D.R. and A.R. Ravishankara, The reaction probabilities of ClONO_2 and N_2O_5 on 40 to 75% sulfuric acid solutions, *J. Geophys. Res.*, 96, 17307-17314, 1991.

Johnston, H.S., Reduction of stratospheric ozone by nitrogen oxide catalysts from supersonic transport exhaust, *Science*, 173, 517, 1971.

Johnston, P.V., R.L. McKenzie, J.G. Keys, and W.A. Matthews, Observations of depleted stratospheric NO_2 following the Pinatubo volcanic eruption, *Geophys. Res. Lett.*, 19, 211-213, 1992.

McCormick, M.P., L.W. Thomason, and C.R. Trepte, Atmospheric effects of the Mt. Pinatubo eruption, *Nature*, 373, 399-404, 1995.

Molina, M.J. and F.S. Rowland, Stratospheric sink for chlorofluoromethanes: chlorine atom catalyzed destruction of ozone, *Nature*, 249, 810, 1974.

Rodriguez, J.M., Probing stratospheric ozone, *Science*, 261, 1128-1129, 1993.

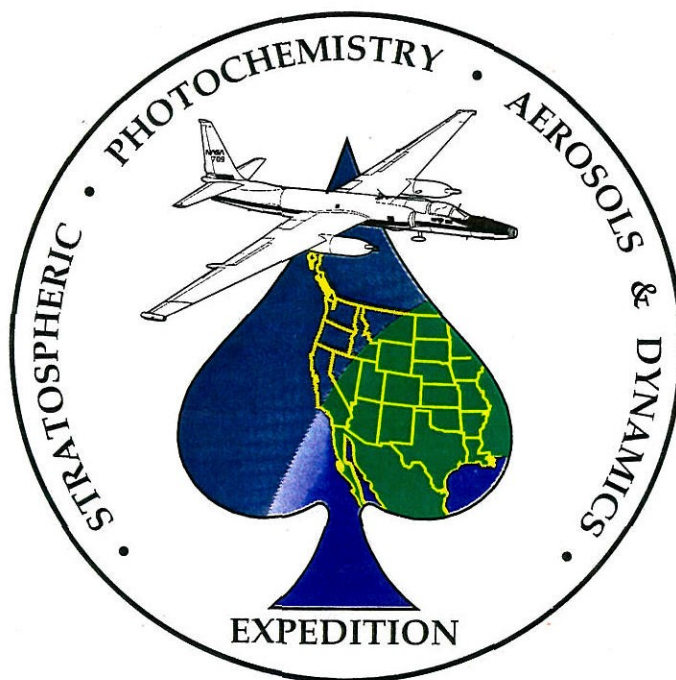
Solomon, S., Progress towards a quantitative understanding of Antarctic ozone depletion, *Nature*, 347, 347-354, 1990.

Toohey, D.W., L.M. Avallone, L.R. Lait, P.A. Newman, M.R. Schoeberl, D.W. Fahey, E.L. Woodbridge, and J.G. Anderson, The seasonal evolution of reactive chlorine in the northern hemisphere stratosphere, *Science*, 261, 1134-1136, 1993.

Webster, C.R., R.D. May, D.W. Toohey, L.M. Avallone, J.G. Anderson, P. Newman, L. Lait, M.R. Schoeberl, J.W. Elkins, and K.R. Chan, Chlorine chemistry on polar stratospheric cloud particles in the Arctic vortex, *Science*, 261, 1130-1134, 1993.

CHAPTER 2

**In Situ Measurements of the NO₂/NO Ratio for Testing
Atmospheric Photochemical Models**





**In Situ Measurements of the NO₂/NO Ratio for Testing
Atmospheric Photochemical Models**

L. Jaeglé

Environmental Engineering Science Department, California Institute of Technology

C.R. Webster and R.D. May

Jet Propulsion Laboratory, California Institute of Technology

D.W. Fahey, E.L. Woodbridge, E.R. Keim, R. Gao and M.H. Proffitt
NOAA Aeronomy Laboratory

R.M. Stimpfle, R.J. Salawitch and S.C. Wofsy
Harvard University

L. Pfister

NASA Ames Research Center

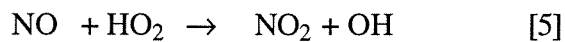
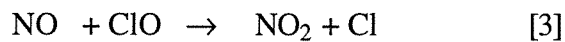
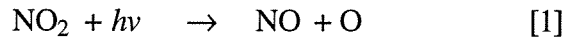
[The text of this chapter appeared in *Geophys. Res. Lett.*, 21, 2555-2558, 1994;

Copyright by the American Geophysical Union]

Abstract. Simultaneous *in situ* measurements of NO₂, NO, O₃, ClO, pressure and temperature have been made for the first time, presenting a unique opportunity to test our current understanding of the photochemistry of the lower stratosphere. Data were collected from several flights of the ER-2 aircraft at mid-latitudes in May 1993 during NASA's Stratospheric Photochemistry, Aerosols and Dynamics Expedition (SPADE). The daytime ratio of NO₂/NO remains fairly constant at 19 km with a typical value of 0.68 and standard deviation of ± 0.17 . The ratio observations are compared with simple steady-state calculations based on laboratory-measured reaction rates and modeled NO₂ photolysis rates. At each measurement point the daytime NO₂/NO with its measurement uncertainty overlap the results of steady-state calculations and associated uncertainty. However, over all the ER-2 flights examined, the model systematically overestimates the ratio by 40% on average. Possible sources of error are examined in both model and measurements. It is shown that more accurate laboratory determinations of the NO + O₃ reaction rate and of the NO₂ cross-sections in the 200-220 K temperature range characteristic of the lower stratosphere would allow for a more robust test of our knowledge of NO_x photochemistry by reducing significant sources of uncertainties in the interpretation of stratospheric measurements. The present measurements are compared with earlier observations of the ratio at higher altitudes.

Introduction

NO₂ and NO, two major constituents of the nitrogen oxide family in the stratosphere, rapidly interchange during the day through a small set of reactions:



Because of the small timescales associated with these reactions (a few minutes at 20 km down to a few seconds at 30 km), a photochemical steady-state exists between daytime concentrations of NO₂ and NO, and their ratio is approximated by the relationship:

$$\frac{[\text{NO}_2]}{[\text{NO}]} = \frac{k_2[\text{O}_3] + k_3[\text{ClO}]}{J\text{NO}_2} \quad [6]$$

where $J\text{NO}_2$ is the photodissociation coefficient for NO₂, and the k 's refer to the temperature-dependent bimolecular rate constants for reactions indicated by the subscripts. In writing equation [6], reactions [4] and [5] are omitted as they account for a negligible fraction of the total NO loss at 20 km. In addition, the reaction of NO₂ with atomic oxygen is also neglected since at the altitudes considered here it contributes less than 0.1% of the total loss of NO₂. NO_x (defined here as NO+NO₂) along with odd-hydrogen and odd-chlorine cycles control stratospheric ozone [McElroy et al., 1992].

Previous simultaneous measurements of NO₂ and NO include long-path solar occultation [Louisnard et al., 1983; Russell et al., 1988], long-path limb-scanning radiometry [Drummond and Jarnot, 1978; Roscoe et al., 1986], *in situ* chemiluminescence detection [McFarland et al., 1986; Fabian et al., 1987], and long path tunable diode laser absorption spectroscopy [Webster and May, 1987; Webster et al.,

1990]. While observations and model results showed generally good agreement within their combined uncertainties, comparisons were somewhat frustrated by high uncertainties in measurements of NO and NO₂ [McFarland et al., 1986], difficulties in solar occultation retrievals [Allen and Delitsky, 1990], or lack of measurements of one or more of the other key variables (ClO, O₃) needed for a complete test of photochemical theory.

The recent addition of new measurement capability for NO₂ to the ER-2 payload in May 1993, combined with simultaneous *in situ* measurements of NO, O₃, ClO, temperature and pressure, provide a unique opportunity to test our current understanding of NO_x photochemistry. In this paper we first compare *in situ* measurements with steady-state predictions as a test of photochemical theory, and then examine the behavior of the ratio as a function of altitude.

The aircraft instruments

The series of flights discussed here were part of SPADE, during the month of May 1993. In flights typically 7-8 hours long, the ER-2 aircraft attains a pressure of about 65 mbar (19 km), covering a maximum latitude range of about $\pm 22^\circ$.

The Aircraft Laser Infrared Absorption Spectrometer (ALIAS) instrument, which is a scanning tunable diode laser spectrometer [Webster et al., 1994], measured NO₂, HCl, N₂O and CH₄ using high resolution laser absorption at wavelengths from 3 to 8 μm . While ALIAS measured NO₂ for the first time during SPADE, numerous measurements using a similar method and laser have been successfully carried out in the past by the Balloon-borne Laser In Situ Sensor (BLISS) instrument [Webster and May, 1987]. Secondary NO_x production or loss is not expected during the 1-second transit time through the halocarbon wax-coated inlet. The measurement uncertainty for five-minute averages of NO₂ depends on the signal size as well as on uncertainties in spectral parameters and calibration. The total uncertainty is typically 13% at 400 pptv, 17% at

200 pptv, and 25% for the smaller volume mixing ratios around 100 pptv (the corresponding signal to noise ratios varying between 16:1 to 5:1).

NO is measured by a chemiluminescence detector with an estimated accuracy of 20% [Fahey et al., 1993]. ClO is measured by resonance fluorescence with a 15% accuracy [Brune et al., 1988], and O₃ by UV absorption [Proffitt et al., 1989] to 5%. All the uncertainties are given as 1 σ .

The models

The predicted steady-state values of NO₂/NO at the local temperatures and pressures were obtained by combining the measured O₃ and ClO in expression [6]. Unless otherwise specified, the temperature-dependent rate constants are from DeMore et al. [1992]. JNO₂ is calculated by a radiative transfer model [Salawitch et al., 1994] which uses ozone profiles from the climatology that are scaled to TOMS satellite column ozone measurements, and albedoes derived from TOMS reflectance maps.

Results/Discussion

Daytime NO₂/NO ratio

NO₂/NO measurements from three flights have been combined in Fig. 1 (open circles) to reconstruct a full sunrise to sunset cycle. The ratio exhibits a remarkable homogeneity between 9 am and 5 pm at a mean value of 0.68 (with a typical standard deviation of ± 0.17), illustrating the relative uniformity of the atmosphere sampled by the ER-2 in May of 1993 during SPADE. Strong midday springtime photolysis of NO₂ shifts the steady-state ratio toward NO. Loss of NO is dominated by reaction [2] with ozone, which contributes on average approximately 90% of the total NO loss.

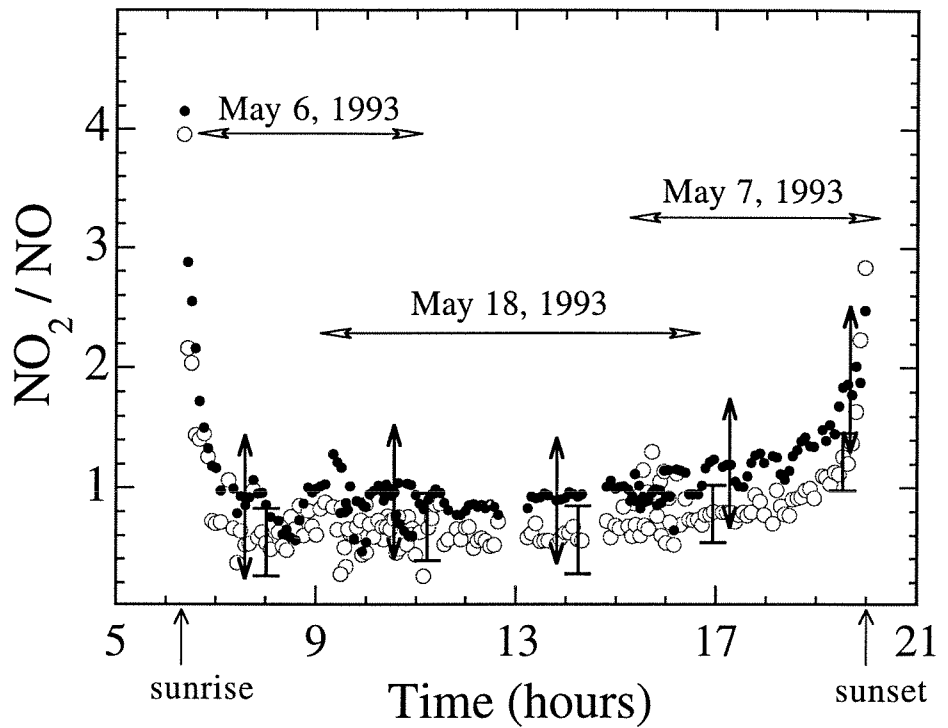


Figure 1: Comparison of measurements (open circles - error bars every 4 hours) and steady-state predictions (small filled circles with double headed arrows as error bars) of NO_2/NO for the SPADE flights of May 6, 7, and 18, 1993. Each measurement point is a 5-minute average. The data was selected for pressures below 70 mbar.

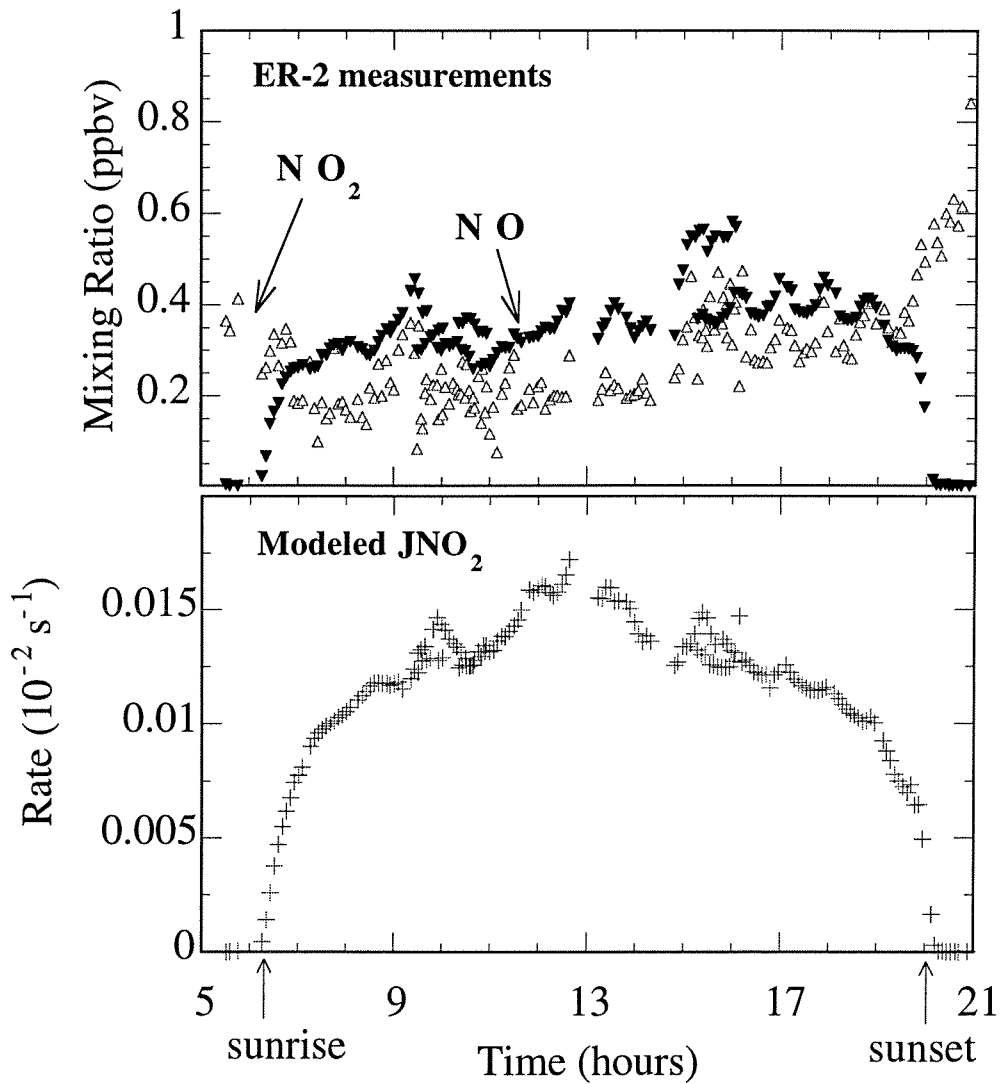


Figure 2: ER-2 observations of NO_2 and NO for the same flights as Fig. 1; modeled JNO_2 used in the steady-state calculations.

The individual measurements of NO₂ and NO, along with the modeled JNO₂ are shown on Fig. 2. At sunset NO is seen to be very rapidly converted to NO₂ as visible and ultraviolet light diminishes. It is the dependence of JNO₂ on solar zenith angles (SZA) larger than 80° that drives the corresponding rapid increase of the ratio. Symmetrically, during sunrise NO₂ is photolyzed to form NO. Aside from random instrumental uncertainties, the observed variability ($\approx 25\%$) in daytime NO₂/NO reflects the transport-driven variability of ozone ($\approx 12\%$), the variability in JNO₂ ($\approx 10\%$) caused by the changing tropospheric albedo as the ER-2 plane flies over different types of surfaces and varying cloud cover, and the temperature changes affecting reaction rate k_2 ($\approx 10\%$).

The calculated algebraic ratios are represented in Fig. 1 as small filled circles. They generally follow the observations, reflecting the validity of the steady-state assumption during daytime. Close to sunset and sunrise the photostationary steady-state assumption no longer applies as the photolysis rate of NO₂ changes too rapidly for equilibrium to be established. Although during daytime at each point along the ER-2 flight tracks the uncertainty in the calculated ratio (represented by double headed arrow) is found to overlap the measurement uncertainty, overall the calculated steady-state expression has a clear tendency to overestimate systematically the observed ratio by 40% *on average*. The significance of this overestimation has been tested using a chi-square test on the difference between model and observations, with a resulting statistical confidence level of 0.01%. Possible sources of this systematic bias, including (1) errors in the rate constants used as input in equation [6]; (2) systematic instrumental bias in the observations, and (3) incomplete knowledge of the NO_x chemistry, are considered below.

Comparison between model and observations: error analysis

The individual error contribution of each input parameter to equation [6] has been calculated following the method of Harries [1982], for conditions typical of the SPADE May flights.

Table 1: Uncertainties in the observed NO₂/NO ratio and its calculation

	Uncertainty	Radiation model	Instrumental	Individual contribution	Total error
k ₂	60%			50%	
k ₃	32%			5%	
JNO ₂		30%		30%	
O ₃			5%	4.5%	
ClO			15%	2%	
(NO ₂ /NO) _{ss}					58.7%
NO ₂			17%		
NO			20%		
(NO ₂ /NO) _{obs}					26.2%

The results are summarized in Table 1 along with 1 σ uncertainties of observed concentrations, calculated JNO₂ and kinetic rate constants based on the temperature-dependent factors listed by DeMore et al. [1992]. The root sum squares show a total uncertainty of 26% in the observed ratio (NO₂/NO)_{obs} and of 59% in the calculated steady-state ratio (NO₂/NO)_{ss}. In Table 1, k₂ and JNO₂ can be identified as the key parameters which contribute most to the model's total uncertainty, and thus they are the variables which have most leverage on the calculated ratio within the limit of their 1 σ uncertainties, while all the other parameters produce errors of 5% or less. The large uncertainty range of k₂ quoted by DeMore et al. especially at the low temperatures (200-220K) of interest here reflects the uncertainties in a given experiment as well as the differences between the various laboratory groups considered.

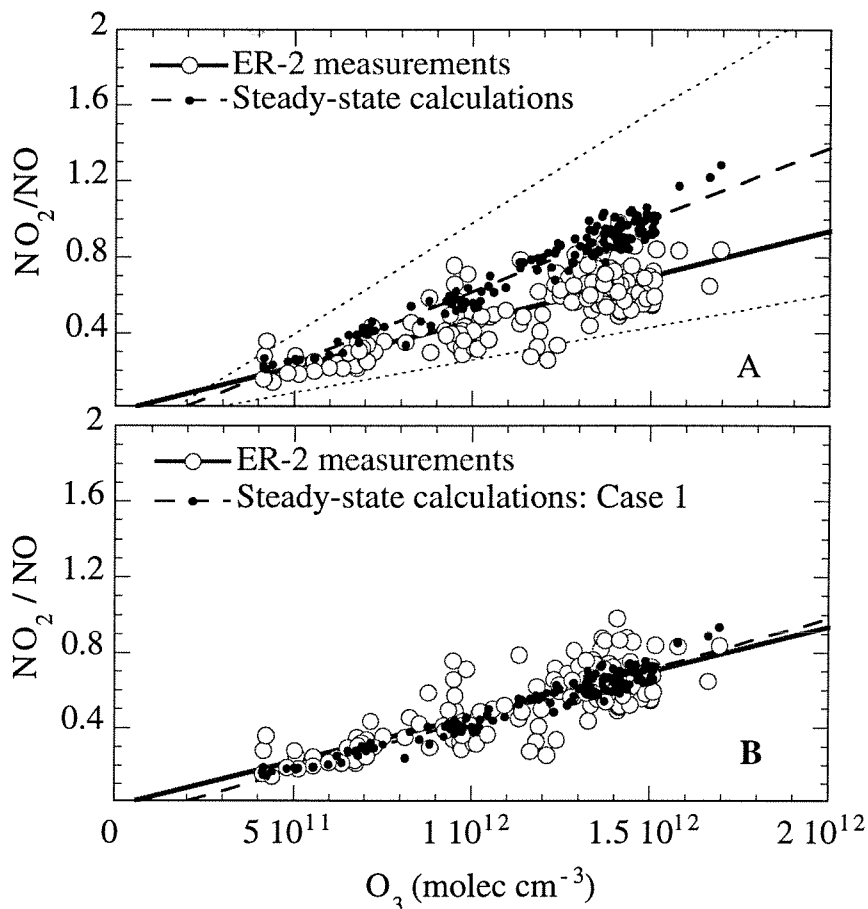


Figure 3: NO_2/NO as a function of ozone, for the flights of May 6, 11, 12, 14, and May 18, 1993 (data selected for high SZA and pressures below 70 mbar). The solid line represents a linear fit to the data points. Also shown is the linear fit corresponding to the steady-state calculation of the ratio (dashed line), with its upper and lower uncertainties (dotted lines). Figure 3a corresponds to the calculation with rates in DeMore et al. [1992], while Fig. 3b shows the results with a rate decreased by 35% for $NO + O_3$ (case 1).

We have plotted in Fig. 3a the ratio from five SPADE flights as a function of ozone. The linear correlation with ozone is expected because, as seen earlier, $k_2[\text{O}_3]$ dominates the numerator of the ratio in [6]. The difference in variability between model and observations is due to the superposition of random errors in the measurements of NO and NO₂. Although most of the data are contained within the two dotted lines (upper and lower limits on the steady-state calculations), there clearly is a systematic overestimation of the calculated steady-state ratio in Fig. 3a. We can see in Fig. 3b that reasonable changes of the two rates k_2 and $J\text{NO}_2$ will tend to reconcile the differences between model and measurements. As an illustration, the effect of decreasing k_2 by 35% (case 1) is shown on Fig. 3b. A similar very good agreement can also be reached, for example, by decreasing k_2 by 25% while increasing $J\text{NO}_2$ by 15%. Interestingly, we note that the measurements reported by Ray and Watson [1981] are close to the 35% reduction in k_2 that is illustrated by case 1.

Simultaneous HO₂ measurements during SPADE [Wennberg et al., 1994] have allowed us to check that reaction [4] contributes to about 1% of the total NO loss. Reaction with BrO, the abundances of which are based on the climatology developed by Wennberg et al., accounts for 2% of the loss. Thus including both these reactions would have only slightly increased the calculated ratio. A systematic underestimation by the radiative transfer model of $J\text{NO}_2$ could result in the observed discrepancy. We note that preliminary $J\text{NO}_2$ values derived by the Composition and Photodissociative Flux Measurement (CPFM) using a spectrometer aboard the ER-2 seem to suggest an even smaller photolysis rate for NO₂ [T. McElroy, personal communication, 1994] leading to an even higher calculated steady-state NO₂/NO. Both radiative transfer calculations and CPFM derivations are using NO₂ cross-sections and quantum yields recommended by DeMore et al. [1992]. Self-reaction of NO₂ and strong temperature dependence of its UV-visible spectrum contribute to difficulties in their laboratory determinations [Roscoe and Hind, 1993]. Furthermore, there are no measurements below 230 K.

The possibility of systematic errors associated with the individual measurements of NO and NO₂ themselves has to be considered. To the best of our knowledge, there is no evidence of such errors. Furthermore, we note that using independent observations of NO₂ by the NOAA instrument [Gao et al., 1994] on the ER-2 flight of May 12 leads to the same overestimation.

Finally, incomplete knowledge of NO_x photochemistry cannot be entirely ruled out until more accurate laboratory studies of the rate constants for reactions [1] and [2] at low temperatures are made.

Behavior of the partitioning between NO₂ and NO as a function of altitude

Figure 4 displays the daytime ratio measured during the May 1993 flights of SPADE along with previous higher altitude balloon observations (all within a few hours of noon). The value of the NO₂/NO ratio is of the order of one in the major part of the stratosphere. The increase up to about 25-30 km follows the ozone concentration profile, as shown by equation [6] which is valid throughout most of the stratosphere. Above 30 km, as the ozone density decreases the capability of the reaction NO + O₃ to convert NO to NO₂, reaction of NO₂ with O becomes increasingly important as atomic O abundance increases due to more efficient O₃ photolysis. Consequently, at increasing altitudes NO becomes the dominant form of the daytime nitrogen oxide family.

The extent to which the measurements of Fig. 4 can be compared is limited mainly by differences in ozone profiles at the time of the respective observations and also, to a lesser degree, by variations in JNO₂ and temperature. In particular, the balloon measurements of NO₂/NO by Ridley et al. [1987] at altitudes which overlap the ER-2 data were reported with ozone abundances higher by 10-50% and temperatures higher by 10K, thus accounting for the higher ratio observed.

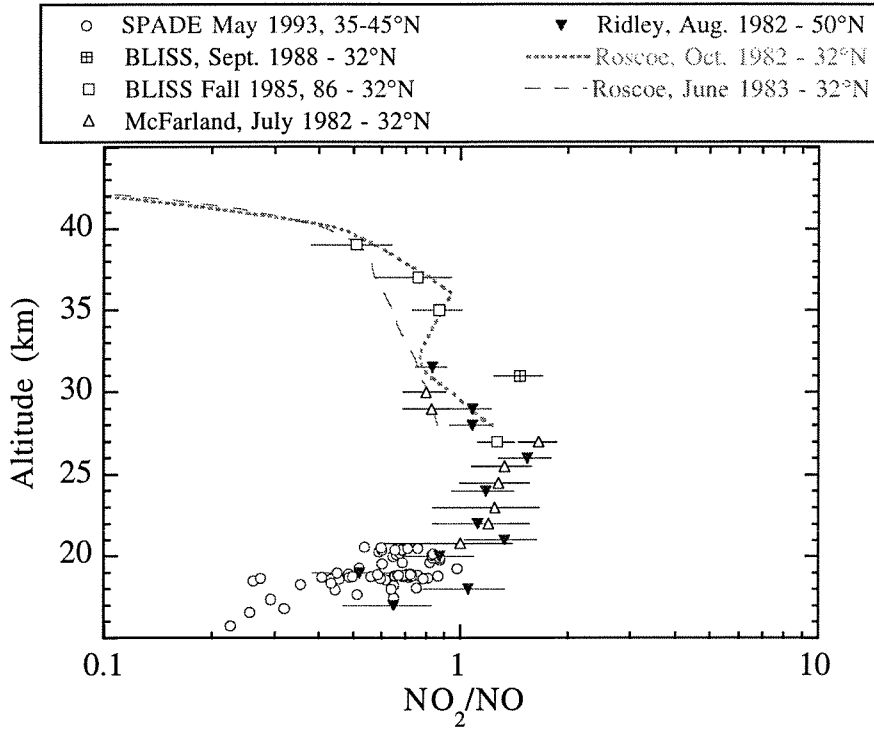


Figure 4: Daytime NO₂/NO as a function of altitude between 15 and 45 km. In addition to the SPADE measurements, higher altitudes points from the balloon instruments: BLISS [Webster et al., 1990], McFarland et al. [1986], Ridley et al. [1987], and Roscoe et al. [1986] are also represented.

References

Allen, M. and M.L. Delitsky, Stratospheric NO, NO₂, and N₂O₅: a comparison of model results with Spacelab 3 Atmospheric Trace Molecule Spectroscopy (ATMOS) measurements, *J. Geophys. Res.*, 95, 14,077-14,082, 1990.

Brune, W.H., E.M. Weinstock, and J.G. Anderson, Mid-latitude ClO below 22 km: Measurements with a new aircraft-borne instrument, *Geophys. Res. Lett.*, 15, 144-147, 1988.

DeMore, W.M., W. B., S.P. Sander, D.M. Golden, R.F. Hampson, M.J. Kurylo, C.J. Howard, A.R. Ravishankara, C.E. Kolb, and M.J. Molina, Chemical Kinetics and Photochemical Data for Use in Stratospheric Modeling: Evaluation Number 10, *JPL Publication 92-20*, 1992.

Drummond, J.R. and R.F. Jarnot, Infrared measurements of stratospheric composition, II, Simultaneous measurements of NO and NO₂, *Proc. Roy. Soc. London, Ser. A*, 364, 237-254, 1978.

Fabian, P., G. Flentje, and W.A. Matthews, Stratospheric NO profiles measured simultaneously using two chemiluminescent balloon-borne sondes, *Planet. Space Sci.*, 35, 609-614, 1987.

Fahey, D.W., S.R. Kawa, E.L. Woodbridge, P. Tin, J.C. Wilson, H.H. Jonsson, J.E. Dye, D. Baumgardner, S. Borrmann, D.W. Toohy, L.M. Avallone, M.H. Proffitt, J. Margitan, M. Loewenstein, J.R. Podolske, R.J. Salawitch, S.C. Wofsy, M.K.W. Ko, D.E. Anderson, M.R. Schoeberl, and K.R. Chan, *In situ* measurements constraining the role of sulfate aerosols in mid-latitude ozone depletion, *Nature*, 363, 509-514, 1993.

Gao, R.S., E.R. Keim, E.L. Woodbridge, S.J. Ciciora, M.H. Proffitt, T.L. Thompson, R.J. McLaughlin, and D.W. Fahey, New photolysis system for NO₂ measurements in the lower stratosphere, *J. Geophys. Res.*, 99, 20,673-20,681, 1994.

Harries, J.E., Stratospheric composition measurements as tests of photochemical theory, *J. Atmos. Terr. Phys.*, 44, 591-597, 1982.

Louisnard, N., G. Fergant, A. Girard, L. Gramont, O. Ladobordowsky, J. Laurent, S. Leboiteux, and M.P. Lemaitre, Infrared absorption spectroscopy applied to stratospheric profiles of minor constituents, *J. Geophys. Res.*, 88, 5365-5376, 1983.

McElroy, M.B., R.J. Salawitch, and K. Minschwaner, The changing stratosphere, *Planet. Space Sci.*, 40, 373-401, 1992.

McFarland, M., B.A. Ridley, M.H. Proffitt, D.L. Albritton, T.L. Thompson, W.J. Harrop, R.H. Winkler, and A.L. Schmeltekopf, Simultaneous *in situ* measurements of nitrogen dioxide, nitric oxide, and ozone between 20 and 31 km, *J. Geophys. Res.*, 91, 5421-5437, 1986.

Proffitt, M. H., M.J. Steinkamp, J.A. Powell, R.J. McLaughlin, O.A. Mills, A.L. Schmeltekopf, T.L. Thompson, A.F. Tuck, T. Tyler, R.H. Winkler, and K.R. Chan, *In situ* ozone measurements within the 1987 Antarctic ozone hole from a high-altitude ER-2 aircraft, *J. Geophys. Res.*, 94, 16,547-16,556, 1989.

Ray, G.W. and R.T. Watson, Kinetics of the reaction $\text{NO} + \text{O}_3 \rightarrow \text{NO}_2 + \text{O}_2$ from 212K to 422K, *J. Phys. Chem.*, 85, 1673-1676, 1981.

Ridley, B.A., M. Mcfarland, A.L. Schmeltekopf, M.H. Proffitt, D.L. Albritton, R.H. Winkler, and T.L. Thompson, Seasonal differences in the vertical distributions of NO, NO₂, and O₃ in the stratosphere near 50°N, *J. Geophys. Res.*, 92, 11,919-11,929, 1987.

Roscoe, H.K. and A.K. Hind, The equilibrium constant of NO₂ with N₂O₄ and the temperature dependence of the visible spectrum of NO₂: a critical review and the implications for measurements of NO₂ in the polar stratosphere, *J. Atmos. Chem.*, 16, 257-276, 1993.

Roscoe, H.K., B.J. Kerridge, L.J. Gray, R.J. Wells, and J.A. Pyle, Simultaneous measurements of stratospheric NO and NO₂ and their comparison with model predictions, *J. Geophys. Res.*, 91, 5,405-5,419, 1986.

Russell, J.M., III, C.B. Farmer, C.P. Rinsland, R. Zander, L. Froidevaux, G.C. Toon, B. Gao, J. Shaw, and M. Gunson, Measurements of odd nitrogen compounds in the stratosphere by the ATMOS Experiment on Spacelab 3, *J. Geophys. Res.*, 93, 1718-1736, 1988.

Salawitch, R.J., S.C. Wofsy, P.O. Wennberg, R.C. Cohen, J.G. Anderson, D.W. Fahey, R.S. Gao, E.R. Keim, E.L. Woodbridge, R.M. Stimpfle, J.P. Koplow, D.W. Kohn, C.R. Webster, R.D. May, L. Pfister, E.W. Gottlieb, H.A. Michelsen, G.K. Yue, J.C. Wilson, C.A. Brock, H.H. Jonsson, J.E. Dye, D. Baumgardner, M.H. Proffitt, M. Loewenstein, J.R. Podolske, J.W. Elkins, G.S. Dutton, E.J. Hints, A.E. Dessler, E.M. Weinstock, K.K. Kelly, K.A. Boering, B.C. Daube, K.R. Chan, and S. W. Bowen, The distribution of hydrogen, nitrogen, and chlorine radicals in the lower stratosphere: implications for changes in O₃ due to emission of NO_y from supersonic aircraft, *Geophys. Res. Lett.*, 21, 2547-2550, 1994.

Webster, C.R., R.D. May, C.A. Trimble, R.G. Chave, and J. Kendall, Aircraft (ER-2) Laser Infrared Absorption Spectrometer (ALIAS) for *in situ* stratospheric measurements of HCl, N₂O, CH₄, NO₂, and HNO₃, *Applied Optics*, 33, 454, 1994.

Webster, C.R., R.D. May, R. Toumi, and J.A. Pyle, Active nitrogen partitioning and the nighttime formation of N₂O₅ in the stratosphere: simultaneous *in situ* measurements of NO, NO₂, HNO₃, O₃, and N₂O using the BLISS diode laser spectrometer, *J. Geophys. Res.*, 95, 13,851-13,886, 1990.

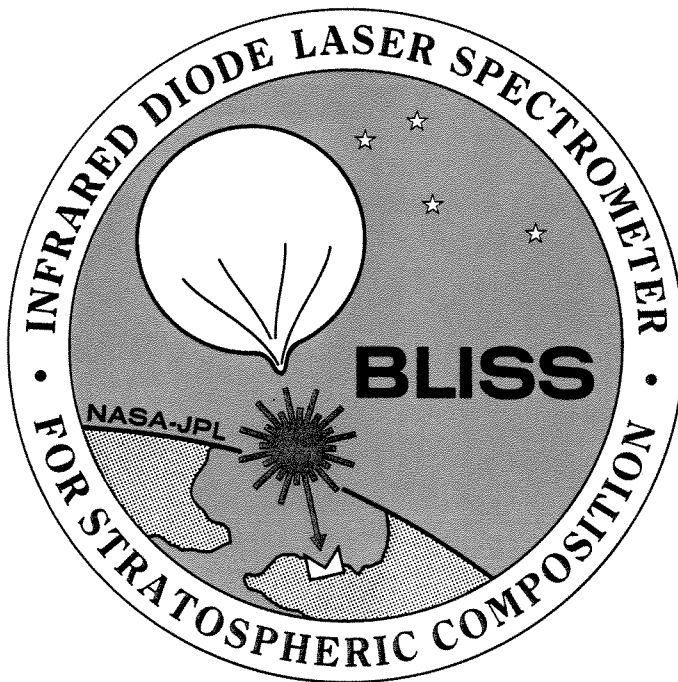
Webster, C.R. and R.D. May, Simultaneous *in situ* measurements and diurnal variations of NO, NO₂, O₃, jNO₂, CH₄, H₂O, and CO₂ in the 40- to 26- km region using

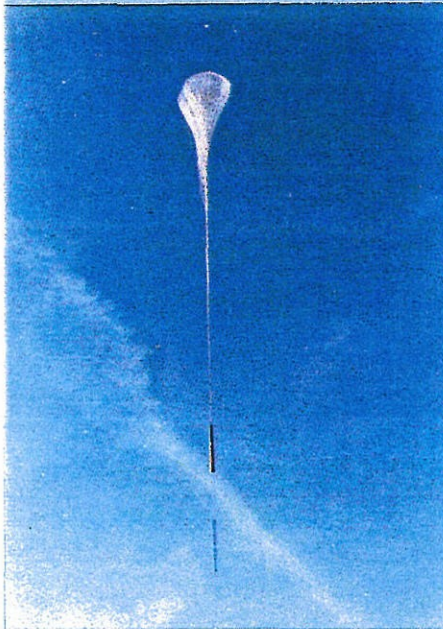
an open path tunable diode laser spectrometer, *J. Geophys. Res.*, 92, 11,931-11,950, 1987.

Wennberg, P.O., R.C. Cohen, R.M. Stimpfle, J.P. Koplw, J.G. Anderson, R.J. Salawitch, D.W. Fahey, E.L. Woodbridge, E.R. Keim, R. Gao, C.R. Webster, R.D. May, D.W. Toohey, L.M. Avallone, M.H. Proffitt, M. Loewenstein, J.R. Podolske, K.R. Chan, and S.C. Wofsy, Removal of stratospheric O₃ by free radicals: *In situ* measurements of OH, HO₂, NO, NO₂, ClO, and BrO, *Science*, 266, 398-404, 1994.

CHAPTER 3

**Balloon Profiles of Stratospheric NO_2 and HNO_3 for Testing
the Heterogeneous Hydrolysis of N_2O_5 on Sulfate Aerosols**





**Balloon Profiles of Stratospheric NO_2 and HNO_3 for Testing the Heterogeneous
Hydrolysis of N_2O_5 on Sulfate Aerosols**

C.R. Webster, R.D. May, M. Allen
Jet Propulsion Laboratory, California Institute of Technology

L. Jaeglé
Environmental Engineering Science Department, California Institute of Technology

M.P. McCormick
NASA Langley Research Center, Atmospheric Sciences Division

[The text of this chapter appeared in *Geophys. Res. Lett.* , 21, 53-56, 1994;

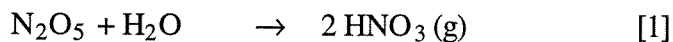
Copyright by the American Geophysical Union]

Abstract. Simultaneous *in situ* measurements of stratospheric NO_2 , HNO_3 , HCl , and CH_4 from 34 to 24 km were made in August 1992 from Palestine, Texas, using the Balloon-borne Laser In Situ Sensor (BLISS) tunable diode laser spectrometer. Although the measurements of NO_2 , HNO_3 , and NO_2/HNO_3 agree well with gas-phase model calculations near 34 km where SAGE II data show little sulfate aerosol, this is not true at the lower altitudes where SAGE II shows high aerosol loadings. At 24 km the BLISS NO_2 and HNO_3 measurements are 70% lower, and 50% higher, respectively, than the gas phase model predictions, with a measured NO_2/HNO_3 ratio 5 times smaller. When the heterogeneous hydrolysis of N_2O_5 and ClONO_2 on sulfate aerosol of surface area densities matching the SAGE II measurements is added to the model, good agreement with the BLISS measurements is found over the whole altitude range.

Introduction

The large increases in number density and surface area of stratospheric liquid sulfuric acid droplets [see, special issue of *Geophysical Research Letters*, volume 19, number 2, 1992] accompanying the June 1991 eruption of Mt. Pinatubo [McCormick and Veiga, 1992] present a unique opportunity for study of heterogeneous chemistry and its sensitivity to an ever-diminishing aerosol loading, as the atmosphere returns to background conditions. Earlier attempts to attribute changes in atmospheric photochemistry to heterogeneous chemistry have been frustrated by three factors: the lower levels of sulfate aerosol associated with earlier volcanic eruptions or with background conditions typical of the pre-Pinatubo period; the measurement uncertainty of earlier instrumentation; and the lack of data relating measurements to tracer fields to normalize dynamical effects.

Models predict that the largest perturbations to stratospheric chemistry caused by heterogeneous reactions are associated with changes in the $\text{NO}_x(=\text{NO}+\text{NO}_2)$ to HNO_3 balance. Two heterogeneous hydrolysis reactions are thought to be of significance: that of N_2O_5 [Cadle et al., 1975], with a reaction probability of 0.1 independent of temperature; and that of ClONO_2 with a reaction probability of only 0.0012, but increasing with decreasing temperature [see DeMore et al., 1992]:



Over the temperature ranges of the mid-latitude lower stratosphere, the ClONO_2 reaction is expected to play a minor role in driving the conversion of NO_x to HNO_3 .

The most direct method of establishing the occurrence of reaction (1) is to measure decreasing reactant, N_2O_5 , and increasing reaction product, HNO_3 , over an altitude range

transitioning from little sulfate aerosol in the middle stratosphere to the heavy loading characteristic of the post-Pinatubo lower stratosphere.

Ironically, remote sensing satellite, shuttle, or balloon instruments with capability for simultaneous N_2O_5 and HNO_3 measurement do not perform well in the regions of high aerosol loading where solar transmission at the suntracker wavelengths is greatly reduced. A re-analysis of ATMOS data by McElroy et al. [1992] has shown that while observed NO_2/HNO_3 ratios at 47°S below 30 km are better represented by a model incorporating heterogeneous chemistry, this same data set at 30°N is matched well by gas phase chemistry alone, although measured N_2O_5 is lower than the gas phase results.

The radicals NO_2 and NO are linked directly to the temporary reservoir N_2O_5 through the diurnal cycles of its nighttime formation and daytime photolysis, and are therefore considered good proxies of the temporary reservoir. Unlike N_2O_5 , several reliable techniques exist for their atmospheric measurement, but the fast daytime photochemistry between them means that an isolated measurement of either gas is insufficient for testing heterogeneous chemistry without the simultaneous measurement of the other partner and of HNO_3 .

The significant decreases in lower stratospheric NO and NO_2 after the eruption of El Chichon [McFarland et al., 1986; Roscoe et al., 1986] demonstrated the importance of heterogeneous chemistry, with models able to approximate the observed changes [Hofmann and Solomon, 1989; Michelangeli et al., 1989], but not the specific mechanism. More recent observations of NO_2 abundances lower than gas phase predictions [Webster et al., 1990] did not include measurement of HNO_3 .

Large differences between observed NO_2 and gas phase model predictions were reported following the eruption of Mt. Pinatubo. Johnston et al. [1992] reported a sudden drop by 35-45% in column NO_2 amounts over New Zealand. Observations of the NO_2 column over Colorado in spring 1992 [Mills et al., 1993] showed strong anti-correlation

with increasing aerosol amount near 25-30 km, the effect saturating at higher aerosol loading.

Conclusive evidence of the occurrence of reaction (1) came from simultaneous *in situ* measurements of NO and NO_y [Fahey et al., 1993]. Reductions in NO_x were observed for both background and volcanic aerosol conditions. Although this study was limited to altitudes ≤ 20 km, values of NO_x/NO_y as low as 5%, and 3 times smaller than gas phase values, were reported.

Balloon measurements of ClO profiles from 15 to 30 km from New Mexico (34°N) by Avallone et al., [1993] and from Greenland (67°N) by Dessler et al. [1993] reported ClO amounts significantly greater than gas phase model predictions, and identified heterogeneous sulfate chemistry as the source of the increases.

In this paper, we report the first simultaneous *in situ* measurements of NO_2 and HNO_3 since the eruption of Mt. Pinatubo over the altitude range 24-34 km from Palestine, Texas (32°N), and compare the data with the Caltech-JPL photochemical model incorporating heterogeneous chemistry constrained by simultaneous satellite measurements of aerosol loading, O_3 , H_2O , temperature and pressure.

The BLISS Instrument

The Balloon-borne Laser In Situ Sensor (BLISS) instrument is a tunable diode laser infrared absorption spectrometer which over the last decade has made stratospheric measurements of numerous gases, including NO, NO_2 , HNO_3 , O_3 , HCl, H_2O , CH_4 , and N_2O [Webster et al., 1990, May and Webster, 1993]. Molecular number densities are measured directly using long-path absorption spectroscopy and harmonic detection techniques to sample a 200-300-m path between payload gondola and lowered retroreflector. For wavelength calibration, unambiguous identification of molecular

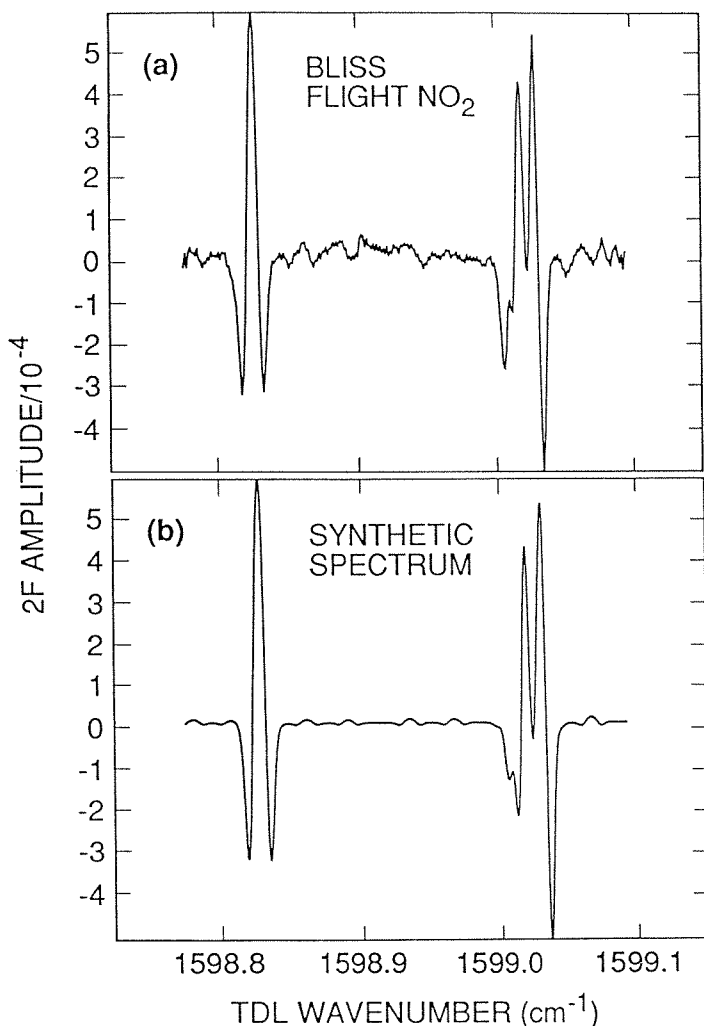


Figure 1: Second harmonic BLISS flight spectrum for NO_2 at 7.4 mbar compared with a synthetic spectrum.

species is ensured by the use of on-board reference cells of NO_2 , HNO_3 , HCl and CH_4 (see Figure 1, and May and Webster [1992]).

The Caltech-JPL Model

A simplified version of the Caltech-JPL one-dimensional time-dependent photochemical model [Allen and Delitsky, 1991] was used, which included chemical

kinetic rate constants based on the JPL compilation of DeMore et al. [1990] and photolysis rate coefficients with a full treatment of the spherical geometry of the atmosphere.

The basic technique adopted was to constrain the model using abundances of: NO_y estimated from the BLISS HNO_3 and NO_2 measurements combined with expected values for ClONO_2 and N_2O_5 ; Cl_y from the BLISS HCl measurements and expected values of ClONO_2 and ClO ; and O_3 and H_2O from the Microwave Limb Sounder (MLS) [Waters et al., 1993] on the Upper Atmospheric Research Satellite. The model was initialized with all the NO_y entered as NO_2 , and the initial values of all the other NO_y species set to zero for maintaining mass balance. This method has the advantage of providing solutions to the coupled system of differential equations unbiased by initial values, but to reach a steady diurnal state the model has to be run for more than 40 model days, mainly due to the long lifetime of HNO_3 below 30 km. A similar procedure was adopted for total free chlorine by entering it exclusively as HCl . The ozone concentration was kept fixed at the observed MLS values.

A first control run including gas-phase chemistry only, was stopped at 4 am (time of the BLISS measurement at 24 km). The resulting atmosphere was then taken as initial conditions before adding the two heterogeneous reactions (1) and (2). The products of both reactions were assumed to be in the gas phase, as laboratory experiments suggest [Reihls et al. 1990]. The adopted aerosol profiles shown in Figure 2 are based on Stratospheric Aerosols and Gas Experiment (SAGE II) measurements in September 1990 and September 1992. Aerosol surface area densities were retrieved from the observed SAGE II extinctions by assuming a lognormal size distribution for the background loading [Yue et al., 1986]. Because the eruption of Mt. Pinatubo generated relatively large particles in the stratosphere [Ansmann et al., 1993], two lognormal size distributions describing the bimodal behavior were required. In order to reach repeatable

diurnal cycles in the cases of post-volcanic and background conditions, additional model times of 3 days, and 2 weeks, respectively, were needed, reflecting the rapidity of the

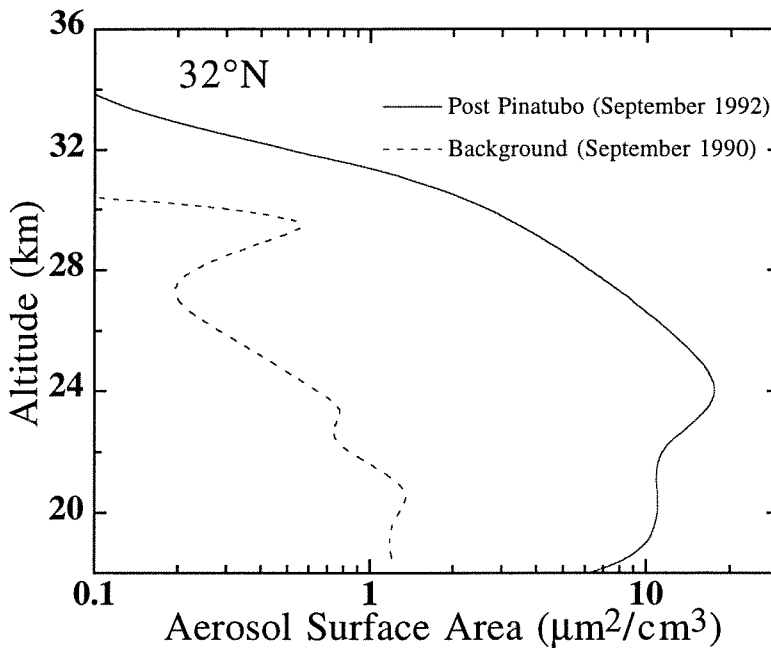


Figure 2: SAGE measurements of the total aerosol surface area density profile at 32°N in Sept. 1992 (close to the BLISS flight date) and in Sept. 1990 (background conditions prior to the eruption of Mt. Pinatubo).

changes introduced by heterogeneous chemistry on enhanced aerosol surface area. Despite the limitations of using a one-dimensional model, the validity of this approach was supported by meteorological data showing zonally-symmetric temperatures and weak winds during August 1992 [G. Manney, private communication].

Results and discussion

Table 1 lists the BLISS measurements for the flight of August 26, 1992. Figure 3 compares the BLISS measurements of NO_2 and HNO_3 mixing ratios between 18 and 36 km with the model predictions. To construct the profile at 4:00 a.m. (solar zenith angle (SZA) of 127°), the measured values at 32 and 34 km were adjusted slightly to correct for the nighttime conversion of NO_2 to N_2O_5 [Webster et al., 1990], based on a simple expression dependent on ozone concentration [Toumi et al., 1991]. Model runs are shown at the same SZA. Nitric acid has a much longer lifetime than NO_2 and does not exhibit diurnal variations, so the values for the measurements at 24, 26 and 34 km are used directly from Table 1 and compared with model predictions in Figure 3. Figure 4 shows a plot of the measured NO_2/HNO_3 ratio as a function of altitude, compared to model predictions.

Table 1. BLISS data for balloon flight of August 26, 1992.

Gas	Local Time	Lat., Long.	Press. (mbar)	Temp. (K)	Mixing Ratio (ppbv)
NO_2	11:54 p.m.	$31^\circ 47, 97^\circ 32$	7.4	231	6.8 ± 0.7
	1:44 a.m.	$31^\circ 35, 98^\circ 45$	9.5	229	3.7 ± 0.7
	4:00 a.m.	$31^\circ 36, 99^\circ 43$	29.1	215	0.7 ± 0.2
HNO_3	12:48 a.m.	$31^\circ 43, 98^\circ 6$	6.7	227	1.5 ± 0.5
	03:32 a.m.	$31^\circ 37, 99^\circ 39$	27.7	216	6.1 ± 0.7
	05:18 a.m.	$31^\circ 39, 100^\circ 5$	29.1	213	7.1 ± 0.8
HCl	11:22 p.m.	$31^\circ 49, 97^\circ 14$	7.2	233	1.98 ± 0.20
	2:34 a.m.	$31^\circ 38, 99^\circ 11$	18.1	219	1.34 ± 0.15
	3:06 a.m.	$31^\circ 38, 99^\circ 27$	25.3	218	1.17 ± 0.12
	4:24 a.m.	$31^\circ 36, 99^\circ 48$	30.2	213	1.17 ± 0.12
CH_4	12:28 p.m.	$31^\circ 45, 97^\circ 52$	7.1	229	820 ± 40
	2:51 a.m.	$31^\circ 38, 99^\circ 21$	21.2	216	1080 ± 50
	4:40 a.m.	$31^\circ 38, 99^\circ 53$	31.0	223	1240 ± 60

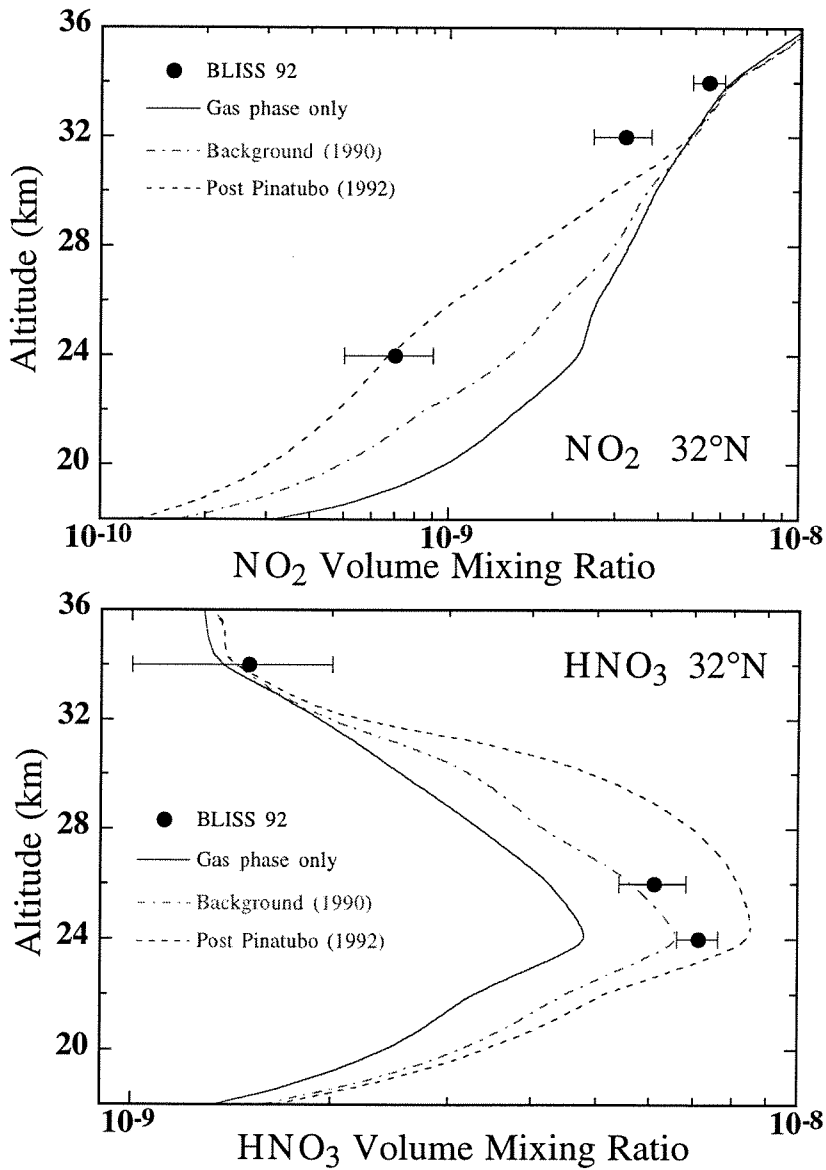


Figure 3: BLISS measurements of NO_2 and HNO_3 mixing ratio between 18 and 36 km compared with model predictions using gas-phase chemistry only (solid line), and including heterogeneous chemistry on background (dash-dot line) and volcanic (dashed line) aerosol.

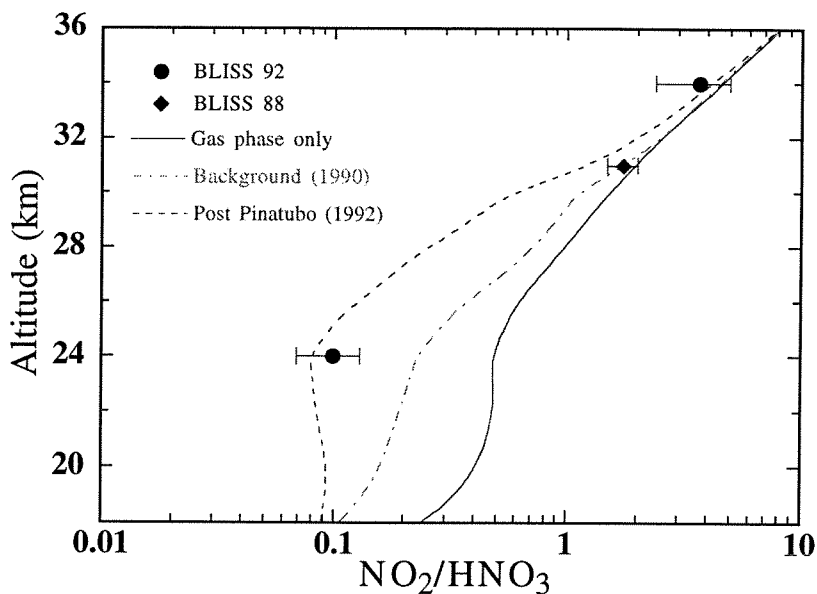


Figure 4: BLISS measurements of the NO_2/HNO_3 ratio between 18 and 36 km compared with model predictions using gas-phase chemistry only (solid line), and including heterogeneous chemistry on background (dash-dot line) and volcanic (dashed line) aerosol. The data point representing $\text{NO}_2/\text{HNO}_3 = 1.74$ at 31 km is from an earlier BLISS flight in 1988.

Immediately apparent from Figures 3 and 4 is the general good agreement between observation and model results at the higher altitudes above 30 km, where aerosol surface area densities are negligible, and model calculations using both gas and heterogeneous chemistry converge. At the lower altitudes, however, as aerosol surface area density increases, the measurements depart markedly from the model calculations using only gas phase photochemistry. At 24 km the measurements of NO_2 and HNO_3 are 70% lower, and 50% higher, respectively, than the gas phase model predictions, with a measured NO_2/HNO_3 ratio 5 times smaller.

When the heterogeneous hydrolysis of N_2O_5 and ClONO_2 on sulfate aerosol of surface area densities matching the SAGE II measurements is added to the models, good agreement with the BLISS measurements of NO_2 and of HNO_3 is found over the whole altitude range. Note that vertical mixing, which the model does not account for, occurs on timescales of 1 to 3 months, compared with the interconversion between NO_x and HNO_3 which reaches steady-state after a little more than a month. This may explain why the model calculations have a tendency to overestimate the long-lived reservoir HNO_3 . The contribution of uncertainty in the estimate of NO_y is minimized by considering the ratio of NO_2/HNO_3 .

The dramatic differences in the ability of the gas phase and heterogeneous models to fit the data are seen in the comparison with the calculated NO_2/HNO_3 ratios (see Figure 4). Good agreement near 34 km is found with or without heterogeneous chemistry included (since aerosol surface area is small). At 24 km, however, a factor of 5 distinguishes the two cases, and the addition of heterogeneous chemistry is needed to match the low observations of NO_2/HNO_3 . Background aerosol loading does not convert enough NO_2 to HNO_3 to account for the observed ratio. For both altitudes, the agreement between heterogeneous model and measurement is remarkable. A measurement of NO_2/HNO_3 of 1.7 at 31 km made close to 4:00 a.m. on an earlier BLISS flight in September 1988 is also shown in Figure 4, and agrees well with the model results.

The BLISS observations of NO_2 and HNO_3 14 months after the eruption of Mt. Pinatubo can be simulated only upon the inclusion of heterogeneous NO_y hydrolysis in model calculations. This result is particularly significant since purely gas-phase calculations initialized with ATMOS 1985 measurements reproduced the ATMOS data set well throughout the whole stratosphere. The observations are consistent with observations of low NO/NO_y ratios near 17-20 km [Fahey et al., 1993].

Acknowledgements. The authors are indebted to Joe Waters and Lucien Froidevaux for providing UARS MLS profiles of O₃, H₂O, temperature, and pressure. Bob Herman and Yuk Yung assisted with the modelling effort. Part of the research described in this paper was carried out by the Jet Propulsion Laboratory, California Institute of Technology, under a contract with the National Aeronautics and Space Administration.

References

Allen, M. and M.L. Delitsky, Stratospheric NO, NO_2 and N_2O_5 : a comparison of model results with Spacelab 3 Atmospheric Trace Molecule Spectroscopy (ATMOS) measurements, *J. Geophys. Res.*, 95, 14077-14082, 1990.

Ansman, A.R., U. Wandinger, and C. Weitkamp, One year observations of Mount Pinatubo aerosol with advanced Raman lidar over Germany at 53.5 °N, *Geophys. Res. Lett.*, 20, 711-714, 1993.

Avallone, L.M., D.W. Toohey, W.H. Brune, R.J. Salawitch, A.E. Dessler, and J.G. Anderson, *In situ* measurements of ClO and ozone: implications for heterogeneous chemistry and mid-latitude ozone loss, *Geophys. Res. Lett.*, 20, 1795-1798, 1993.

Cadle, R.D., P. Crutzen, and D. Ehhalt, Heterogeneous Chemical Reactions in the Stratosphere, *J. Geophys. Res.*, 80, 3381-3385, 1975.

DeMore, W.M., S.P. Sander, C.J. Howard, A.R. Ravishankara, D.M. Golden, C.E. Kolb, R.F. Hampson, M.J. Kurylo, and M.J. Molina, Chemical Kinetics and Photochemical Data for Use in Stratospheric Modeling: Evaluation Number 10, *JPL Publication 92-20*, 1992.

Dessler, A.E., R.M. Stimpfle, B.C. Daube, R.J. Salawitch, E.M. Weinstock, D.M. Judah, J.D. Burley, J.W. Munger, S.C. Wofsy, J.G. Anderson, M.P. McCormick, and W.P. Chu, Balloon-borne measurements of ClO, NO, and O_3 in a volcanic cloud: an analysis of heterogeneous chemistry between 20 and 30 km, *Geophys. Res. Lett.*, 20, 2527-2530, 1993.

Fahey, D.W., S.R. Kawa, E.L. Woodbridge, P. Tin, J.C. Wilson, H.H. Jonsson, J.E. Dye, D. Baumgardner, S. Borrmann, D.W. Toohey, L.M. Avallone, M.H. Proffitt, J. Margitan, M. Loewenstein, J.R. Podolske, R.J. Salawitch, S.C. Wofsy, M.K.W. Ko, D.E. Anderson, M.R. Schoeberl, and K.R. Chan, *In situ* measurements constraining the role of sulphate aerosols in mid-latitude ozone depletion, *Nature*, 363, 509-514, 1993.

Hofmann, D.J. and S. Solomon, Ozone destruction through heterogeneous chemistry following the eruption of El Chichon, *J. Geophys. Res.*, 94, 5029-5041, 1989.

Johnston, P.V., R.L. McKenzie, J.G. Keys, and A.W. Matthews, Observations of depleted stratospheric NO₂ following the Pinatubo volcanic eruption, *Geophys. Res. Lett.*, 19, 211-213, 1992,

May, R.D. and C.R. Webster, *In situ* Stratospheric Measurements of HNO₃ and HCl near 30 km using the BLISS Tunable Diode Laser Absorption Spectrometer, *J. Geophys. Res.*, 94, 16,343-16,350, 1989.

May, R.D. and C.R. Webster, Data processing and calibration for tunable diode laser harmonic absorption spectrometers, *J. Quant. Spectr. Rad. Transfer*, 49, 335-347, 1993.

McCormick, M.P. and R.E. Veiga, SAGE II measurements of early Pinatubo aerosols, *Geophys. Res. Lett.*, 19, 155-158, 1992.

McElroy, M.B., R.J. Salawitch, and K. Minschwaner, The Changing Stratosphere, *Planet. Space Sci.*, 40, 373-401, 1992.

McFarland, M., B.A. Ridley, M.H. Proffitt, D.L. Albritton, T.L. Thompson, W.J. Harrop, R.H. Winkler, and A.L. Schmeltekopf, Simultaneous *in situ* measurements of nitrogen dioxide, nitric oxide, and ozone between 20 and 31 km, *J. Geophys. Res.*, 91, 5421-5437, 1986.

Michelangeli, D., M. Allen, and Y.L. Yung, The effect of El Chichon volcanic aerosols on the chemistry of the stratosphere through radiative coupling, *J. Geophys. Res.*, 94, 18429-18443, 1989.

Mills, M.J., A.O. Langford, T.J. O'Leary, K. Arpag, H.L. Miller, M.H. Proffitt, R.W. Sanders, and S. Solomon, *Geophys. Res. Lett.*, 20, 1187-1190, 1993.

Reihs, C.M., D.M. Golden and M.A. Tolbert, Nitric acid uptake by sulfuric acid solutions under stratospheric conditions: determination of Henry's law solubility, *J. Geophys. Res.*, 95, 16545-16550, 1990.

Roscoe, H.K., B.J. Kerridge, L.J. Gray, R.J. Wells, and J.A. Pyle, Simultaneous measurements of stratospheric NO and NO_2 , and their comparison with model predictions, *J. Geophys. Res.*, 91, 5405-5419, 1986.

Toumi, R., J.A. Pyle, C.R. Webster, and R.D. May, Theoretical interpretation of N_2O_5 measurements, *Geophys. Res. Lett.*, 18, 1213-1216, 1991.

Waters, J.W., L. Froidevaux, W.G. Read, G.L. Manney, L.S. Elson, D.A. Flower, R.F. Jarnot, and R.S. Harwood, Stratospheric ClO and O_3 from the MLS on the UARS satellite, *Nature*, 362, 597-602, 1993.

Webster, C. R., R.D. May, D. Toohey, L.M. Avallone, J.G. Anderson, P.A. Newman, L.R. Lait, M.R. Schoeberl, J. Elkins, and K.R. Chan, Chlorine chemistry on polar stratospheric cloud particles in the Arctic winter, *Science*, 261, 1130-1134, 1993.

Webster, C.R., R.D. May, R. Toumi, and J. Pyle, Active Nitrogen Partitioning and the Nighttime Formation of N_2O_5 in the Stratosphere: Simultaneous *In situ* Measurements of NO, NO_2 , HNO_3 , O_3 , N_2O , and jNO_2 using the BLISS Diode Laser Spectrometer, *J. Geophys. Res.*, 95, 13,851-13,866, 1990.

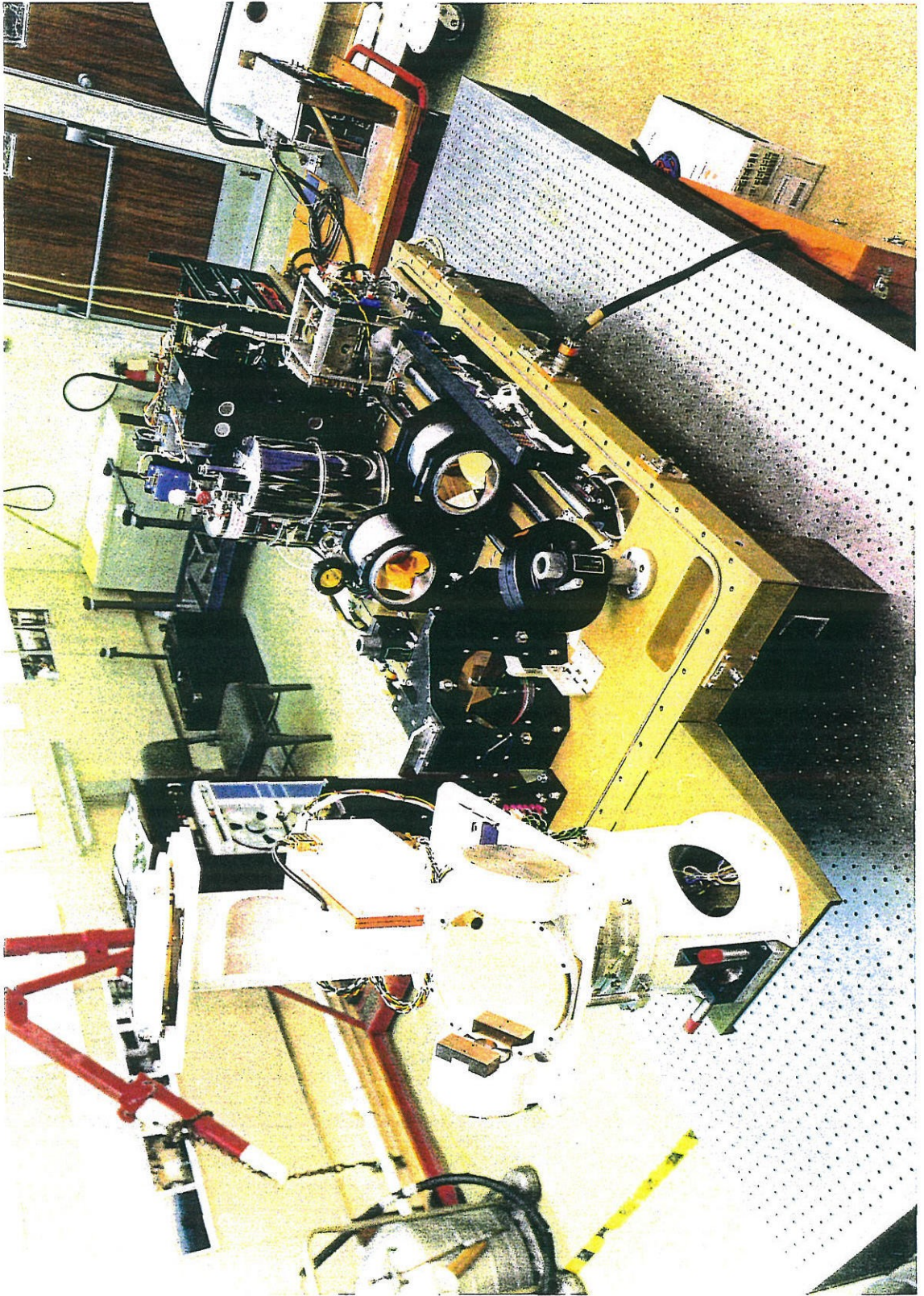
World Meteorological Organization, Scientific Assessment of Ozone Depletion: 1991, *WMO Rep. No. 25*, Global Ozone Res. and Monit. Proj., Geneva, 1991.

Yue, G.K., M.P. McCormick, and W.P. Chu, Retrieval of composition and size distribution of stratospheric aerosols with the SAGE II satellite experiment, *J. Atm. Ocean. Technol.*, 3, 371-380, 1986.

CHAPTER 4

Partitioning of Inorganic Chlorine in the Stratosphere:
Simultaneous Balloon Profiles of HCl, ClONO₂, HOCl and ClO





**Partitioning of Inorganic Chlorine in the Stratosphere:
Simultaneous Balloon Profiles of HCl, ClONO₂, HOCl and ClO**

Lyatt Jaeglé

Environmental Engineering Science Department, California Institute of Technology

Geoffrey C. Toon, Bhaswar Sen, Jean-François Blavier, Robert A. Stachnik
Jet Propulsion Laboratory, California Institute of Technology

Yuk L. Yung, M. Allen

Division of Geological and Planetary Sciences, California Institute of Technology

Abstract. Simultaneous observations of stratospheric HCl, ClONO₂, and HOCl from the MkIV fourier transform infrared spectrometer, complemented with ClO measurements by the Submillimeterwave Limb Sounder, are used to examine the partitioning of inorganic chlorine at mid-latitudes between 1990 and 1994. Comparison of these balloon-borne observations to results from a photochemical model constrained to the conditions (tracer profiles) present for each individual flight show that over most of the altitude range sampled (16-39 km) there is broad agreement. However, two regions of divergence are systematically present in all the examined flight data: (1) above 30 km, the model underestimates HCl and overestimates ClO and HOCl, (2) below 22 km, the model underestimates ClONO₂ and overestimates HCl. To reconcile model calculations with the observations at high altitudes, an additional pathway to convert ClO to HCl is necessary. The second disagreement suggests a stronger pressure/altitude dependence of the ClONO₂/HCl ratio than is currently represented by photochemical models in the lower stratosphere. We demonstrate that a mechanism such as a pressure dependent quantum yield in the photolysis of ClONO₂ (Nickolaisen et al., 1996) is qualitatively consistent with the MkIV observations.

Introduction

The partitioning of inorganic chlorine between its reactive forms (ClO, Cl₂O₂, Cl) and longer lived reservoirs (HCl, ClONO₂ and HOCl) is thought to control the rate of ozone destruction in the stratosphere, along with varying contributions from the odd-nitrogen, odd-hydrogen and bromine families [WMO, 1995]. Our understanding of the photochemical reactions governing this partitioning is therefore central to the ability of models to accurately predict the impact of anthropogenic chlorine on the ozone layer.

Over the last few years, comparisons between atmospheric observations and model calculations have made clear that, although we can qualitatively describe levels of inorganic chlorine species, at least two substantial quantitative discrepancies remain.

The first problem concerns the tendency of models to underpredict HCl at high altitudes (above ~30 km) while overpredicting ClO [Stachnick et al., 1992; McElroy and Salawitch, 1989; Natarajan and Callis, 1991; Allen and Delitsky, 1991; Toumi and Bekki, 1993; Michelsen et al., 1995]. This has been linked to the long-standing issue of ozone production deficit in the upper stratosphere [Crutzen and Schmailzl, 1983; Jackman et al., 1986; Eluszkiewicz and Allen, 1993; Crutzen et al., 1995], where models predict too much ozone loss compared to observations. Among the mechanisms found to possibly enhance HCl above 30 km are a small channel producing HCl in ClO + OH → Cl + HO₂ (reaction a), or in ClO + HO₂ → HOCl + O₂ (reaction b), as well as an increase in the rate of Cl + HO₂ → HCl + O₂ (reaction c). Laboratory measurements have put upper bounds on these channels of 14% for (a) and 4% for (b), and the uncertainty on (c) is 50% [DeMore et al., 1994].

The second problem has been revealed by recent *in situ* measurements of HCl and ClO made from NASA's ER-2 aircraft, which show that HCl observations at 20 km are 50% lower than model predictions [Webster et al., 1993; Webster et al., 1994; Salawitch et al., 1994]. The discrepancy between *in situ* balloon observations of ClO below 20 km and

the much lower model predictions has also pointed to a missing mechanism in our understanding of the partitioning between HCl and ClONO₂ [Avallone et al., 1993]. Furthermore, a general underprediction of the ClONO₂/(HCl+ClONO₂) ratio by a 2D model has been noted at the 550K potential temperature height (~21 km) in data collected by instruments on the Upper Atmospheric Research Satellite [Dessler et al., 1995].

Balloon-borne observations made by the JPL MkIV interferometer offer a unique opportunity to reexamine these inconsistencies in our understanding of inorganic chlorine partitioning. This data set is ideal in that it presents us with the only truly simultaneous observations of HCl, ClONO₂ and HOCl made in the same airmass. In addition, the high quality stratospheric profiles of these species span an extremely wide altitude range, extending from 16 to 39 km. A further important constraint is added to this data set by the ClO observations made by the Submillimeterwave Limb Sounder (SLS) sharing the same balloon gondola. By comparing proposed alternative models to these measurements, we self-consistently examine and constrain the underlying processes determining the speciation of chlorine in the stratosphere.

Instrument/model descriptions

The balloon flights took place out of Fort Sumner, New Mexico (34°N, 104°W), and Daggett, California (35°N, 115°W), on seven occasions since 1989. In this analysis we discuss the sunset occultations of September 27, 1990 (34.2°N, 106°W), May 5, 1991 (37.5°N, 111.8°W), April 3, 1993 (34.8°N, 115.5°W), September 25, 1993 (34°N, 109.4°W) and May 22, 1994 (36.6°N, 109.7°W). The MkIV instrument is a Fourier Transform Infra-Red spectrometer [Toon et al., 1991], which, in addition to HCl, ClONO₂, and HOCl [Toon et al., 1996a], measures reactive nitrogen species (NO₂, NO, HNO₃, HNO₄), as well as tracers (O₃, H₂O, CO, CH₄, C₂H₆, N₂O) and organic chlorine species [Toon et al., 1996b]. On two occasions (September 25, 1993 and April 3, 1993),

the SLS instrument [Stachnik et al., 1992] flew on the same balloon payload, and observed ClO and HCl simultaneously.

The photochemical model used in this study is an extension of the Caltech/JPL model described in Allen and Delitsky [1991] and incorporates 50 chemical species in the NO_y, Cl_y, Br_y, HO_x, O_x and CHO_x families. Most reaction rates and photolysis cross sections are based on the compilation by DeMore et al. [1994]. Heterogeneous processes on sulfate aerosols are also included, among which are hydrolysis of N₂O₅, BrONO₂ and ClONO₂, as well as HCl+ClONO₂ → Cl₂+HNO₃, HOCl+HCl → Cl₂+H₂O [Hanson et al., 1994a, 1994b, 1995]. These last three reactions play a very minor role in the mid-latitude conditions studied here.

For each balloon flight examined, the model is constrained by MkIV observations of H₂O, O₃, CH₄, CO and C₂H₆, which are all kept fixed at their measured values. Total nitrogen (NO_y) and chlorine (Cl_y) are obtained by summing up the individually measured species. The aerosol surface area is specified from SAGE-II satellite observations close in time and space to the balloon flights (G. Maddrea and L. Thomason, personal communication).

Results/Discussion

The MkIV altitude profiles of HCl, ClONO₂, and HOCl are presented in figure 1, for three balloon flights (September 1993, April 1993, and May 1991). Also shown are the SLS observations of ClO and HCl. The main reservoir, HCl, steadily increases with altitude, while ClONO₂ reaches a maximum close to 26 km, and then decreases as it is increasingly destroyed by photolysis. For these flights, the ratio ClONO₂/HCl reaches a maximum between 0.75 and 0.85 (Fig. 2).

The abundance of ClONO₂ in the stratosphere is set through a balance between its formation via the termolecular reaction between ClO and NO₂ and destruction via

photolysis. Furthermore, conversion of ClONO₂ and ClO to HCl involves the reactions $\text{ClO} + \text{NO} \rightarrow \text{Cl} + \text{NO}_2$ and $\text{Cl} + \text{CH}_4 \rightarrow \text{HCl} + \text{CH}_3$. Ozone plays an important role in determining the balance between the two chlorine reservoirs [Brasseur and Solomon, 1986] as it intervenes both directly through the reaction $\text{O}_3 + \text{Cl} \rightarrow \text{ClO} + \text{O}_2$, and indirectly by competing with ClO to react with NO. While the role of ozone in determining the partitioning between HCl and ClONO₂ is prevalent below 24 km, above that altitude, CH₄ constitutes a dominant source of HCl via its reaction with Cl. Furthermore, reaction of Cl with formaldehyde (H₂CO) becomes increasingly important at high altitudes, contributing up to 20% of the HCl production at 40 km.

Overall, the photochemical model reproduces the main features of the observations, in particular in the region of maximum ClONO₂ (~25 km). However, there is a systematic underprediction of HCl above 30 km by 0.1-0.4 ppbv (~20%), accompanied by a pronounced overprediction of ClO by about 50%. In the same region, HOCl tends to be overpredicted by more than 100%. As discussed in the introduction, this is a well known problem seen in other observational studies, most recently by Michelsen et al. [1995] when analyzing the ATMOS ATLAS 2 and 3 data sets.

HCl underprediction above 30 km

The underprediction of HCl and overprediction of ClO above 30 km indicate that the partitioning between these two species is not accurately described in the photochemical model. Assuming a 5% yield in reaction (a), producing HCl improves the agreement with HCl and ClO (case 2 on Fig. 1). The discrepancy between observed and modeled HOCl is reduced from 100% to 50%.

Examining ratios, instead of individual species, provide stricter constraints as the uncertainty due to the total Cl_y specified in the model is eliminated. Figure 2 illustrates

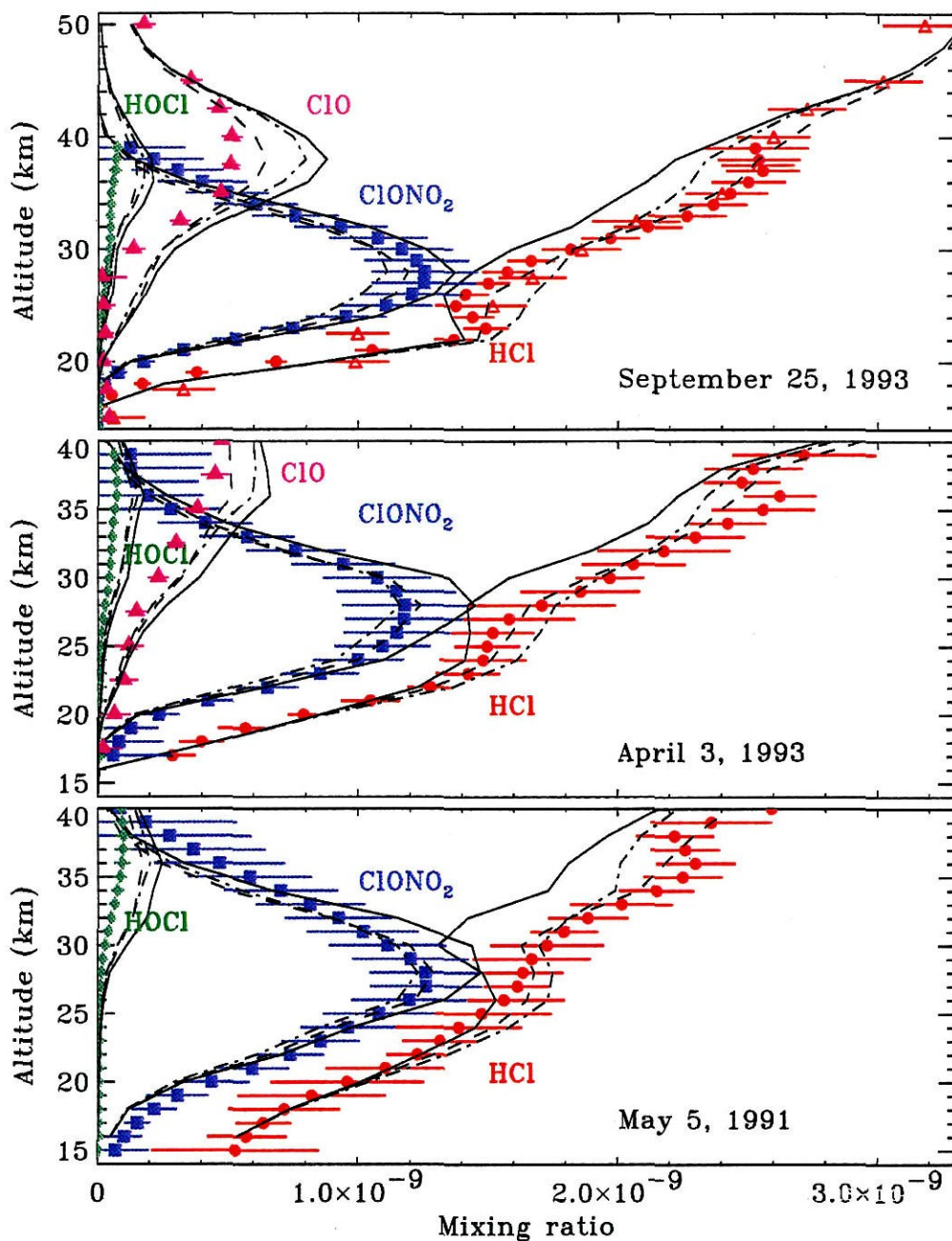


Figure 1: MkIV sunset measurements of HCl (solid circles), ClONO₂ (solid squares), and HOCl (solid diamonds) on September 25, 1993 (34°N), April 3, 1993 (34.2°N) and May 5, 1991 (37.5°N). SLS observations of ClO (full triangles) are also shown on the two top panels, as well as SLS observations of HCl (empty triangles) on the top panel. All error bars reflect 1-sigma uncertainties. The lines show the photochemical model results for three cases: a standard case with JPL 1994 chemistry (case1, —); inclusion of a 5% HCl yield in reaction OH + ClO (case2, - - -); and inclusion of a 3% HCl yield in HO₂ + ClO (case 3, — · — ·).

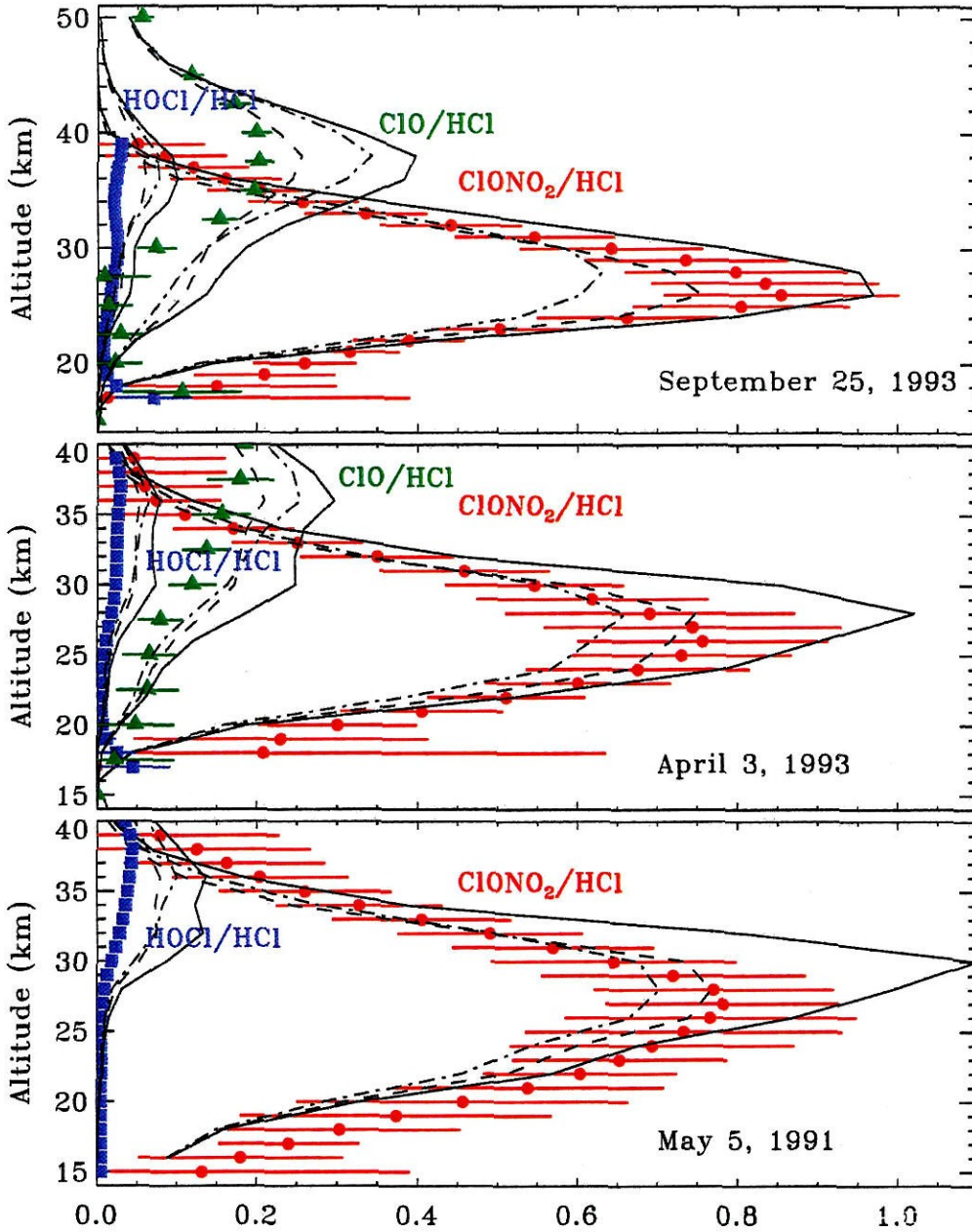


Figure 2: Same as Fig. 1, but for the observed and modeled ratios ClONO₂/HCl, HOCl/HCl, and ClO/HCl.

the better agreement for ClO/HCl with the 5% HCl channel in reaction (a). The observed ClONO₂/HCl ratio is generally bracketed between the 0% (standard model) and 5% channels for most altitudes above 22 km. A higher HCl yield for reaction (a) while further improving agreement with ClO and HOCl above 35 km would worsen it for the ClONO₂/HCl ratio below 25 km. If we include a 3% yield in (b), the general shape of HCl is not as well reproduced (case 3 in Fig. 1), and the predicted ClONO₂/HCl ratio tends to be too low compared to observations (Fig. 2).

Upper estimates of 2-5% were obtained for production of HCl in HOCl photolysis [Butler and Phillips, 1983; Vogt and Schindler, 1992]. Including such a channel produces the same effect as reaction (b). Furthermore, a reduction of the rate constant for reaction HCl + OH by 60% is necessary to match the ClO, but the resulting ClONO₂/HCl is underpredicted by 40%. These results, illustrated here for three balloon flights, are similar for the two other MkIV balloon flights in May 1994 and September 1990 (not shown here) that we examined.

For any of the modifications discussed above, the HOCl/HCl ratio is poorly modeled. HOCl is produced in the stratosphere by reaction of ClO with HO₂, and destroyed mainly by photolysis (reaction with OH contributes to less than 10% of the loss). From SLS observations of HO₂ and ClO, we have calculated the expected steady-state HOCl, which is larger than the observations of HOCl. It is thus possible that either photolysis of HOCl is too fast or that its production is too slow. However, we note that HOCl measurements by Chance et al. (1995) tend to be up to a factor of two larger than the MkIV observations above 35 km, and are generally well predicted by the steady-state expression based on simultaneous ClO and HO₂ measurements.

We conclude from this analysis that for any of the proposed processes to resolve the HCl deficit in the MkIV data, it must be an altitude-selective reaction, affecting the partitioning of HCl and ClO above 30 km, while only slightly affecting the partitioning between HCl and ClONO₂ below that altitude. For example, a temperature/pressure

dependent yield for HCl in either reaction (a) or (b), or a wavelength dependent HCl production from HOCl photolysis, are among the possibilities. The extensive set of species and their diurnal variations measured during the September 1993 flight should provide more information and possible identification of the exact mechanism responsible for the discrepancy in chlorine partitioning at high altitudes. This analysis is currently under way (Stachnik et al., 1996).

ClONO₂/HCl below 22 km

The standard model run clearly underpredicts the ClONO₂/HCl ratio below 22 km by factors between 2 and 10. The model shows HCl to be the largely predominant chlorine reservoir at these altitudes, while the observations indicate that ClONO₂ is present in amounts representing up to 20% of HCl at 18 km.

In recent laboratory measurements, Nickolaisen et al. [1996] have studied the photolysis of chlorine nitrate using broadband flash photolysis and have discovered a pressure and wavelength dependence in the product yields of this reaction. Translating these measurements to the atmosphere has proved to be a difficult task and requires the ability to solve the spectral distribution of the pressure effect. At this point no parameterization of the quantum yield as a function of density and pressure is available for application to modeling studies.

If such an effect is indeed present in the lower stratosphere, then ClONO₂ would have a longer lifetime than previously believed. The sensitivity of the model calculated ClONO₂/HCl ratio to the ClONO₂ photolysis rate (J_{ClONO_2}) is well illustrated in Fig. 3, where we have chosen an arbitrary pressure dependent quantum yield, α , for the photolysis rate ($J_{\text{ClONO}_2(\text{model})} = \alpha J_{\text{ClONO}_2(\text{JPL94})}$) such that at 20 km, $\alpha = 1/2, 1/3$, and $1/5$ respectively. The change in ClONO₂ is almost linearly proportional to $1/\alpha$. ClO itself is only affected to a small degree because, while J_{ClONO_2} is lower, there is more ClONO₂ available to produce ClO. The two effects partially balance each other and the

overall effect is a small decrease in ClO. For the pressure dependence needed to 'fit' the MkIV observations, JClONO₂ is reduced by 40% at 20 km, and ClO itself is reduced by less than 10%.

For each altitude level, we can extract the overall quantum yield that reproduces best the observations. The corresponding quantum yield is presented in Fig. 4 as a function of density. This modeling effort is somewhat frustrated by the large uncertainties in the observations at low altitudes. For this reason, we have applied a similar procedure to four other MkIV balloon flights. All flights seem consistent with a pressure dependent-effect appearing for densities above about 1.5×10^{18} molec cm⁻³.

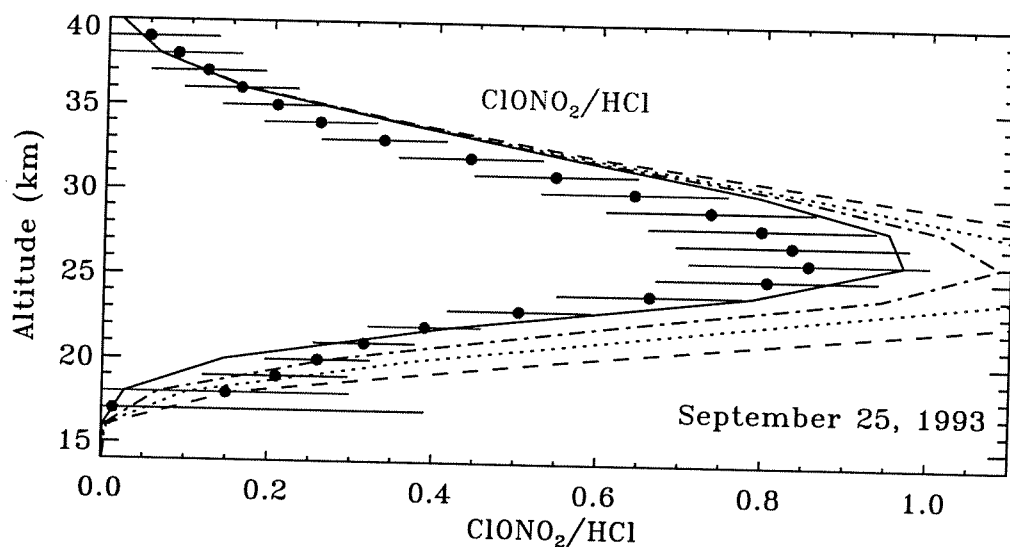


Figure 3: The ClONO₂/HCl ratio on September 1993: model sensitivity to the ClONO₂ photolysis rate (JClONO₂). The solid line shows calculations with standard model (JPL 1994). The dashed dotted line corresponds to $J_{\text{ClONO}_2} = 1/2 J_{\text{ClONO}_2}$ (JPL 1994), the dotted line, to $J_{\text{ClONO}_2} = 1/3 J_{\text{ClONO}_2}$ (JPL 1994), and the dashed line, to $J_{\text{ClONO}_2} = 1/5 J_{\text{ClONO}_2}$ (JPL 1994) [see text].

Two flights (May 1991 and September 1990) exhibit a smaller pressure dependence than the others. In their laboratory experiment, Nickolaisen et al. observed a wavelength dependence of the quantum yield, which was strongly reduced for wavelength longer than 300 nm. Radiative transfer calculations show that the observed ozone profiles corresponding to these two flights result in a different distribution of the spectral intensity, with smaller contributions of the longer wavelengths. Thus these simultaneous observations of ClONO₂ and HCl seem consistent with both a pressure and wavelength dependent photolysis of ClONO₂.

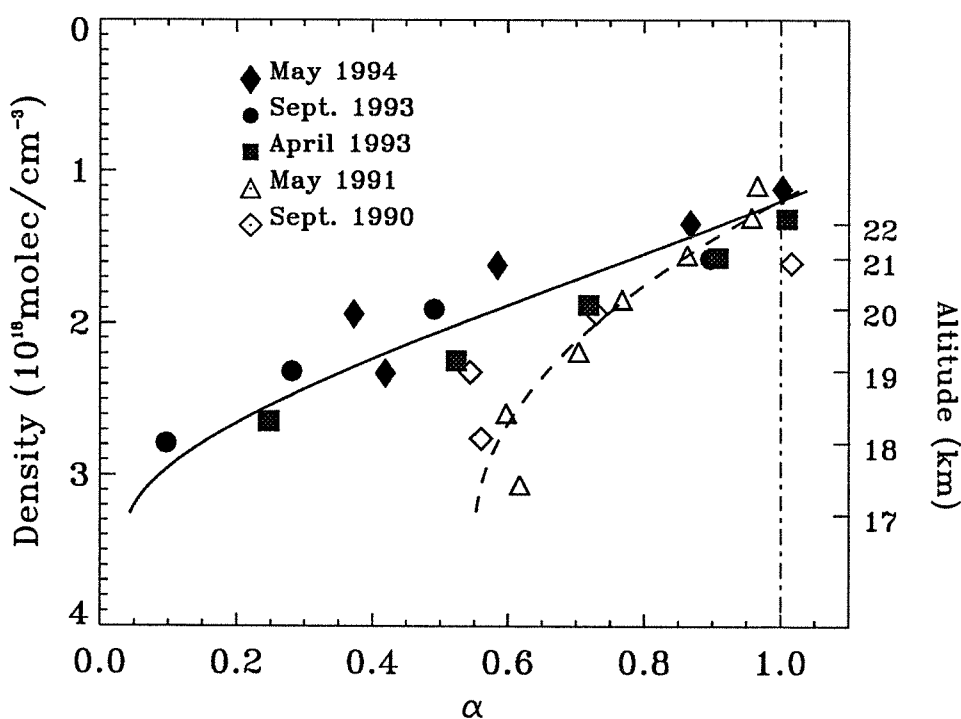


Figure 4: Needed quantum yield in $J\text{ClONO}_2$ (α) to obtain the best match to the observations of ClONO₂/HCl as a function of density/altitude. Each set of symbols corresponds to the analysis described in the text, applied to a different balloon flight: May 1994 (full diamonds), September 1993 (circles), April 1993 (squares), May 1991 (empty triangles), September 1990 (empty diamonds). The solid curve shows a polynomial fit to these points for the first three of these flights, while the dashed curve corresponds to the last two flights (May 1991 and September 1990).

In all of the above, we have assumed that HCl and ClONO₂ are in steady state equilibrium. We must note that in the lower stratosphere below 20 km, both chlorine reservoirs have very long lifetimes (on the order of a month or more), and therefore horizontal mixing and vertical transport might shift the partitioning away from equilibrium. However, it seems likely that such processes - if important - would not affect the ClONO₂/HCl ratio in any systematic way, as observed by the MkIV, but rather would tend to increase the scatter in this ratio.

Implications for the stratosphere / Summary

In situ observations from the ER-2 in 1993 have revealed that the levels of HCl were as low as half of the model predictions, and therefore 30-50% of the inorganic chlorine around 20 km could not be accounted for by the sum of measured HCl, ClO and inferred steady-state ClONO₂ (Webster et al., 1994). It was found that a reduction of JClONO₂ by a factor of 3 to 5 (thereby increasing the inferred steady-state ClONO₂) was needed at 20 km in order to entirely close the budget. Our study of the MkIV data, with direct observations of ClONO₂, supports a JClONO₂ reduction by a factor of 1.5-2.5 at 20 km. Thus, although improving agreement between model and observations of HCl, the introduction of a pressure dependent photolysis rate for ClONO₂ consistent with the MkIV observations of the ClONO₂/HCl ratio does not seem to entirely resolve the chlorine budget as observed from the ER-2.

In a separate study of the MkIV organic and inorganic chlorine budget for the September 1993 flight, comparison between measured and expected chlorine levels lead us to make a case for a missing inorganic chlorine species, HClO₄, produced on sulfate aerosols [Jaeglé et al., 1996]. Because we assumed a very long lifetime (5-10 months) for this species, its effect would be to temporarily reduce the inorganic chlorine available while not significantly affecting the relative partitioning among HCl, ClONO₂ and ClO. For this reason, we have separated the two studies.

It is tempting to suggest that perhaps a small pressure dependent JClONO₂ in combination with a partial sequestering of HCl at the time of the ER-2 missions would resolve the inconsistencies noted between the HCl and ClO *in situ* observations [Webster et al., 1993; Stimpfle et al., 1993], as well as for the MkIV inorganic and organic chlorine observations.

The view of the partitioning between HCl and ClONO₂ as measured by the MkIV instrument is one that seems somewhat different from observations by the ATMOS instrument [Michelsen et al., 1995]: ATMOS ClONO₂/HCl was consistently close to 0.5, being a factor of 2 lower than model predictions, while for MkIV ClONO₂/HCl was close to 0.8.

A comparison of the ozone profiles observed in these two studies show that for the seasons (September and April-May) and latitudes (32-37°N) of the MkIV flights, ozone profiles exhibit high values, while the ATMOS mid-latitude (43.2°N, November) and high-latitude (69°N, February) cases shows low ozone levels, in accordance with the expected climatology. Thus, the dissimilarity between the observations of the two platforms reflects real atmospheric differences.

Taken together, the MkIV observations of HCl, ClONO₂, and HOCl have allowed a quantitative analysis of the chlorine family partitioning. A source of HCl restricted to altitudes higher than 30 km is needed to reconcile model calculations with these observations. In this paper, we demonstrated that the observed ClONO₂/HCl ratio is consistent with the existence of a pressure/altitude dependent effect such as one affecting the photolysis of chlorine nitrate.

ACKNOWLEDGEMENTS. Part of the research described in this paper was carried out by the Jet Propulsion Laboratory, California Institute of Technology under contract with

NASA. This research is also supported in part by NASA grant NAGW-413 to the California Institute of Technology.

REFERENCES

- Allen, M. and M.L. Delitsky, Inferring the abundances of ClO and HO₂ from Spacelab 3 Atmospheric Trace Molecule Spectroscopy observations, *J. Geophys. Res.*, 96, 2913-2919, 1991.
- Avallone, L.M., D.W. Toohey, W.H. Brune, R.J. Salawitch, A.E. Dessler, and J.G. Anderson, Balloon-borne *in situ* measurements of ClO and ozone: implications for heterogeneous chemistry and mid-latitude ozone loss, *Geophys. Res. Lett.*, 20, 1795-1798, 1993.
- Brasseur, G. and S. Solomon, Aeronomy of the middle atmosphere, *D. Reidel publishing company*, 1986.
- Butler, P.J.D. and L.F. Phillips, Upper limit for the atomic oxygen yield in the 308-nm photolysis of HOCl, *J. Phys. Chem.*, 84, 821-826, 1983.
- Chance, K., W.A. Traub, K.W. Jucks, P. Ciarpallini, R.A. Stachnik, R.J. Salawitch, and H.A. Michelsen, submitted to *Science*, 1995.
- Crutzen, P.J., J.U. Grooss, C. Bruhl, R. Muller, and J.M. Russell, A reevaluation of the ozone budget with HALOE UARS data - no evidence for the ozone deficit, *Science*, 268, 705-708, 1995.
- Crutzen, P.J. and U. Schmailzl, Chemical budgets of the stratosphere, *Planet. Space Sci.*, 31, 1009-1032, 1983.
- DeMore, W.B., S.P. Sander, D.M. Golden, R.F. Hampson, M.J. Kurylo, C.J. Howard, A.R. Ravishankara, C.E. Kolb, and M.J. Molina, Chemical Kinetics and Photochemical Data for Use in Stratospheric Modeling: Evaluation Number 10, *JPL Publication 94-26*, 1994.
- Dessler, A.E., D.B. Considine, G.A. Morris, M.R. Schoeberl, J.M. Russell, A.E. Roche, J.B. Kumer, J.L. Mergenthaler, J.W. Waters, J.C. Gille, and G.K. Yue, Correlated

observations of HCl and ClONO₂ from UARS and implications for stratospheric chlorine partitioning, *Geophys. Res. Lett.*, 22, 1721-1724, 1995.

Eluszkiewicz, J. and M. Allen, A global analysis of the ozone deficit in the upper-stratosphere and lower mesosphere, *J. Geophys. Res.*, 98, 1069-1082, 1993.

Hanson, D.R. and A.R. Ravishankara, Heterogeneous chemistry of bromine species in sulfuric-acid under stratospheric conditions, *Geophys. Res. Lett.*, 22, 385-388, 1995.

Hanson, D.R., A.R. Ravishankara, and S. Solomon, Heterogeneous reactions in sulfuric acid aerosols: a framework for model calculations, *J. Geophys. Res.*, 99, 3615-3625, 1994a.

Hanson, D.R. and A.R. Ravishankara, Reactive uptake of ClONO₂ onto sulfuric-acid due to reaction with HCl and H₂O, *J. Phys. Chem.*, 98, 5728-5735, 1994b.

Jackman, C. H., R.S. Stolarski, and J.A. Kaye, Two-dimensional monthly average ozone balance from Limb Infrared Monitor of the Stratosphere and Stratospheric and Mesospheric Sounder data, *J. Geophys. Res.*, 91, 1103-1116, 1986.

Jaeglé, L., Y.L. Yung, G.C. Toon, B. Sen, and J.-F. Blavier, Balloon observations of organic and inorganic chlorine in the stratosphere: the role of HClO₄ production on sulfate aerosols, submitted to *Geophys. Res. Lett.*, 1996.

McElroy, M.B. and R.J. Salawitch, Stratospheric ozone: impact of human activity, *Planet. Space Sci.*, 37, 1653-1672, 1989.

Michelsen, H.A., R.J. Salawitch, M.R. Gunson, C. Aellig, N. Kaempfer, M.M. Abbas, M.C. Abrams, T.L. Brown, A.Y. Chang, A. Goldman, F.W. Irion, M.J. Newchurch, C.P. Rinsland, G.P. Stiller, and R. Zander, Stratospheric chlorine partitioning: constraints from shuttle-borne measurements of HCl, ClNO₃ and ClO, submitted to *Geophys. Res. Lett.*, 1995.

Natarajan, M. and L.B. Callis, Stratospheric photochemical studies with Atmospheric Trace Molecule Spectroscopy (ATMOS) measurements, *J. Geophys. Res.*, 96, 9361-9370, 1991.

Nickolaisen, S.L., S.P. Sander, and R.R. Friedl, Pressure dependent yields and product branching ratios in the broadband photolysis of chlorine nitrate, submitted to *J. Phys. Chem.*, 1996.

Salawitch, R.J., S.C. Wofsy, P.O. Wennberg, R.C. Cohen, J.G. Anderson, D.W. Fahey, R.S. Gao, E.R. Keim, E.L. Woodbridge, R.M. Stimpfle, J.P. Koplw, D.W. Kohn, C.R. Webster, R.D. May, L. Pfister, E.W. Gottlieb, H.A. Michelsen, G.K. Yue, J.C. Wilson, C.A. Brock, H.H. Jonsson, J.E. Dye, D. Baumgardner, M.H. Proffitt, M. Loewenstein, J.R. Podolske, J.W. Elkins, G.S. Dutton, E.J. Hintsa, A.E. Dessler, E.M. Weinstock, K.K. Kelly, K.A. Boering, B.C. Daube, K.R. Chan, and S.W. Bowen, The distribution of hydrogen, nitrogen, and chlorine radicals in the lower stratosphere: implications for changes in O₃ due to emission of NO_y from supersonic aircraft, *Geophys. Res. Lett.*, 21, 2543-2546, 1994.

Stachnik, R.A., G.C. Toon, H.M. Pickett, and R.J. Salawitch, in preparation, 1996.

Stachnik, R.A., J.C. Hardy, J.A. Tarsala, J.W. Waters, and N.R. Erickson, Submillimeterwave heterodyne measurements of stratospheric ClO, HCl, O₃, HO₂: first results, *Geophys. Res. Lett.*, 19, 1931-1934, 1992.

Stimpfle, R. M., J.P. Koplw, R.C. Cohen, D.W. Kohn, P.O. Wennberg, D.M. Judah, D.W. Toohey, L.M. Avallone, J.G. Anderson, R.J. Salawitch, E.L. Woodbridge, C.R. Webster, R.D. May, M.H. Proffitt, K. Aiken, J. Margitan, M. Loewenstein, J.R. Podolske, L. Pfister, and K.R. Chan, The response of ClO radical concentrations to variations in NO₂ radical concentrations in the lower stratosphere, *Geophys. Res. Lett.*, 21, 2543-2546, 1994.

Toon, G.C., B. Sen, and J.-F. Blavier, Inorganic chlorine measured by balloon-borne solar absorption spectrometry, *Geophys. Res. Lett.*, manuscript in preparation for *Geophys. Res. Lett.*, 1996a.

Toon, G.C., B. Sen, and J.-F. Blavier, Sources of stratospheric chlorine measured by balloon-borne solar absorption spectrometry, in preparation for *Geophys. Res. Lett.*, 1996b.

Toon, G.C., The JPL MkIV interferometer, *Optics and Photonics News*, 2, 19-21, 1991.

Toumi, R. and S. Bekki, The importance of the reactions between OH and ClO for stratospheric ozone, *Geophys. Res. Lett.*, 20, 2447-2450, 1993.

Vogt, R. and R.N. Schindler, Product channels in the photolysis of HOCl, *J. Photochem. Photobiol. A: Chem.*, 66, 133-140, 1992.

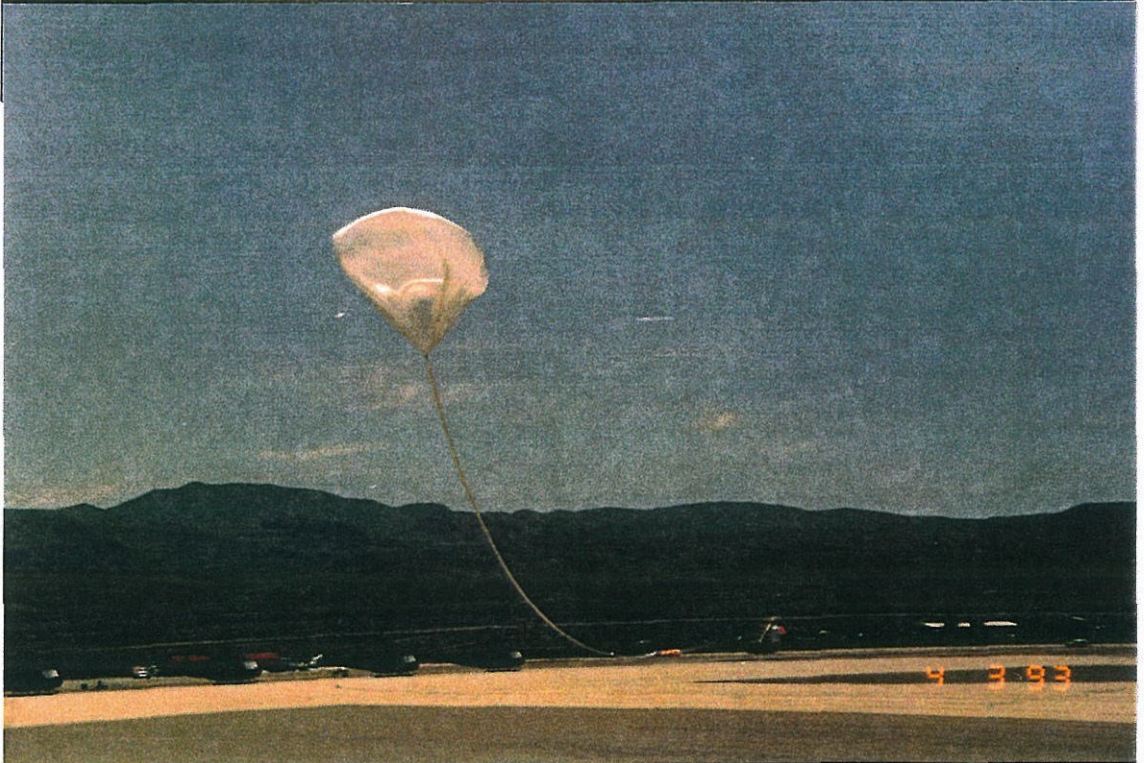
Webster, C.R., R.D. May, L. Jaeglé, S.P. Sander, M.R. Gunson, G.C. Toon, J.M. Russell III, R. Stimpfle, J. Koplow, R.J. Salawitch, and H.A. Michelsen, Hydrochloric acid and the chlorine budget of the lower stratosphere, *Geophys. Res. Lett.*, 21, 2575-2578, 1994.

Webster, C.R., R.D. May, D.W. Toohey, L.M. Avallone, J.G. Anderson, and S. Solomon, *In-situ* measurements of the ClO/HCl ratio - heterogeneous processing on sulfate aerosols and polar stratospheric clouds, *Geophys. Res. Lett.*, 20, 2523-2526, 1993.

WMO, *Scientific Assessment of Ozone Depletion: 1994*, Global Ozone Research and Monitoring Project - Report No. 37, World Meteorological Organization, Geneva, 1995.

CHAPTER 5

**Balloon Observations of Organic and Inorganic Chlorine in the Stratosphere:
the Role of HClO₄ Production on Sulfate Aerosols**



**Balloon Observations of Organic and Inorganic Chlorine in the Stratosphere:
the Role of HClO₄ Production on Sulfate Aerosols**

Lyatt Jaeglé

Environmental Engineering Science Department, California Institute of Technology

Yuk L. Yung

Division of Geological and Planetary Sciences, California Institute of Technology

Geoffrey C. Toon, Bhaswar Sen, Jean-François Blavier

Jet Propulsion Laboratory, California Institute of Technology

[The text of this chapter is submitted to the *Geophysical Research Letters*]

Abstract. Simultaneous observations of stratospheric organic chlorine (CCl₃F, CCl₂F₂, CCl₂FCClF₂, CHClF₂, CH₃Cl, CCl₄) and inorganic chlorine (HCl, ClONO₂, HOCl) were made in September 1993 out of Fort Sumner, New Mexico, using the JPL balloon-borne MkIV interferometer. These measurements have been used to examine the atmospheric chlorine budget. Between 15 and 20 km, a significant fraction (20 - 60%) of the inorganic chlorine could not be accounted for by the sum of measured HCl, ClONO₂, and HOCl. Laboratory measurements of the reaction of ClO radicals on sulfuric acid solutions have indicated that, along with HCl, small amounts of perchloric acid, HClO₄, were formed. Therefore, we investigate here the possibility that the deficit in inorganic chlorine can be explained by heterogeneous production of HClO₄ on stratospheric sulfate aerosols. A photochemical box model is used to determine the impact of this new species on the partitioning of inorganic chlorine in the stratosphere. It is shown that in the enhanced aerosol loading conditions resulting from Mt. Pinatubo's eruption, HClO₄ is photochemically stable enough that it could represent a significant reservoir of chlorine in the lower stratosphere, sequestering up to 0.2 ppbv (or 50%) of the total inorganic chlorine at 16 km. The occurrence of this new species could bring to closure the inorganic chlorine budget deficiency made apparent by recent ER-2 aircraft *in situ* measurements of HCl.

Introduction

Once organic chlorine (CCly) has reached the stratosphere in the form of halocarbons, it is converted by photolysis and reaction with radicals to inorganic chlorine (Cly). Most of the inorganic chlorine species thought to play an important role in the stratosphere have been detected (HCl, ClONO₂, HOCl, ClO, OClO), and a few others (Cl₂, Cl, Cl₂O₂, ClNO, ClNO₂) occur at abundances too small to be observable with current techniques. These compounds represent only a small subset of the many possible chlorine-containing compounds. In particular, higher oxides like ClO₃, ClO₄, Cl₂O, Cl₂O₇, and oxo acids like HClO₂, HClO₃, HClO₄ have been characterized in the laboratory environment (Greenwood and Earnshaw, 1985), and their possible importance for stratospheric chemistry is still subject to speculation (Sander et al., 1995, 1989). As most of the higher oxides of chlorine tend to be unstable, they could be present in the stratosphere only in small quantities, but may possibly play an important role in the loss of stratospheric ozone (Prasad and Lee, 1994). On the other hand, if any oxo acid were to be formed under stratospheric conditions, it might be stable enough to constitute an important reservoir of chlorine, depending on its loss processes.

The first evidence for a serious discrepancy in our understanding of the partitioning of the inorganic chlorine in the lower stratosphere was presented by Webster et al. (1994, 1993). These recent *in situ* measurements aboard NASA's ER-2 aircraft revealed abundances of HCl in the lower stratosphere (~19 km) that represent about half of the values predicted by models. Consequently, 30-50 % of Cly could not be accounted for by comparison of *in situ* measurements of HCl, ClO, and calculated steady-state ClONO₂, with Cly inferred from N₂O.

In this paper, we first present evidence of a discrepancy in the chlorine budget as shown by MkIV balloon measurements in September 1993. We then investigate the possible source of the missing chlorine, emphasizing a possible heterogeneous formation of HClO₄. Finally we discuss the implications of the production of HClO₄ for the mid-

latitude lower stratosphere in the context of the high aerosol loading conditions present after Mt. Pinatubo's eruption in 1991.

Missing Chlorine: MarkIV observations

The MkIV interferometer is a Fourier Transform Infra-Red spectrometer, which has flown on seven balloon flights since 1989 from New Mexico and California (Toon et al., 1996a). The set of measurements discussed here were taken on the flight of September 25, 1993, out of Fort Sumner, New Mexico. This flight was exceptional in that a very clear tropopause allowed data to be taken nearly all the way down to the ground. The many gases measured between 5 and 39 km included species in the families of inorganic chlorine (HCl, ClONO₂, HOCl), organic chlorine (CCl₃F, CCl₂F₂, CCl₂FCClF₂, CHClF₂, CH₃Cl, CCl₄), reactive nitrogen species (HNO₃, NO₂, NO, HNO₄), as well as tracers (O₃, H₂O, CH₄, CO, C₂H₆, N₂O, SF₆). In addition the Submillimeterwave Limb Sounder (Stachnik et al., 1992), on the same balloon payload, observed ClO simultaneously.

We use these observations to calculate the chlorine budget. MkIV measures approximately 86% of the chlorine-bearing source gases. Adding to these gases an estimate of CH₃CCl₃ based on MkIV CFC-11 together with an empirical relationship between CH₃CCl₃ and CFC-11 (Elkins et al., 1995), we account for 99% of the inorganic chlorine in the troposphere (~3.8 ppbv; WMO, 1995). Furthermore, the sum ClONO₂+HCl+HOCl+ClO accounts for 82-100% of the total inorganic chlorine. We also include estimates of COFCl (0.01 - 3% of Cly in the stratosphere) from a 2-D model calculation, and of COCl₂ (0.1-15%), for which we used the model profile of Kindler et al. (1995) which compares well with observations in the lower stratosphere (Wilson et al., 1988). The resulting total organic and inorganic chlorine is presented in Fig. 1. A more detailed description of these measurements and the data reduction can be found in Toon et al. (1996b and 1996c).

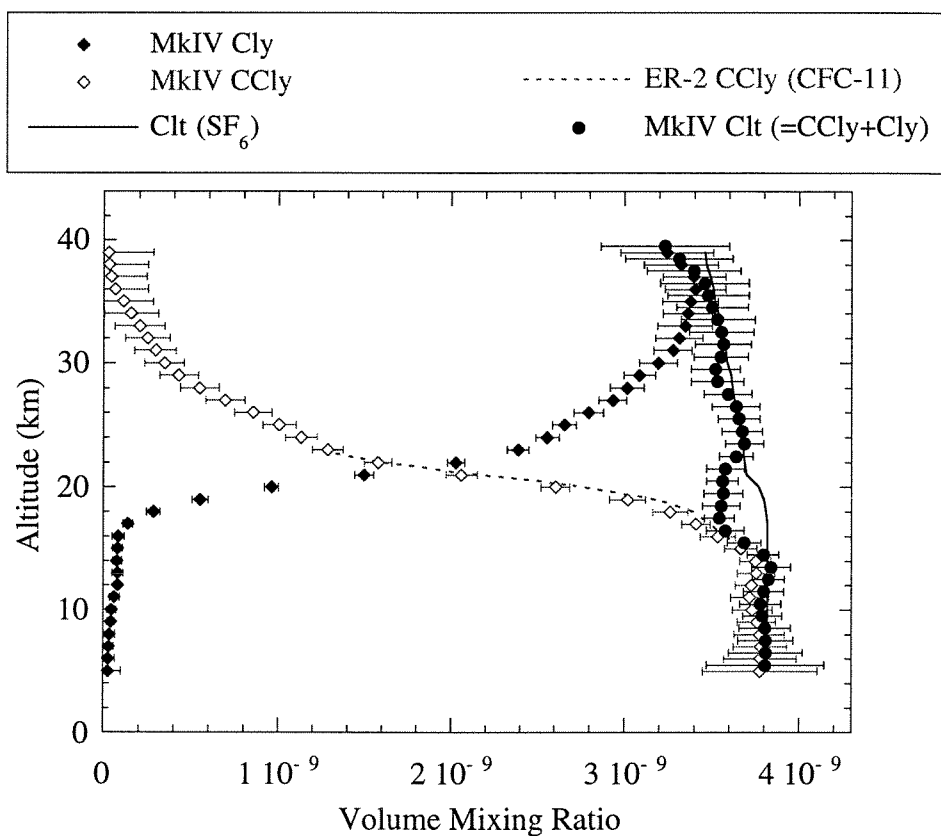


Figure 1: MkIV interferometer sunset measurements of organic (CCl₄: open diamonds) and inorganic (Cly: solid diamonds) chlorine between 5 and 39 km on September 25, 1993 (34° N, 109.4° E). The solid circles represent the sum of observed Cly and CCl₄. For better representation, these numbers have been interpolated to a grid shifted by 0.5 km. The error bars correspond to 1-s precision errors. The solid line is the calculated total chlorine based on the age of the air (see text). The dashed line shows the corresponding CCl₄ as derived from the MkIV CFC-11 using empirical relationships determined from in situ organic chlorine observations aboard the ER-2 (Elkins et al., 1995).

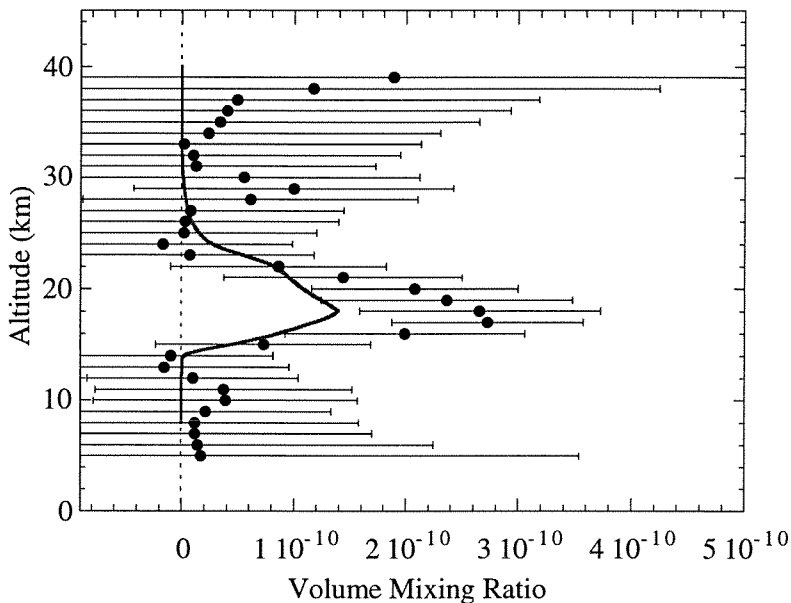


Figure 2: Comparison between MkIV observations of the chlorine deficit (circles with error bars), and calculated vertical profiles of HClO₄ (solid line).

We compare the sum of measured Cly and CCly to the expected amount of total chlorine (Cl_t). Cl_t is a direct function of the age of the air (Woodbridge et al., 1995), which is usually defined as the time elapsed since an air parcel has entered the stratosphere at the tropical tropopause (Rosenlof, 1995). We based our calculation of the age of the air on the MkIV SF₆ measurements between 12 and 21 km, assuming a growth rate of 9% per year for SF₆. For altitudes above 21 km where no SF₆ observations were available, we assumed linearly increasing age reaching a maximum age of 5 years at 40

km. To infer Clt from the age, we used the record of tropospheric total chlorine documented by the World Meteorological Organization (WMO, 1995; WMO, 1992).

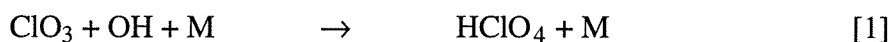
Based on our current knowledge of stratospheric chemistry, the sum of chlorine species measured by the MkIV interferometer supplemented with the other few species discussed above, should account for all of the chlorine present in the stratosphere. However, Fig. 1 shows a striking discrepancy between predicted and observed total chlorine: there is evidence of ~0.3 ppbv of missing chlorine concentrated in a layer around 17 km. Good agreement between MkIV CCl_y and *in situ* organic chlorine measurements aboard the ER-2 (Elkins et al., 1995) yield a high level of confidence in the ability of MkIV to measure total organic chlorine. Also, for this same September 1993 MkIV data set, Sen et al. (1996) examined the fluorine budget which shares many of the species involved in the chlorine budget, and found very good agreement with model predictions for both fluorine sources and reservoirs. On this basis, we attribute the missing chlorine to the inorganic chlorine family.

The difference between Clt and the sum Cly+CCly is illustrated in Fig. 2. The error bars shown are the 1- σ precision propagated errors, and do not include an estimate of systematic errors, which are mainly due to spectroscopic uncertainties. Although these uncertainties are substantial, they are mostly altitude independent and therefore do not detract from the significance of the deficit. Such a feature was not observed in the ATMOS Spacelab 3 observations (Zander et al. 1992), which took place in 1985. However, an important difference between the two observations is that the MkIV balloon flight took place in an atmosphere with levels of sulfate aerosols still high after Mt. Pinatubo's eruption in 1991 (surface areas of 3-6 $\mu\text{m}^2/\text{cm}^3$), while the ATMOS experiment flew in a relatively clean atmosphere ($< 1 \mu\text{m}^2/\text{cm}^3$). The ATMOS ATLAS-3 mission chlorine retrievals (Zander et al., 1995) and the other MkIV balloon flights made in 1992 and 1993 do not extend to altitudes low enough to reveal the presence or the absence of missing chlorine. In the following section, we will speculate that the missing

chlorine suggested by the MkIV measurements is held in HClO₄, a species which could be produced on sulfate aerosols.

Perchloric acid and sulfate aerosols

The possibility of HClO₄ formation in the stratosphere was first discussed by Simonaitis and Heicklen (1975). They proposed a three body reaction,



with a rate constant estimated to be similar to that of NO₂ + OH + M. However, ClO₃ itself can be formed from only two sources: photolysis of Cl₂O₃ and OClO + O + M (Sander and Friedl, 1995). Both require OClO, which occurs at significant levels only in the polar springtime (Solomon et al., 1987). Thus this process can only contribute to very small amounts of perchloric acid at mid-latitudes. More recently, Prasad and Lee (1994) presented another possibility:



where the ClO·O₃ radical would be formed via reaction of ClO·O₂ with ozone. The stability of ClO·O₂ is itself still subject to discussion (Prasad and Lee, 1994) and the existence of ClO·O₃ is hypothetical.

Martin et al. (1980) obtained experimental measurements of the ClO heterogeneous reactivities on sulfuric acid solutions. These authors monitored the loss of ClO at a constant vapor pressure of H₂O (5.10⁻⁴ Torr) and over a temperature range of 240-293 K. The following temperature-dependent uptake reaction probability was derived:

$$\gamma(T) = \exp[-9.361 + (3.22 \pm 1.43)(1000/T - 3.867)] \quad [a]$$

The main chlorine containing product was found to be HCl (accounting for 60-100% of the ClO lost), and, interestingly, small amounts of HClO₄ were also detected (Martin et al., 1979):



Moreover, formation of HCl and perchloric acid was seen from reactions of Cl radicals and Cl₂ molecules on sulfuric acid. It is unclear what mechanism would cause HClO₄ formation in sulfuric acid. To our knowledge, no other measurements of ClO uptake on sulfuric acid have been published; however, preliminary measurements by Zhang et al. (personal communication) seem to suggest a slower reaction probability. Martin et al. examined the possible significance of HCl formation via [4] for stratospheric chemistry. They concluded that [4] contributes to a slight reduction of the Cl/HCl ratio at 20 km under background aerosol loading conditions. The impact of [3] has not been examined, and is an interesting possibility to consider under volcanic aerosol levels. Recent *ab initio* characterization of perchloric acid (Francisco, 1995) have shown that the molecule, under the form HOClO₃, is stable to thermal decomposition.

If it appears that under some conditions HClO₄ could be formed in substantial amounts in the stratosphere, we need to need to examine the possible loss mechanisms of this molecule.

Loss processes

Very little is known about the loss processes of HClO₄ in the stratosphere, and we base our considerations on analogies with the chemistry of HCl. It is likely that HClO₄ would be more stable than HCl towards reaction with OH (Simonaitis and Heicklen [1975]; Prasad and Lee [1994]). Therefore, we assumed a rate constant for reaction of OH with HClO₄ to be ten times slower than that with HCl. As perchloric acid is a weak absorber (Karelin et al., 1975), its loss by photolysis is probably negligible and we have chosen it to be equal to the HCl photolysis rate. Other loss mechanisms could exist, like reaction with NO or other radicals, but these might be slower than that with OH, as is the case for HCl. Alternatively, HClO₄ could be removed by inclusion into sulfate aerosols. We are

not aware of any measurements of the solubility of perchloric acid in sulfuric acid solutions, so we estimated its Henry's law constant from basic thermodynamical properties in water (Colussi et al. and Grela, 1993; Karapet'yants and Karapet'yants, 1970) and comparison with HCl solubilities in water and sulfuric acid (Hanson et al., 1994; Clegg and Brimblecombe, 1990). Taking into account the dissociation of HClO₄ to form the perchlorate ion in solution, ClO₄⁻, we obtain a Henry's law constant of about 10⁶ M.atm⁻¹ at 200K (compared to 6.10⁴ M.atm⁻¹ for HCl). Thus, less than 10⁻² % of the HClO₄ will be sequestered in the aerosol phase. However, if we use *ab initio* calculations of the heat of formation of HClO₄ (Francisco, 1995), the value obtained for Henry's law would be much higher and a significant fraction of HClO₄ could be in the aerosol phase. Direct laboratory measurements would be necessary to settle this issue.

Model Description

To assess the impact of the heterogeneous production of perchloric acid on the chlorine budget, we have implemented the simple HClO₄ chemistry outlined above (using the upper limit for HClO₄ yield from ClO uptake on sulfuric acid, i.e. 40%) in a photochemical box model (Jaeglé et al., 1996). Heterogeneous processes also included are hydrolysis of N₂O₅ and ClONO₂ (Hanson et al., 1994). In the following, we have neglected uptake of HClO₄ by aerosols.

Given the large lifetime of HClO₄ (two-ten months in the lower stratosphere), we need to take into account the progressive decrease of the aerosol surface area over the three years following Mt. Pinatubo's eruption in June 1991. We have therefore performed our calculations for this three year period. The surface area evolution as a function of altitude is based on a time dependent 2-D model calculation by Tie et al. (1994) at 45°N, which we adjusted to match the aerosol profile measured by the SAGE II satellite close in space and time to the balloon measurement. The altitude profiles for O₃, H₂O, CH₄ have been

constrained to the conditions observed by the MarkIV balloon instrument on September 25, 1993. Cly was taken as the difference between total chlorine, Clt, and CCl_y.

Model results / Discussion

The calculated profile for HClO₄ in September of 1993 is presented in Fig. 2. The model results are dependent on the assumptions made for HClO₄ chemistry and they show that HClO₄ is produced in a thin layer between 16 and 22 km, where most of the aerosol surface area is contained and the temperatures are below 210 K. The altitude and magnitude of the peak in mixing ratio depend on the assumption made for ClO reactivity on aerosols, as well as on the magnitude of the loss term. In particular, an exponential dependence on temperature as described by Martin et al. yields a profile of HClO₄ peaking around 22 km (not shown here). Laboratory measurements of ClONO₂ hydrolysis (Hanson et al., 1994) have shown that the rates of heterogeneous reactions are extremely sensitive to the water content of the sulfuric acid aerosol. We have therefore attempted to extrapolate the measurements of Martin et al. to more dilute sulfuric acid aerosols, by using a dependence on sulfuric acid weight percent (WH₂SO₄) instead of temperature. We obtained the following expression:

$$\gamma(\text{WH}_2\text{SO}_4) = 10 [3.65 - 0.094 * \text{WH}_2\text{SO}_4] \quad [\text{b}]$$

This has the main effect of increasing the uptake coefficient for dilute aerosols found in the lower stratosphere. As can be seen in Fig. 2, the mixing ratio of HClO₄ predicted by the model peaks at 16 km, with a shape similar to the observations of missing chlorine, but reaching a lower maximum. Given the uncertainties associated with both the chemistry of HClO₄ and this idealized calculation, we have not attempted to obtain a better match with the observed deficit. In order to conserve the amount of chlorine at each level, we have not introduced any vertical diffusion which would have the effect of

smoothing this profile vertically. In a separate calculation we have tested the impact of reaction [1], and have found that the amounts of HClO₄ formed were negligible.

Figure 2 illustrates the fact that heterogeneous production of HClO₄ is a possible candidate to explain qualitatively the missing chlorine inferred from the MkIV measurements. Even though the sticking coefficient for ClO in reaction [3] is small, it could be very effective at producing HClO₄ because of the very slow gas-phase loss of this species. Thus, in the presence of aerosols, HClO₄ could constitute a chlorine reservoir with a lifetime longer than that of HCl, its main impact being to reduce the amount of chlorine available to form HCl and ClONO₂.

The impact of the rapid increase followed by a slow decrease of aerosol levels as caused by Mt. Pinatubo would be a delayed response of HClO₄ concentrations is shown in Fig. 3. The only time-varying input in our model calculation was the aerosol surface area (Fig. 3a). At 16 km the surface area peaked seven months after the eruption of Mt. Pinatubo and decreased thereafter roughly exponentially, with a time constant of approximately 22 months. HClO₄/Cly itself reached a maximum of 35-45% six months after the peak in surface area, and then slowly decreased as OH destroyed it. HCl follows the mirror image of HClO₄, and is reduced by 45% at 16 km and by 35 % at 18 km. To distinguish the effect of HClO₄ chemistry and the perturbation introduced by N₂O₅ and ClONO₂ hydrolysis, we have represented a model calculation including only standard chemistry (dashed lines). The uptake of ClO on sulfate aerosols has little effect on the relative partitioning of other chlorine species: production of HCl via reaction [4] is slow compared to the Cl + CH₄ reaction, confirming the results of Martin et al. (1980). The calculated evolution of ClO can also be seen in Fig. 3d: the increase in surface area results in a smaller and less prolonged increase in ClO when HClO₄ chemistry is included. The main effect of HClO₄ is that it acts as a temporary sink for inorganic chlorine thereby lowering the amount of Cly available for HCl formation.

We have attempted to detect HClO₄ in the stratosphere using the MkIV infrared spectra, but the large abundance of N₂O and H₂O lines in the region where we would expect to see an absorption feature (Karelin et al., 1975), and the lack of high-resolution spectral information, have not allowed us to clearly prove or disprove the presence of HClO₄.

Implications for the stratosphere

In situ measurements from the ER-2 aircraft of HCl in the lower stratosphere made in 1992 and 1993 have revealed a serious discrepancy in our understanding of the partitioning of inorganic chlorine at mid-latitudes: the observed levels of HCl were as low as half of the model predictions, and therefore 30-50% of the inorganic chlorine around 20 km could not be accounted for by the sum of measured HCl, ClO and inferred steady-state ClONO₂ (Webster et al., 1994). These measurements were made in the northern hemisphere, in the presence of high aerosol loading resulting from Mt. Pinatubo's eruption, and, as evidenced in Fig. 2, could be consistent with heterogeneous formation of HClO₄.

More recent *in situ* observations by this same instrument indicated a recovery of HCl, with mixing ratios slowly increasing as a function of time as the aerosol loading is decreasing (Webster et al., 1996). Southern hemisphere observations, with low aerosol levels, show little to no deficit. The progressive recovery of the *in situ* HCl observations between 15 and 20 km is qualitatively consistent with a slow release of the sequestered Cl₂ possibly in the form of perchloric acid (Webster et al., 1996), as predicted by the box model calculation.

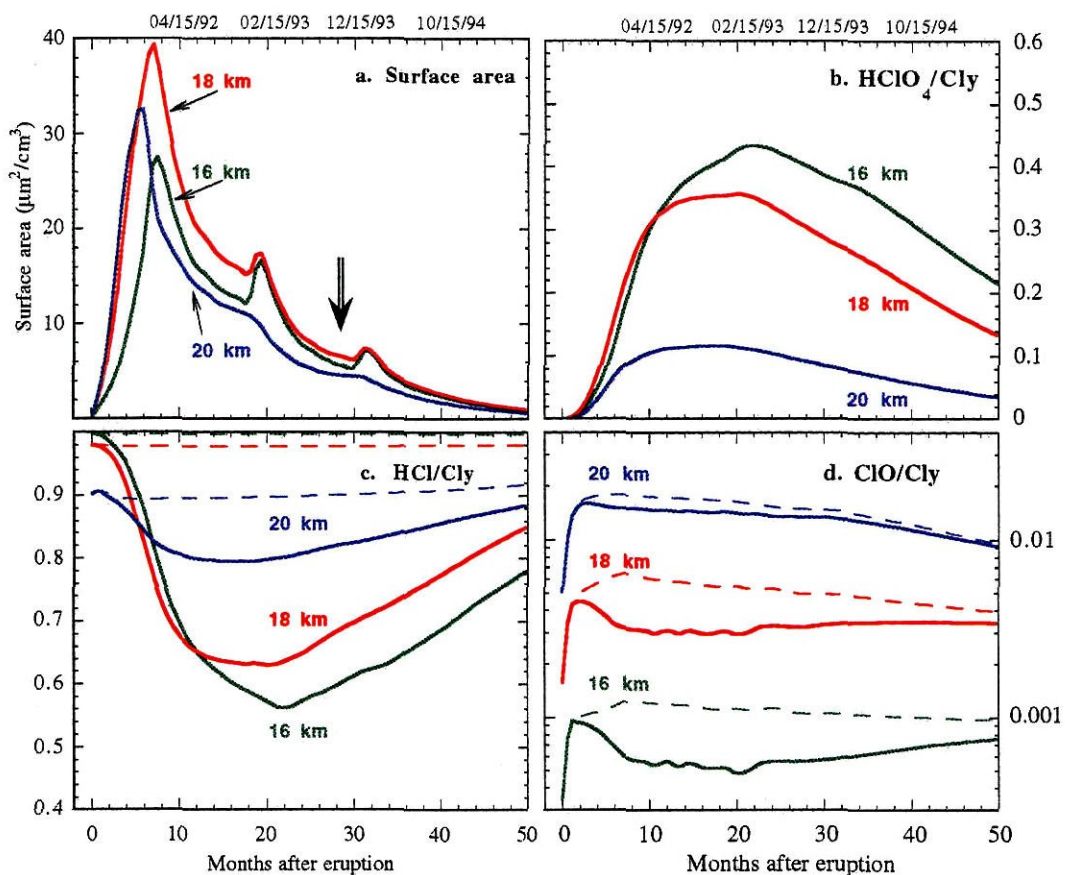


Figure 3: Time dependent box model calculation since Mt. Pinatubo's eruption. (a) Aerosol surface area evolution at 16, 18 and 20 km (2D model output by Tie et al., 1994). The solid lines represent model calculations including HClO₄ chemistry (see text) for (b) HClO₄/Cly, (c) HCl/Cly, and (d) ClO/Cly. The dashed lines illustrate the effect of changing surface area considering only standard heterogeneous chemistry (N₂O₅ and ClONO₂ hydrolysis). The arrow on panel (a) indicates the time of the MkIV balloon flight.

Thus, volcanic eruptions such as Mt. Pinatubo's may have the effect of temporarily reducing the available Cl_y for conversion to HCl, and ClO, thereby rendering ozone molecules less vulnerable to loss via chlorine catalytic cycles. Whether this mechanism could take place in the winter polar regions, where high ClO concentrations and large surface areas provided by polar stratospheric cloud (PSC) particles coexist, is an interesting issue to consider. While PSC surfaces have been shown to be unreactive towards ClO (Kenner et al., 1993), they could constitute a net sink for species like HClO₄ by analogy with HCl (which is converted to Cl₂ on PSCs). However, the stoichiometry of HCl loss and ClO production demonstrated by *in situ* observations in the Arctic winter of 1991-1992 (Webster et al., 1993) and reflecting the role of $\text{HCl} + \text{ClONO}_2 \rightarrow \text{Cl}_2 + \text{HNO}_3$ would tend to disprove such a loss mechanism, or might suggest that at the time of the observations no mid-latitude HClO₄ had yet reached the isolated Arctic vortex.

Conclusions

Observations of organic and inorganic chlorine by the MkIV instrument show a significant deficit in Cl_y around 17 km. We have proposed that perchloric acid might sequester a fraction of the inorganic chlorine in the presence of high levels of sulfate aerosols. This hypothesis provides a qualitative explanation for the current imbalance in the chlorine budget observed in this study, and might provide a possible explanation for the low HCl aircraft measurements. More robust conclusions await laboratory determinations of the possible production and loss mechanisms outlined in this paper, as well as possible detection of the species in the stratosphere.

ACKNOWLEDGEMENTS. The authors would like to thank S. Sander, C. Webster, R. Martin, S. Martin, and R. Zhang for helpful discussions, and X. Tie for providing his 2-D model output. Part of the research described in this paper was carried out by the Jet

Propulsion Laboratory, California Institute of Technology, under contract with the National Aeronautics and Space Administration (NASA). This research is also supported in part by NASA grant NAGW-413 to the California Institute of Technology.

REFERENCES

Clegg, S.L. and P. Brimblecombe, Solubility of volatile electrolytes in multicomponent solutions with atmospheric applications, in *Chemical Modeling of Aqueous Systems II*, edited by D.C. Melchior and R.L. Bassett, pp 58-73, American Chemical Society, Washington D.C., 1990.

Colussi, A.J. and M.A. Grela, Kinetics and thermochemistry of chlorine- and nitrogen-containing oxides and peroxides, *J. Phys. Chem.*, *97*, 3775-3779, 1993.

Elkins, J.W., D.W. Fahey, J.M. Gilligan, G.S. Sutton, T.J. Baring, C.M. Volk, R.E. Dunn, R.C. Myers, S.A. Montzka, P.R. Wamsley, A.H. Hayden, J.H. Butler, T.M. Thompson, T.H. Swanson, E.J. Dlugokencky, P.C. Novelli, D.F. Hurst, J.M. Lobert, S.J. Ciciora, R.J. McLaughlin, T.L. Thompson, R.H. Winkler, P.J. Fraser, L.P. Steele, and M.P. Lucarelli, Airborne gas chromatograph for *in situ* measurements of long-lived species in the upper troposphere and lower stratosphere, *Geophys. Res. Lett.*, in press, 1995.

Francisco, J.S., *Ab initio* characterization of HOClO₃ and HClO₄: implications for atmospheric chemistry, *J. Phys. Chem.*, *99*, 13422-13425, 1995.

Greenwood, N.N. and A. Earnshaw, Chemistry of the elements, *Pergamon Press*, 920-1039, 1985.

Hanson, D.R., A.R. Ravishankara, and S. Solomon, Heterogeneous reactions in sulfuric acid aerosols: a framework for model calculations, *J. Geophys. Res.*, *99*, 3615-3625, 1994.

Jaeglé, L., G.C. Toon, B. Sen, J.-F. Blavier, R.A. Stachnik, Y.L. Yung, and M. Allen, Partitioning of inorganic chlorine in the stratosphere: simultaneous balloon profiles of HCl, ClONO₂, HOCl and ClO, in preparation for *Geophys. Res. Lett.*, 1996.

Karapet'yants, M. Kh. and M.L. Karapet'yants, Thermodynamic constants of inorganic and organic compounds, Ann Arbor - Humphrey Science publishers, 1970.

Karelin, A.I., Z.I. Grigorovich, and V. Ya. Rosolovskii, Vibrational spectra of perchloric acid-I. Gaseous and liquid HClO₄ and DClO₄, *Spectrochim. Acta*, 31a, 765-775, 1975.

Kenner, R.D., I.C. Plumb, and K.R. Ryan, Laboratory measurements of the loss of ClO on Pyrex, ice and NAT at 183 K, *Geophys. Res. Lett.*, 20, 193-196, 1993.

Kindler, T.P., W.L. Chameides, P.H. Wine, D.M. Cunnold, F.N. Alyea, and J.A. Franklin, The fate of atmospheric phosgene and the stratospheric chlorine loadings of its parent compounds: CCl₄, C₂Cl₄, C₂HCl₃, CH₃CCl₃, and CHCl₃, *J. Geophys. Res.*, 100, 1235-1251, 1995.

Martin, L.R., H.S. Judeikis, and M. Wun, Heterogeneous reactions of Cl and ClO in the stratosphere, *J. Geophys. Res.*, 85, 5511-5518, 1980.

Martin, L.R., A.G. Wren, and M. Wun, Chlorine atom and ClO wall reaction products, *Int. J. Chem. Kinet.*, 11, 543-557, 1979.

Prasad, S.S. and T.J. Lee, Atmospheric chemistry of the reaction ClO + O₂ ⇌ ClO·O₂: where it stands, what needs to be done, and why?, *J. Geophys. Res.*, 99, 8225-8230, 1994.

Rosenlof, K.H., Seasonal cycle of the residual mean meridional circulation in the stratosphere, *J. Geophys. Res.*, 100, 5173-5191, 1995.

Sander, S.P. and R.R. Friedl, Experimental and theoretical studies of atmospheric inorganic chlorine chemistry, *Advances in Physical Chemistry*, in press, 1995.

Sander, S.P., R.R. Friedl, and Y.L. Yung, Rate of formation of the ClO dimer in polar stratospheric chemistry: implications for ozone loss, *Science*, 245, 1095-1098, 1989.

Sen, B., G.C. Toon, J.-F. Blavier, and C.H. Jackman, Balloon-borne observations of mid-latitude fluorine abundance, *J. Geophys. Res.*, in press, 1996.

Simonaitis, R. and J. Heicklen, Perchloric acid: a possible sink for stratospheric chlorine, *Planet. Space Sci.*, 23, 1567-1569, 1975.

Solomon, S., G.H. Mount, R.W. Sanders, and A.L. Schmeltekopf, Visible and near-ultraviolet spectroscopy at McMurdo Station, Antarctica 2. Observations of OCIO, *J. Geophys. Res.*, 92, 8329, 1987.

Stachnik, R.A., J.C. Hardy, J.A. Tarsala, J.W. Waters, and N.R. Erickson, Submillimeterwave heterodyne measurements of stratospheric ClO, HCl, O₃, HO₂: first results, *Geophys. Res. Lett.*, 19, 1931-1934, 1992.

Tie, X.X., G.P. Brasseur, B. Briegleb, and C. Granier, Two-dimensional simulation of Pinatubo aerosols and its effect on stratospheric ozone, *J. Geophys. Res.*, 99, 20,545-20,562, 1994.

Toon, G.C., B. Sen, and J.-F. Blavier, Balloon-borne measurements of stratospheric composition by FTIR solar absorption spectrometry, manuscript in preparation for *J. Geophys. Res.*, 1996a.

Toon, G.C., B. Sen, and J.-F. Blavier, Inorganic chlorine measured by balloon-borne solar absorption spectrometry, manuscript in preparation for *Geophys. Res. Lett.*, 1996b.

Toon, G.C., B. Sen, and J.-F. Blavier, Sources of stratospheric chlorine measured by balloon-borne solar absorption spectrometry, manuscript in preparation for *Geophys. Res. Lett.*, 1996c.

Webster, C.R., et al., Interhemispheric asymmetry in the stratospheric HCl concentrations, manuscript in preparation for *J. Geophys. Res.*, 1996.

Webster, C.R., R.D. May, L. Jaeglé, S.P. Sander, M.R. Gunson, G.C. Toon, J.M. Russell III, R. Stimpfle, J. Koplow, R.J. Salawitch, and H.A. Michelsen, Hydrochloric acid and the chlorine budget of the lower stratosphere, *Geophys. Res. Lett.*, 21, 2575-2578, 1994.

Webster, C.R., R.D. May, D.W. Toohey, L.M. Avallone, J.G. Anderson, P. Newman, L. Lait, M.R. Schoeberl, J.W. Elkins, and K.R. Chan, Chlorine chemistry on polar stratospheric cloud particles in the Arctic winter, *Science*, 261, 1130-1134, 1993.

Wilson, S.R., P.J. Crutzen, G. Schuster, D.W.T. Griffith, and G. Helias, Phosgene measurements in the upper troposphere and lower stratosphere, *Nature*, 334, 689-691, 1988.

Woodbridge, E.L., J.W. Elkins, D.W. Fahey, L.E. Heidt, S. Solomon, T.J. Baring, T.M. Gilpin, W.H. Pollock, S.M. Schauffler, E.L. Atlas, M. Loewenstein, J.R. Podolske, C.R. Webster, R.D. May, J.M. Gilligan, S.A. Montzka, K.A. Boering, and R.J. Salawitch, Estimates of total organic and inorganic chlorine in the lower stratosphere from *in situ* measurements during AASE II, *J. Geophys. Res.*, 100, 3057-3064, 1995.

World Meteorological Organization, *Scientific Assessment of Ozone Depletion: 1994*, Global Ozone Research and Monitoring Project - Report No. 37, World Meteorological Organization, Geneva, 1995.

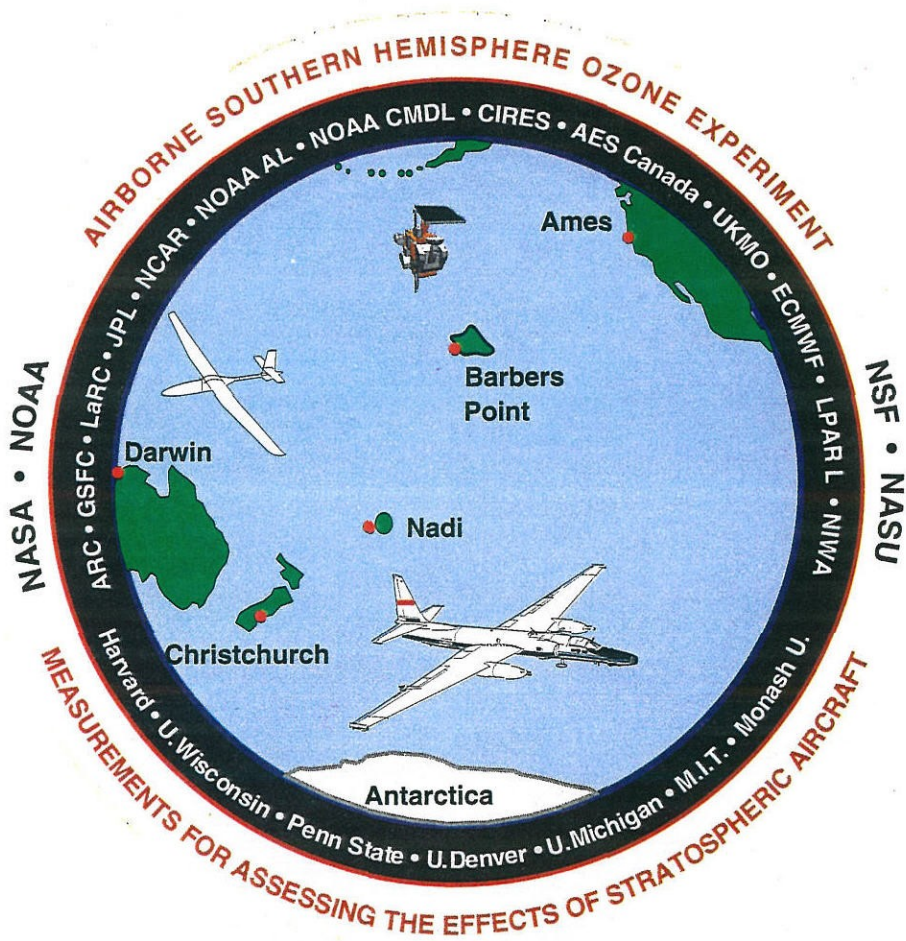
World Meteorological Organization, *Scientific Assessment of Ozone Depletion: 1991* Global Ozone Research and Monitoring Project - Report No. 25, World Meteorological Organization, Geneva, 1992.

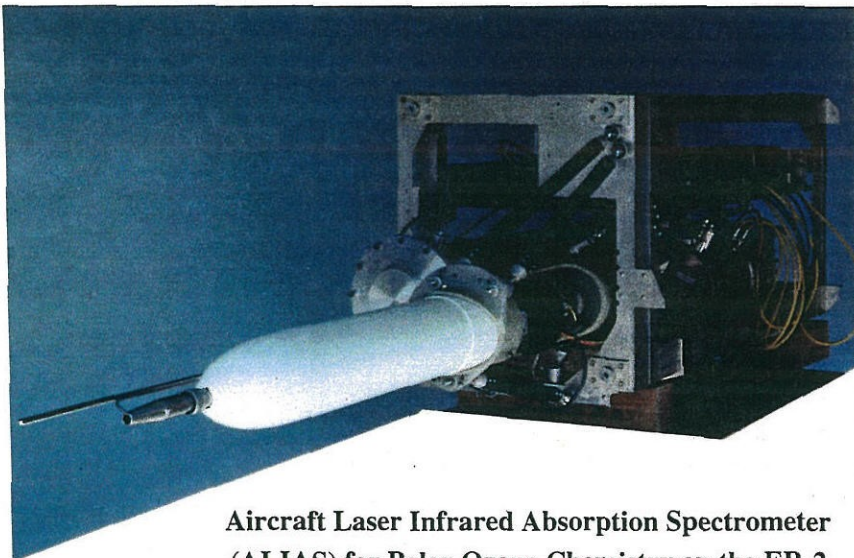
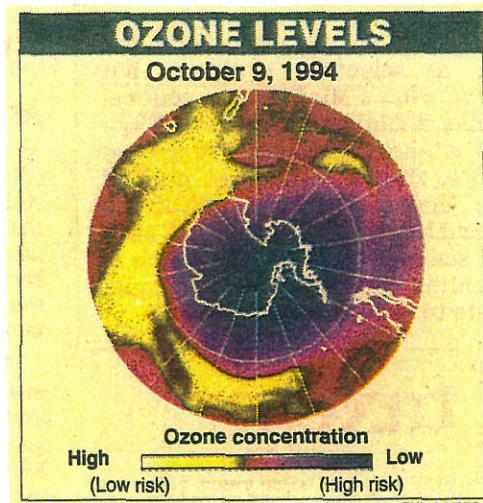
Zander, R., E. Mahieu, M.R. Gunson, C. Aellig, M.C. Abrams, A.Y. Chang, F.W. Irion, A. Goldman, H. Michelsen, M. Newchurch, C.P. Rinsland, R.J. Salawitch and G.P. Stiller, The 1994 northern mid latitude budget of stratospheric chlorine derived from ATMOS/ATLAS 3 observations, submitted to *Geophys. Res. Lett.*, 1995.

Zander, R., M.R. Gunson, C.B. Farmer, C.P. Rinsland, F.W. Irion, and E. Mahieu, The 1985 chlorine and fluorine inventories in the stratosphere based on ATMOS observations at 30° North latitude, *J. Atmos. Chem.*, 15, 171-186, 1992.

CHAPTER 6

Evolution and Stoichiometry of Heterogeneous Processing in the Antarctic Stratosphere





Aircraft Laser Infrared Absorption Spectrometer (ALIAS) for Polar Ozone Chemistry on the ER-2

**Evolution and Stoichiometry of Heterogeneous Processing
in the Antarctic Stratosphere**

L. Jaeglé¹, C. R. Webster², R. D. May², D. C. Scott²,
R. M. Stimpfle³, D. Kohn³, P. O. Wennberg³,
D. W. Fahey⁴, M. H. Proffitt⁴, K. K. Kelly⁴,
J. Elkins⁵, D. Baumgardner⁶, J. E. Dye⁶, J. C. Wilson⁷,
R. F. Pueschel⁸, K. R. Chan⁸,
R. J. Salawitch², A. F. Tuck⁴, S. J. Hovde⁴, Y. L. Yung⁹

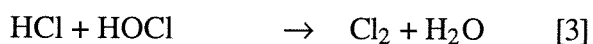
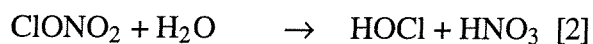
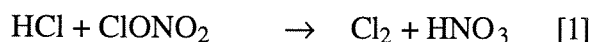
1. Environmental Engineering Science Division,
California Institute of Technology, Pasadena, CA 91125
2. Atmospheric Chemistry Division, Jet Propulsion Laboratory,
California Institute of Technology, Pasadena, CA 91109
3. Department of Chemistry, Harvard University, Cambridge, MA 02138
4. Aeronomy Laboratory, NOAA, Boulder, CO 80303
5. Climate Monitoring and Diagnostic Laboratory,
NOAA, Boulder, CO 80303
6. National Center for Atmospheric Research,
Boulder, CO 80307
7. Department of Engineering, University of Denver,
Denver, CO 80208
8. NASA Ames Research Center, Moffett Field, CA 94035
9. Division of Geological and Planetary Sciences,
California Institute of Technology, Pasadena, CA 91125

Abstract. Simultaneous *in situ* measurements of HCl and ClO have been made for the first time in the southern hemisphere, allowing a systematic study of the processes governing chlorine activation between 15 and 20 km in the 1994 Antarctic winter. Data for several other gases (N₂O, CH₄, CO, H₂O, O₃, NO, NO_y, OH, HO₂, CFCs), particulates and meteorological parameters were collected from the ER-2 aircraft out of New Zealand as part of the 1994 Airborne Southern Hemisphere Ozone Experiment/Measurements of Atmospheric Effects of Stratospheric Aircraft (ASHOE/MAESA) campaign. Observations from the ER-2 in the fall (April-May), prior to polar night, show that chlorine activation begins with 60-75% of inorganic chlorine as HCl. By mid-winter (July-August), near total removal of HCl is observed. The wintertime loss of HCl in air recently exposed to extreme temperatures is found to be correlated with high levels of reactive chlorine (ClO and its dimer, Cl₂O₂) in the linear fashion expected from the stoichiometry of the heterogeneous reaction of hydrochloric acid with chlorine nitrate on polar stratospheric clouds (PSCs): $\text{HCl} + \text{ClONO}_2 \rightarrow \text{Cl}_2 + \text{HNO}_3$. To constrain the role of different heterogeneous reactions and PSC type, we have used a photochemical trajectory model which includes heterogeneous sulfate and PSC chemistry. Model calculations of the evolution of reactive gases are compared with the *in situ* observations. In addition, simultaneous measurements of OH and HO₂ are used as a diagnostic for the occurrence of the heterogeneous reaction $\text{HOCl} + \text{HCl} \rightarrow \text{Cl}_2 + \text{H}_2\text{O}$, which would contribute to suppressed levels of HO_x inside the vortex. It is shown that the amount of chlorine activation is not strongly dependent of the composition of PSCs. However, HO_x levels exhibit different signatures depending on the type of heterogeneous surfaces that affected chlorine activation. Furthermore, this analysis implies that in the edge region of the Antarctic vortex, the observed near total removal of HCl can result from latitudinal excursions of air parcels in and out of sunlight during the winter, which photochemically resupply HOCl and ClONO₂ as oxidation partners for HCl. Such excursions generate very rapid ozone depletion which can be slowed down when mixing between processed and non-processed air occurs.

1. Introduction

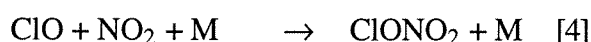
Stratospheric inorganic chlorine ($Cl_y = HCl + ClONO_2 + HOCl + ClO + 2 Cl_2O_2 + OClO + 2 Cl_2 + Cl$) is produced primarily from the emission of man-made chlorofluorocarbons (CFCs) and hydrofluorocarbons (HCFCs) at the surface of the earth followed by transport to the stratosphere where their photochemical breakdown releases chlorine atoms (WMO, 1995). At mid- and low-latitudes inorganic chlorine mainly comprises the stable inactive reservoir forms HCl and $ClONO_2$. During the Antarctic winter, abrupt and sustained shifts in the partitioning of chlorine from HCl and $ClONO_2$ to photochemically reactive chlorine forms (or $Cl_x = ClO + Cl + 2 Cl_2O_2 + 2 Cl_2 + OClO$) are believed to occur as a result of heterogeneous conversion on the surfaces of polar stratospheric cloud particles (Crutzen and Arnold, 1986; McElroy et al., 1986; Solomon et al., 1986). The high levels of reactive chlorine throughout the polar winter initiate massive ozone loss in the Antarctic polar spring (Farman et al., 1985; Hofmann et al., 1994). Many observational studies (Tuck et al., 1989; Anderson et al., 1991; Toohey et al., 1993; Webster et al. 1993; Waters et al., 1993; Pyle et al., 1994), as well as gas-phase and heterogeneous laboratory studies (Molina and Molina, 1987; Tolbert et al., 1987; Leu, 1988) have helped elucidate the mechanisms for heterogeneous processing and for the gas phase catalytic cycles ultimately responsible for the springtime ozone loss. The integration of this accumulated set of data has allowed modeling studies of these processes (Crutzen et al., 1992; Salawitch et al., 1993; Lefèvre et al., 1994; Chipperfield, 1995).

In our current understanding of the polar stratosphere, three principal heterogeneous reactions are believed to convert inorganic chlorine reservoirs to Cl_x (Solomon, 1990):

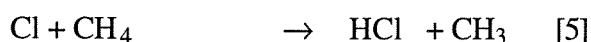


The surfaces on which these reactions take place are provided by the particles making up polar stratospheric clouds (PSCs) (McCormick et al., 1982), which are ternary $\text{HNO}_3/\text{H}_2\text{SO}_4/\text{H}_2\text{O}$ systems of different compositions and phases (Carslaw et al. 1993; Tabazadeh et al., 1994), and form at the cold temperatures typical of the winter polar vortex. The gaseous products of [1]-[3], Cl_2 and HOCl (which are seen to desorb from the PSC surfaces in laboratory observations), are rapidly converted to ClO and Cl_2O_2 , the two dominant forms of Cl_x in the polar stratosphere (Anderson et al., 1991). While the occurrence of reaction [1] is supported by the stoichiometry of HCl loss and ClO production from *in situ* observations in the Arctic (Webster et al., 1993), no direct evidence for the occurrence of reactions [2] or [3] has yet been found in the stratosphere.

In addition to providing sites for heterogeneous chemical reactions, PSCs can sequester a significant fraction of stratospheric HNO_3 in condensed forms (Toon et al., 1986). Growth and subsequent sedimentation of these particles leads to denitrification, further enhancing ozone loss (Fahey et al., 1990). Indeed, while chlorine radicals control the rate at which ozone is being destroyed, the duration of the destruction of O_3 is limited by the resupply of reactive nitrogen which sequesters Cl_x in the form of ClONO_2 (Salawitch et al., 1988). Given photochemical decomposition of HNO_3 to NO_2 under sufficient levels of sunlight, conversion of ClO back to ClONO_2 can take place via:



HCl itself is reformed through the slower reaction:



Thus, understanding the factors controlling chlorine activation and deactivation is central to predicting ozone loss rates in the polar regions.

In this paper, we present simultaneous *in situ* measurements of HCl and ClO in the Antarctic lower stratosphere during the fall and winter of 1994, which were carried as part of the Airborne Southern Hemisphere Ozone Experiment/Measurements of Atmospheric Effects of Stratospheric Aircraft (ASHOE/MAESA) campaign.

Observations of HCl and ClO, in combination with the other reactive gases measured, NO, OH, HO₂, and complemented by aerosol measurements, as well as precursors and tracers observations, constitute a powerful set of indicators on the impact of chlorine chemistry in the perturbed environment of the polar vortex. The capability of simultaneous measurements of HCl and ClO for the first time in the Antarctic may provide additional insight into the heterogeneous processes taking place in a vortex generally colder and more extensive than that of the Arctic: while ClO by itself reflects the amount of recent processing that has taken place, HCl, on the other hand, keeps a much longer “memory” of the heterogeneous conversion because of its very slow recovery, and provides a useful measure of the accumulated effect of chlorine activation.

To interpret the chemical and dynamical factors affecting the chemical composition of the stratosphere during the Antarctic winter, this study uses a photochemical box model along trajectories. Because it takes into account the temperature history of an air parcel, this approach has already proved useful in studying stratospheric chemistry under polar conditions (Austin et al., 1989; Jones et al., 1989; Schoeberl et al., 1993; Lutman et al., 1994a, 1994b). In particular, trajectory models compared well with satellite and *in situ* observations of high ClO levels (Jones et al., 1989; Lutman et al., 1993a) and quantitatively predicted the relaxation of these enhanced ClO concentrations following encounters with PSCs (Schoeberl et al., 1993; Lutman et al., 1994b).

We begin in section 2 by briefly describing the data collected by instruments aboard the ER-2 during ASHOE/MAESA. Sections 3 and 4 will present observations of the conversion of chlorine reservoirs to reactive chlorine, and how these can be analyzed to gain quantitative information on the stoichiometry of the processes responsible for chlorine activation. We describe the Lagrangian photochemical model in section 5. In section 6, model simulation results are presented and compared with observations. Implications on the evolution of reactive gases throughout the polar winter along with

their impact on ozone loss will be discussed in section 7. We conclude by presenting in section 8 a summary of the results obtained in this investigation.

2. Observations and instruments

The Aircraft Laser Infrared Absorption Spectrometer (ALIAS) instrument is a

Table 1 - Instruments on board the ER-2.

Observed quantities	Techniques	Accuracy (%)	Reference
HCl, N ₂ O, CH ₄ , CO	Tunable diode-laser absorption	10, 5, 5, 10	Webster et al., 1994
ClO	Resonance fluorescence	15	Brune et al., 1989
NO, NO _v	NO/O ₃ chemiluminescence	20, 20	Fahey et al., 1989
OH, HO ₂	Laser-induced fluorescence	20, 20	Wennberg et al., 1994
CFCs	Gas chromatograph	2	Elkins et al., 1995
O ₃	Differential UV absorption	5	Proffitt et al., 1989
H ₂ O	Lyman- α hygrometer	10	Kelly et al., 1989
Aerosols size and concentration (0.06-0.2 μ m diameter)	Focused cavity spectrometer	100	Jonsson et al., 1995
Aerosols size and concentration (0.2 - 20 μ m diameter)	Multi-angle spectrometer	100	Baumgardner et al., 1992
Aerosols size, concentration, and composition	Impactor	100	Pueschel et al., 1989

scanning tunable diode laser spectrometer (Webster et al., 1994) which measures HCl (Webster et al., 1995a), CO (Herman et al., 1995) N₂O and CH₄ using high resolution laser absorption at wavelengths from 3 to 8 μ m in an 80-meter multipass cell. The measurement uncertainty depends on signal size as well as on uncertainties in spectral parameters. The total uncertainty (1σ) for 30 second averages of HCl is typically 10% at 1 ppbv, and 30% for the mixing ratios below 0.3 ppbv. The minimum detectable HCl

amount is about 0.1 ppbv, although in some flights this can be as low as 0.05 ppbv. Table 1 briefly summarizes information on the other instruments on board the ER-2. In addition, temperature and pressure are measured by the Meteorological Measurement System instrument (Scott et al., 1990) with accuracies of ± 0.3 mbar and ± 0.3 K.

The series of flights discussed here were part of the ASHOE/MAESA mission, between the months of April and October of 1994. In southern flights out of Christchurch, New Zealand (44°S , 172°E), the ER-2 aircraft typically sampled air from 15 km (~ 120 mbar), to 20 km (~ 55 mbar). The length of ER-2 aircraft flights is limited to 8 hours, and therefore from Christchurch the ER-2 predominantly sampled the edge region of the Antarctic vortex (southern flights generally penetrated $\sim 1\text{-}3^{\circ}$ of latitude inside the vortex up to $\sim 67^{\circ}\text{S}$).

3. Chlorine activation and recovery

In this section we first describe observations of the chlorine partitioning prior to polar night (April-May), deriving empirical relations for reference levels that will allow us to assess the amount of change in HCl and ClONO₂ when heterogeneous processing takes place during the winter. We then present HCl and ClO measurements during the flight of August 6, 1994, where processed air was encountered. Finally, we summarize the evolution the HCl and ClO observations spanning the four ASHOE/MAESA phases, from April to October 1994.

3.1 Initial partitioning

At mid-latitudes away from polar processing, most of inorganic chlorine (Cl_y) is in the form of its reservoirs, HCl and ClONO₂, with small contributions from ClO and HOCl. The concentration of HOCl can be calculated from its steady-state relationship with observed concentrations of ClO, OH and HO₂:

$$[\text{HOCl}^*] = k_{\text{ClO}+\text{HO}_2} [\text{ClO}] [\text{HO}_2] / (k_{\text{HOCl}+\text{OH}} [\text{OH}] + J_{\text{HOCl}}) \quad [6]$$

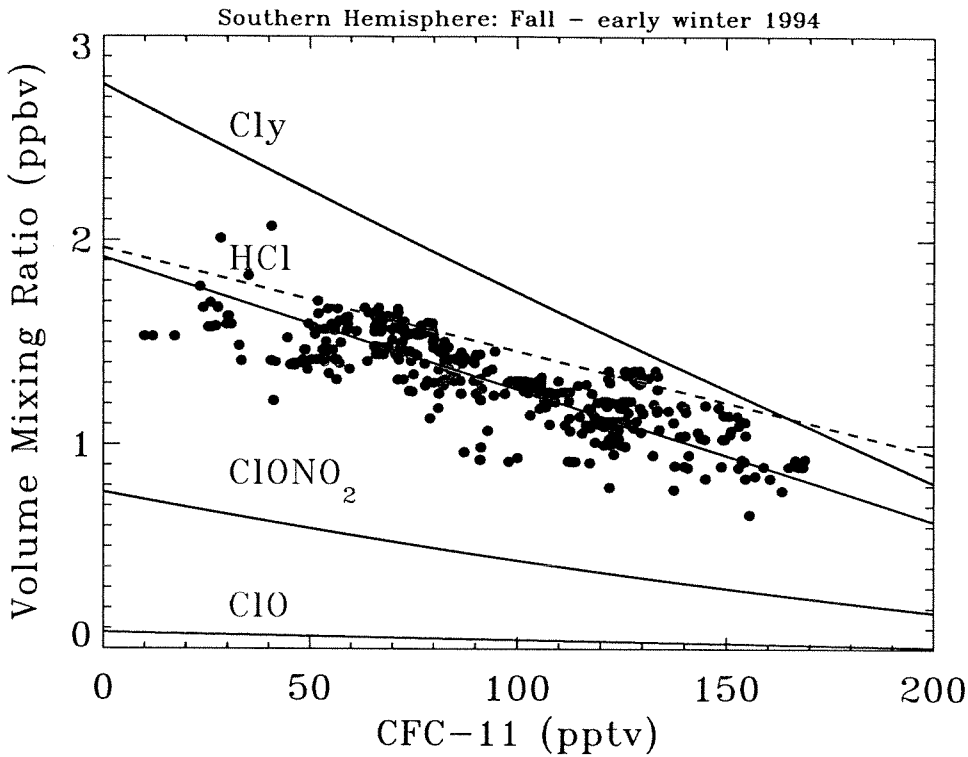


Figure 1: *Unperturbed Antarctic Atmosphere: Partitioning of chlorine species observed in the fall and early winter of 1994, represented as a function of CFC-11. Five flights were used for the HCl data (circles): April 13, May 23, May 24, June 1 and June 3, 1994 (latitude between 40°S and 67°S). The relationship obtained (solid line) is: $HCl^*(CFC-11) = 1.175 + 4.23e-7 \times CFC-11$, with HCl in ppbv, and CFC-11 in pptv. When no CFC-11 measurements were available, an empirical relation between N_2O and CFC-11 is used instead. Cl_y is based on interpolated measurements of organic halogens. A fit to ClO observations is also shown, as well as the inferred chlorine nitrate: $ClONO_2^* = Cl_y - HCl - ClO - HOCl^*$. The relationship obtained is: $ClONO_2^*(CFC-11) = 0.764 - 0.0037 \times CFC-11 + 4.e-6 \times (CFC-11)^2$. The data were selected for pressures above 80 mbar, and $ClO < 50$ pptv. The dashed line corresponds to the $HCl(CFC-11)$ relationship for the Northbound flight of May 28, 1994.*

We will assume ER-2 observations in the fall to be representative of the unperturbed atmosphere. In order to identify chemical changes in either the chlorine reservoirs (HCl and ClONO₂) or the radical (ClO) in an air parcel, we need to establish the expected amounts of these species relative to a dynamical tracer such as N₂O or CFC-11 (Fig. 1). The total inorganic chlorine, Cl_y, expected in an air parcel is based on organic chlorine measurements aboard the ER-2, and is calculated for each CFC-11 value (or N₂O, when no CFC-11 observations are available) according to an empirical relationship (Elkins et al., 1995). Flights north of Christchurch (45-20°S) have slightly higher values of HCl (dashed line in Fig. 1), because of stronger ClONO₂ photolysis at these latitudes. In the late fall of 1994, the measured HCl represents 60-75% of Cl_y at 20 km.

The remaining 40-25% of inorganic chlorine is present as ClONO₂, ClO, and HOCl. ClO is observed at levels typically less than 5% of Cl_y. Using equation [6], we calculated HOCl* to be less than 1% of the budget for this altitude range. Because we do not have measurements of chlorine nitrate, we infer it from:

$$[\text{ClONO}_2^*] = [\text{Cl}_y] - [\text{HCl}] - [\text{ClO}] - [\text{HOCl}^*] \quad [7]$$

for which we then derive a relation as a function of CFC-11 (see figure caption for Fig. 1). (Throughout this paper, we will denote chemical species which are inferred from other *in situ* observations by the symbol *). For these southern hemisphere flights, the ClONO₂ calculated from its steady-state relation with ClO and NO₂ is very close to ClONO₂* (Webster et al., 1995a).

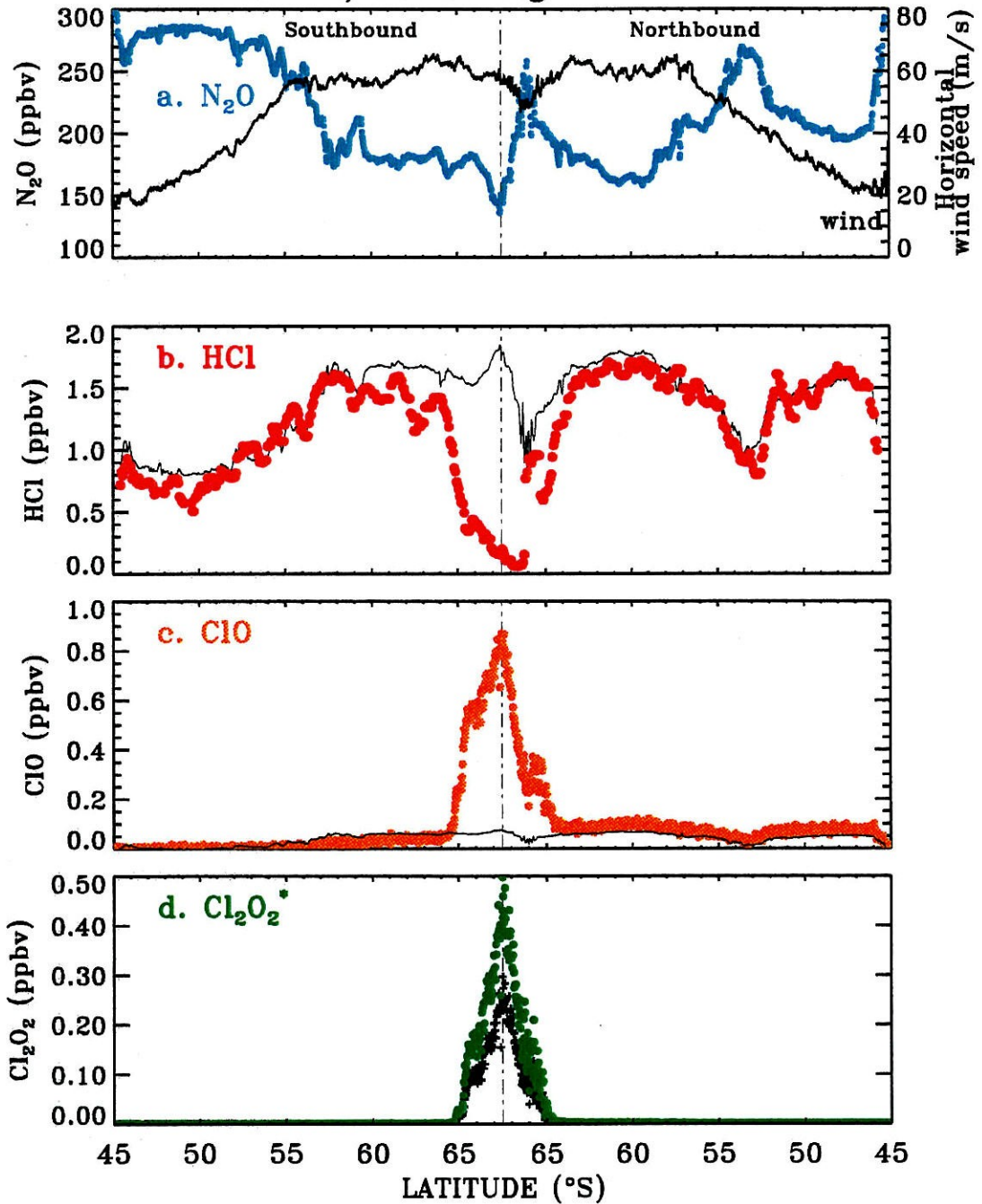
3.2 PSC processing in winter

By late Fall, the vortex is well established (Manney and Zurek, 1993; Schoeberl and Hartmann, 1991) and temperatures reach very low levels. During the flight of August 6, 1994, the ER-2 reached a maximum latitude of 67.7°S before diving down to 15 km, climbing back to its cruise altitude of 19 km and returning to New Zealand. At most

latitudes, the observations of HCl closely follow the expected reference HCl (Fig. 2). Poleward of 64°S, HCl abruptly decreases to

Figure 2: Flight of August 6, 1994: mixing ratios of (a) N_2O , (b) HCl, (c) ClO, (d) $Cl_2O_2^*$, calculated with JCl_2O_2 from DeMore et al. (1994) (black plus) and JCl_2O_2 from Huder and DeMore (1995) (green dots), are plotted as a function of latitude. In panel (a) the solid line shows the horizontal wind speed. In panel (b) and (c), the black lines show the empirically predicted unprocessed levels of HCl and ClO respectively (see Fig. 1). The high values of N_2O on the first part of the southbound leg indicate the tropical origin of the air sampled there (Tuck et al., 1995a) therefore, for this part of the flight we have used the empirical HCl(CFC-11) relation typical of low latitudes (dashed line in Fig. 1).

ASHOE/MAESA flight : 940806



very low values, while ClO increases to reach a maximum of about 0.8 ppbv. Comparing the HCl observations to the predicted reference levels clearly shows that this decrease (by 90%) cannot be due to dynamical descent in the vortex, which would have been reflected in the long-lived tracer N₂O. We therefore identify the observed loss of HCl and associated high values of ClO with recent chemical conversion.

At low temperatures and high ClO levels, a significant fraction of active chlorine can be present as Cl₂O₂, the ClO dimer (Molina and Molina 1987; Sander et al., 1989). Assuming that Cl₂O₂ is in photochemical steady-state equilibrium with the observed ClO, we can calculate it from the expression:

$$[\text{Cl}_2\text{O}_2^*] = (k_{\text{ClO}+\text{ClO}} [\text{ClO}]^2) / (k_{\text{Cl}_2\text{O}_2+\text{M}} [\text{M}] + J_{\text{Cl}_2\text{O}_2}) \quad [8]$$

Where M is a third body, N₂ or O₂, and [M] thus represents the atmospheric density. The reaction rate constants for the ClO self reaction ($k_{\text{ClO}+\text{ClO}}$) and the dimer thermal decomposition ($k_{\text{Cl}_2\text{O}_2+\text{M}}$) are taken from DeMore et al. (1994). The dimer absorption cross-sections are taken from the recent laboratory measurements by Huder and DeMore (1995). The corresponding photolysis rate ($J_{\text{Cl}_2\text{O}_2}$) is calculated taking into account the albedo and overhead ozone variations along the ER-2 flight track (Salawitch et al., 1994). At high solar zenith angles (> 80°), the steady-state assumption no longer holds, and we have corrected Cl₂O₂* by the expected departure we derived from comparison with a time-dependent model (Kawa et al., 1992). A similar approach was used to correct the steady-state HOCl*. On the flight of August 6, 1994, Cl₂O₂ constitutes up to 0.5 ppbv, or 65% of the active chlorine (ClO + 2 Cl₂O₂* = 1.9 ppbv) at the peak ClO value.

Huder et al.'s new determination of the dimer cross-sections yield a photolysis rate 40% lower than values calculated using currently recommended cross-sections (DeMore et al., 1994). Previous measurements seem to overestimate the cross section of Cl₂O₂ due to improperly accounted for contamination by Cl₂O. This has a large impact on our predicted steady-state abundances of Cl₂O₂. As illustrated in Fig. 2d, Cl₂O₂* would be

40% lower if we used the cross-sections in DeMore et al. Throughout this paper, we have adopted the recent absorption cross sections reported by Huder and DeMore (1995).

3.3 Evolution of HCl and ClO through the vortex lifetime

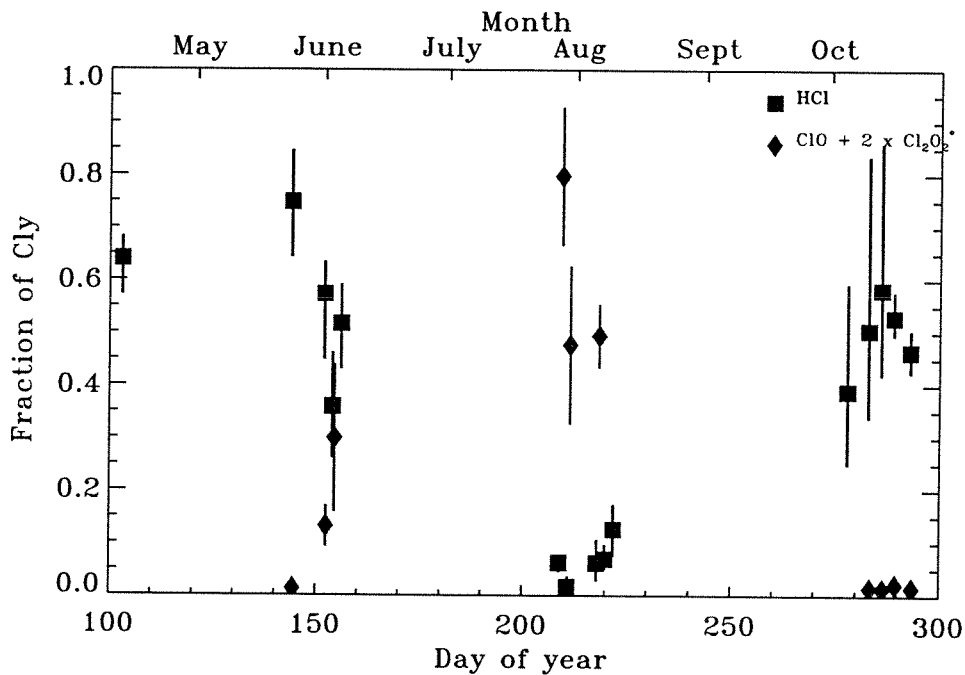


Figure 3: Time evolution of chlorine species inside the vortex between April and October 1994. The medians of observations are represented by the symbols (squares = HCl/Cl_y; diamonds = (ClO + 2 Cl₂O₂*)/Cl_y) with their minimum and maximum, as the vertical bars. The points are selected for latitudes poleward of the maximum horizontal wind speed (~ south of 64°S).

From measurements of HCl and ClO between April and October 1994, a picture of the evolution of inorganic chlorine partitioning at the inner edge of the vortex is built up before, during and after the period when temperatures are cold enough for PSC formation

(Fig. 3). We have selected observations obtained over 2-3° latitude inside the vortex, the edge of which we define by the polar jet wind maximum as measured aboard the ER-2 (Table 1 in Tuck et al., 1995a). The release of active chlorine, $\text{ClO} + 2 \text{Cl}_2\text{O}_2 (= \text{Cl}_x)$, mirrors the evolution of cold temperatures in the vortex, which promote growth of PSCs during the period between June and late August, and whose surfaces provide sites for heterogeneous reactions [1]-[3]. The levels of HCl were first seen to decrease in early June of 1994. By early August, HCl was extensively processed and high levels of active chlorine were present inside the vortex. By October, photochemical recovery of HCl, through reaction [5], is nearly complete. On two occasions, October 10 and 13, the ER-2 sampled air where recovery of HCl to extremely high levels ($\text{HCl}/\text{Cl}_y \sim 1$) had taken place in a low ozone environment (Webster et al., 1995b; Wamsley et al., 1995).

4. Stoichiometry of chlorine processing

In the previous section we saw how the balance between reactive and reservoirs chlorine gases is dramatically altered in the Antarctic vortex from late fall to late winter. Now we attempt to characterize the behavior of the processing events in terms of the stoichiometry of heterogeneous reactions taking place. Due to the limited range of the ER-2, flights during ASHOE/MAESA were confined mostly to the edge region of the Antarctic vortex, where temperatures are not as consistently cold as in the deepest part of the vortex, and where no major denitrification or dehydration events were observed at the 20 km level during the winter months of this campaign (Fahey et al., 1995). Thus, in many ways this region of the Antarctic vortex is similar to the Arctic vortex. In the following, we will see how observations from both hemispheres can be analyzed in parallel to gain better insight into the mechanisms at work.

From observations obtained in the vortex prior to PSC processing, as shown in Fig. 1, we have a knowledge of the expected unperturbed levels of HCl and ClONO_2 . The difference between a measured mixing ratio for HCl and a reference value calculated

from the simultaneously measured CFC-11 (or N₂O) represents the chemical loss, defined as follows:

$$\Delta\text{HCl} = \text{HCl}^* (\text{CFC-11}) - \text{HCl} \quad [9]$$

We can use the same approach for ClONO₂^{*}, as inferred from the inorganic chlorine budget residual:

$$\Delta\text{ClONO}_2^* = \text{ClONO}_2^* (\text{CFC-11}) - \text{ClONO}_2^* \quad [10]$$

By convention, and for simplicity, the sign in these expressions is such that for a net loss in HCl, ΔHCl is positive (the same applies for ClONO₂^{*}). Webster et al. (1993) demonstrated how the values of ΔHCl, ΔClONO₂^{*}, and ClO + 2 Cl₂O₂^{*} associated with each air parcel can give us information on the stoichiometry of PSC processing, since the net effect of heterogeneous reactions [1]-[3] is to increase ΔHCl, ΔClONO₂^{*}, and ClO + 2 Cl₂O₂^{*}. Because of the large temperature dependence of heterogeneous reactions [1] - [3], the degree of chlorine activation depends on a balance between exposure time to cold temperatures, as well as on the time spent in sunlight, which allows reformation of ClONO₂ (Schoeberl et al., 1993).

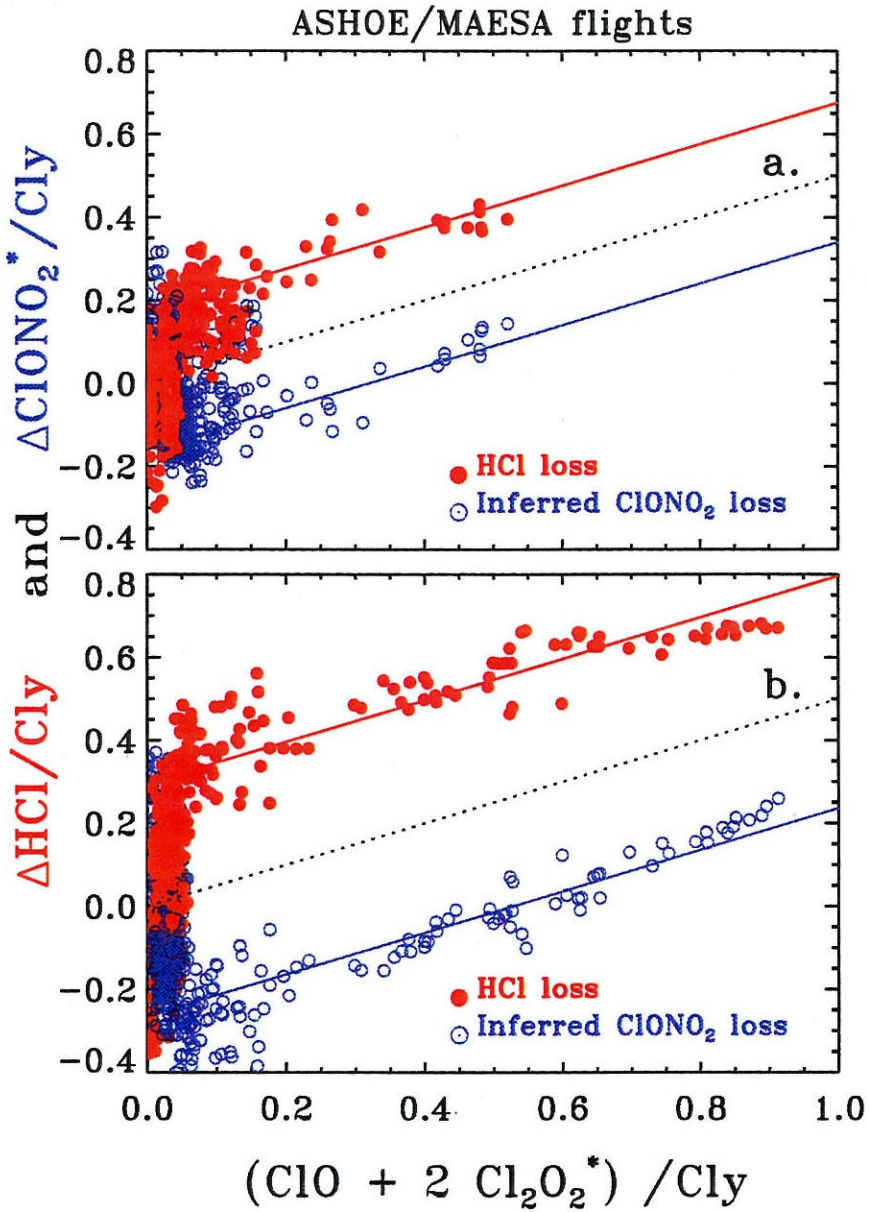
Compact relationships between losses in chlorine reservoirs and production of reactive chlorine gases are seen for ASHOE/MAESA flights during the Antarctic winter. As we will show, these relationships are consistent with the stoichiometry of recent heterogeneous processing. Figure 4 presents ΔHCl and ΔClONO₂^{*}, as a function of levels of ClO + 2 Cl₂O₂^{*}. All the mixing ratios have been normalized to Cl_y to account for variations in chlorine loading between air parcels (for a simple conversion to mixing ratios, the air parcels in the vortex generally contained 2-3 ppbv of inorganic chlorine). In early June 1994 (Fig. 4a), reactive chlorine accounted for 50% of Cl_y in the southern-most part of the flight, where HCl had been reduced by about 50%. Chlorine activation is more extensive at the end of July and in early August (Fig. 4b), where in some air masses, up to 90% of chlorine was in the form of reactive chlorine and little HCl was observed. In their analysis of the AASE-II observations, Webster et al. (1993) saw a

striking 1:2 slope for the correlation between ΔHCl and $\text{ClO} + 2 \text{Cl}_2\text{O}_2^*$ corresponding to the stoichiometry of reaction [1] as depicted in Fig. 5a for the flights of December 12, 1991, and January 20, 1992. One can notice that the observations of HCl and inferred ClONO_2 depart from the 1:2 slope for the highest values of active chlorine. This was not seen as clearly in Webster et al., and is evidenced here by the use of Cl_2O_2 cross-sections based on Huder and DeMore (1995), which results in enhanced Cl_2O_2^* , instead of Burkholder et al. (1990), as discussed in section 3.1. The interpretation of this departure from the 1:2 slope is discussed further below.

For ASHOE/MAESA flights, the slope of the correlation is also close to 1:2; however, there is a vertical offset. In other words, $\Delta\text{HCl} > 1/2 (\text{ClO} + 2 \text{Cl}_2\text{O}_2)$. This would imply that some of the reactive chlorine had been converted back to ClONO_2 prior to this processing event. Indeed, while ΔClONO_2 also increases with increasing Cl_x , ClONO_2 losses are mostly negative, i.e., there is a net gain of ClONO_2 compared to inferred values in the late fall.

The compactness of the slopes in Fig. 4 and 5 is indicative of the fact that the process of activation/deactivation is very similar for all the air parcels sampled, and that their temperature history followed fairly similar evolutions for each individual flight. This is what we would expect, as the ER-2 flight tracks during ASHOE/MAESA were usually designed to follow potential temperature surfaces. Under adiabatic conditions, air is transported along such surfaces of constant potential temperature. The different patterns in Fig. 4 and 5 suggest that the observations correspond to different stages of processing. We can interpret these data if we consider the following four cases reflecting separate temperature history regimes:

Figure 4: Loss of HCl (ΔHCl) and ClONO_2^* (ΔClONO_2^*) as a function of reactive chlorine, $\text{ClO} + 2 \text{Cl}_2\text{O}_2^*$. All these quantities have been normalized to the total inorganic chlorine, Cl_y . ASHOE/MAESA flights of (a) June 1 and 3, 1994, (b) July 28, and August 6, 1994. Observations corresponding to N_2O values greater than 260 ppbv, and pressures above 70 mbar have been excluded from these figures. The dashed line has a slope of 1:2. The two solid lines correspond to slopes of 1:2 going through the observations for $(\text{ClO} + 2 \text{Cl}_2\text{O}_2^*)/\text{Cl}_y > 0.2$. The intercepts at the origin are (a) -0.17 for ΔHCl , +0.16 for ΔClONO_2^* ; (b) -0.3 for ΔHCl , +0.26 for ΔClONO_2^* .



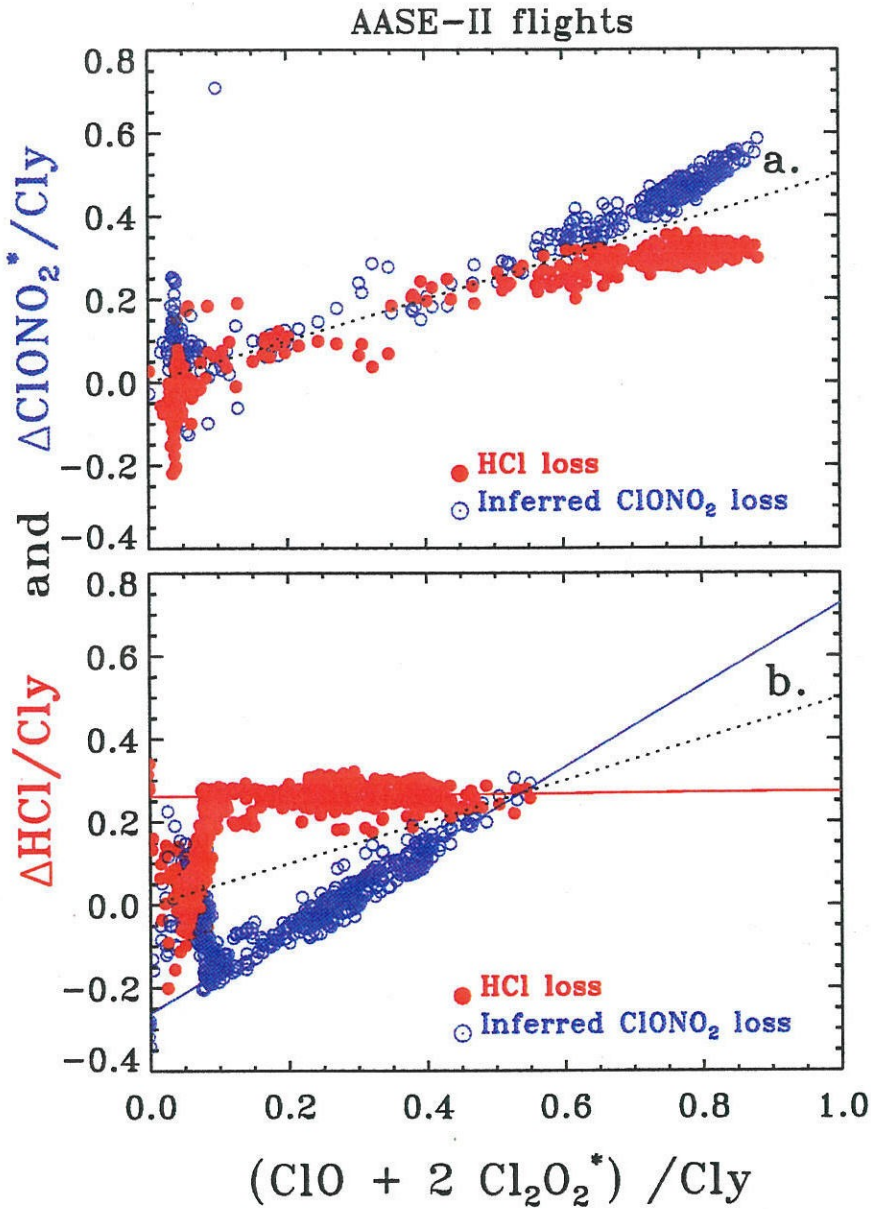


Figure 5: Same as for Fig. 4, but for AASE-II flights of (a) December 12, 1991 and January 20, 1992, (b) February 13 and 17, 1992 (a fit to the points yields a slope of 0.012 for ΔHCl , and 0.99 for ΔClONO_2^*).

1.) *On-going or recent processing*: $\Delta\text{HCl} = \Delta\text{ClONO}_2 = 1/2(\text{ClO} + 2 \text{Cl}_2\text{O}_2)$. Reaction [1] dominates the conversion process; and the combination of reactions [2] + [3] is equivalent to reaction [1], and therefore yields the same net stoichiometry, where one HCl is converted to one Cl_2 . The AASE-II flights of December 12, 1991, and January 20, 1992, fall in this category (Fig. 5a) (Webster et al., 1993).

2.) *Recovery of ClONO₂*: $\Delta\text{HCl} = a(\text{ClO} + 2 \text{Cl}_2\text{O}_2) + b$, $\Delta\text{ClONO}_2 = (\text{ClO} + 2 \text{Cl}_2\text{O}_2) + b$. Following 1.), if there is sufficient sunlight, NO_2 is produced from HNO_3 (photolysis or reaction with OH) and reacts with ClO via [4] to form chlorine nitrate. Thus, ΔClONO_2 decreases (gain of ClONO_2) linearly with reactive chlorine, with a slope of 1. This can be seen during the AASE-II flights of February 12 and 17, 1992. HCl recovers much more slowly, as indicated by the small slope of ΔHCl in Fig. 5b.

3.) *Multiple processing*: $\Delta\text{HCl} = 1/2(\text{ClO} + 2 \text{Cl}_2\text{O}_2) + c$, $\Delta\text{ClONO}_2 = 1/2(\text{ClO} + 2 \text{Cl}_2\text{O}_2) - c$. At the edge of the Antarctic vortex, temperature is cold enough for multiple processing events to take place, interrupted by excursions into sunlight that allow partial recovery of ClONO_2 . Events 1.) and 2.) can follow each other several times until all of HCl has been consumed. The ASHOE/MAESA flights in Fig. 4 show a 1:2 slope offset by 30% Cl_y , implying that the accumulated effect of 1.) and 2.) was to convert 30% of Cl_y back to ClONO_2 .

4.) *Low HCl levels*: $\Delta\text{HCl} = \text{constant}$, $\Delta\text{ClONO}_2 = (\text{ClO} + 2 \text{Cl}_2\text{O}_2) + d$. When most of HCl has been consumed, the rate for [1] becomes very slow. At cold enough temperatures, ClONO_2 can be directly converted to HOCl through [2] on sulfate aerosols or Type II PSCs (this reaction is ineffective on NAT - see Fig. 6). Such a case would be translated into a slope of 1:1 for ClONO_2 and of zero for HCl. This is illustrated in Fig. 4b, where ΔHCl is seen to depart from the 1:2 line for $\Delta\text{HCl} \sim 0.65$. It is more clearly apparent in Fig. 5a for values of $(\text{ClO} + 2 \text{Cl}_2\text{O}_2)/\text{Cl}_y$ larger than 0.6. Note that without temperature history consideration, we cannot distinguish between cases 4.) and 2.).

From these observations, it seems that even though processing begins with more HCl than ClONO₂, partial recovery of ClONO₂ allows near complete heterogeneous loss of HCl. Interestingly, this would suggest that the conversion to active chlorine is HCl limited in the edge region of the Antarctic vortex. The high amounts of ClONO₂, inferred here, form the so-called chlorine nitrate “collar”, first discovered in ground-based measurements (Farmer et al., 1987) and remote soundings from aircraft (Toon et al., 1989) in the springtime Antarctic, and subsequently measured in the Arctic (von Clarmann et al., 1993; Toon et al., 1994; Oelhaf et al., 1994). Observations aboard the Upper Atmospheric Research Satellite have revealed a global picture of this collar which surrounds the Antarctic vortex between 50 and 60°S and is present from July to September (Roche et al., 1993; 1994).

Representing the measurements in the manner depicted in Figures 4 and 5 provides a clear picture of the various stages of PSC processing. More precise questions on the exact influence of the recent temperature history and the individual roles of heterogeneous reactions can be answered using a photochemical model along trajectories which is described in the next section.

5. Photochemical model along trajectories

To gain insight in the mechanisms at work in the repartitioning of chlorine species during the polar winter, we use a Lagrangian photochemical model along trajectories adapted from the Caltech-JPL model (Nair et al., 1996). The model includes 50 species in the NO_y, Cl_y, Br_y, HO_x and O_x families. A full methane oxidation scheme is included. Close to 200 gas phase reactions, 50 photolytic reactions, and 6 heterogeneous reactions on various surfaces are used. Most reaction rates are based on the compilation by DeMore et al. (1994). Absorption cross-sections are also taken from DeMore et al., except for HOBr and Cl₂O₂, for which more recent laboratory measurements by Rattigan et al. (personal communication) and Huder and DeMore (1995) are used. The photolysis

rates are calculated using climatological ozone profiles scaled to Total Ozone Mapping Spectrometer (TOMS) overhead ozone corresponding to the end point of the trajectory.

The main heterogeneous reactions and their uptake probabilities, corresponding to

Table 2 - List of heterogeneous reactions probabilities.

Reaction	Surface type			
	H ₂ SO ₄	NAT	SAT	Ice
ClONO ₂ + HCl → Cl ₂ + HNO ₃	[b]	[d]	[d]	0.2 [a]
ClONO ₂ + H ₂ O → HOCl + HNO ₃	[b]	1e-3 [a]	[e]	0.1 [a]
HOCl + HCl → Cl ₂ + H ₂ O	[c]	[f]	= NAT	0.3 [a]
N ₂ O ₅ + H ₂ O → 2HNO ₃	0.1 [a]	0.0003 [a]		0.1 [a]
BrONO ₂ + H ₂ O → HOBr + HNO ₃	0.5 [g]	0.006 [h]	=NAT	0.3 [a]
N ₂ O ₅ + HCl → ClONO ₂ + HNO ₃		0.003 [a]		0.03 [a]

[a] DeMore et al., (1994); [b] Hanson et al., (1994b); [c] Hanson et al., (1994a); [d] Hanson et al. (1993); [e] Zhang et al., (1993); [f] Abbatt and Molina, (1992); [g] Hanson et al., (1995); [h] Lary et al., (1995)

different types of surfaces adopted in this work, are listed in Table 2.

Fig. 6 illustrates the temperature dependence of the three main heterogeneous reactions ([1]-[3]) for different surface types. Recently, the high reactivity of bromine compounds on heterogeneous surfaces has been observed in the laboratory (Hanson and Ravishankara, 1995; Abbatt, 1994).

Elucidating the exact phase and composition of the PSC particles is not in the scope of this work and is addressed elsewhere (Del Negro et al., 1995). Instead, we use simplified assumptions for each flight examined, based on the observed surface area and composition of the aerosols. Many uncertainties still remain on the early phase of the formation and growth mechanism of polar stratospheric clouds, which can be characterized as Type I or Type II PSCs. The possible composition of Type I PSCs

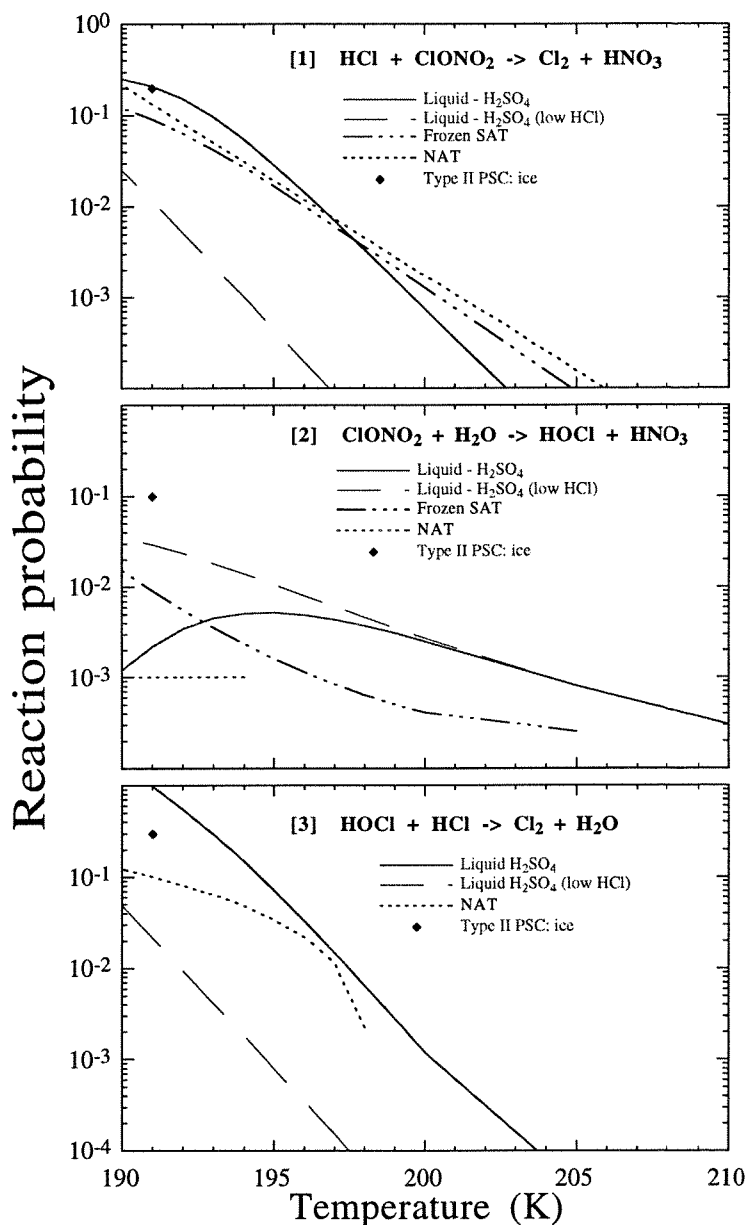


Figure 6: Heterogeneous reaction probabilities as a function of temperature on sulfuric acid, sulfuric acid tetrahydrate (SAT), nitric acid tetrahydrate (NAT), and ice for reactions [1] $\text{HCl} + \text{ClONO}_2 \rightarrow \text{Cl}_2 + \text{HNO}_3$; [2] $\text{ClONO}_2 + \text{H}_2\text{O} \rightarrow \text{HOCl} + \text{HNO}_3$; [3] $\text{HOCl} + \text{HCl} \rightarrow \text{Cl}_2 + \text{H}_2\text{O}$. The dependence on HCl levels is shown for reactivities on sulfuric acid (low HCl = 0.01 ppbv).

include: nitric acid trihydrate (NAT), nitric acid dihydrate (NAD), supercooled H_2O - HNO_3 , supercooled ternary solutions $\text{HNO}_3/\text{H}_2\text{SO}_4/\text{H}_2\text{O}$ (STS), and sulfuric acid tetrahydrate (SAT) (Hanson and Mauersberger, 1988; Wornop et al., 1993; Tabazadeh et al., 1994; Molina et al., 1993; Zhang et al., 1993). Type II PSCs are composed of water ice (Steele et al., 1983).

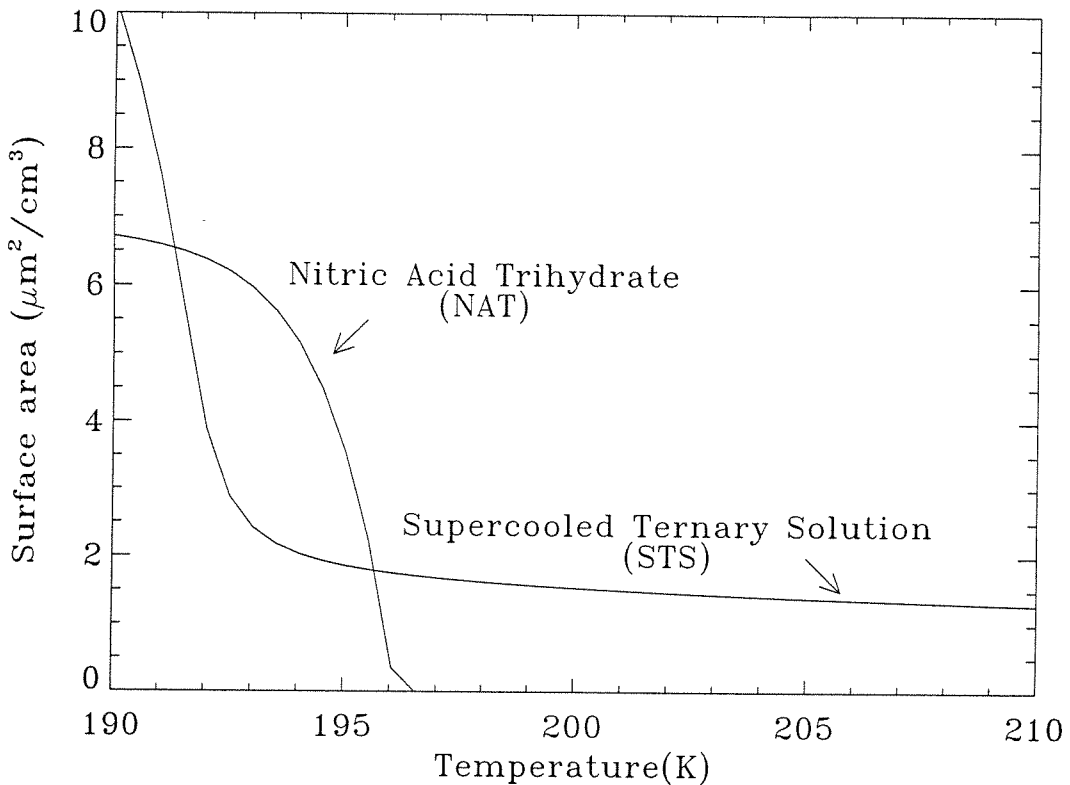


Figure 7: Model calculated aerosol surface area growth as a function of temperature. Nitric acid trihydrate (with assumed radius = $1 \mu\text{m}$), and supercooled ternary solution (formulation of Carslaw et al., 1995) surface areas as a function of temperature. Condition used: $p = 55 \text{ mbar}$, $\text{H}_2\text{O} = 5 \text{ ppmv}$, $\text{HNO}_3 = 10 \text{ ppbv}$, $\text{H}_2\text{SO}_4 = 0.5 \text{ ppbv}$.

In the model, the composition and volume growth of supercooled ternary solution is obtained according to the formulation of Carslaw et al. (1995), and we assume heterogeneous reactions to take place with the same reactivities as on sulfate aerosols.

The presence of NAT particles is predicted as a function of H₂O and HNO₃ local partial pressures, using the saturation vapor pressures given by Hanson and Mauersberger (1988). The corresponding surface area is calculated from the amount of condensed species using a specified radius of 1 μm . Condensed species are returned to the gas phase when the clouds evaporate. An example of calculated growths of STS and NAT aerosols as a function of temperature is shown in Fig. 7.

Unless otherwise specified, H₂O, CH₄, and O₃ are kept fixed at their measured values. If no measurements are available for a particular flight, these species are obtained from empirical tracers relationships inferred from other flights. Total nitrogen (NO_y), chlorine (Cl_y) and bromine (Br_y) are conserved during the calculation. Whenever possible, initial conditions are taken from observational data. Initialization of most other species is obtained from steady-state conditions at the latitude of the end point of the calculations.

To investigate the impact of the temperature and latitude history of the air parcels encountered by the ER-2, we couple the photochemical model with ten-day trajectories calculations. Daily analysis of wind and temperatures obtained from the European Centre for Medium-range Weather Forecasts (ECMWF) were used to calculate three dimensional backtrajectories (Tuck et al., 1995a). Latitude, longitude, pressure and temperature once derived are used as input to the photochemical model which is run forward along the trajectory, with a time-step varying between 30 minutes and 1 minute.

6. Model results along trajectories

Because it simulates the interaction between meteorology and photochemistry, Lagrangian photochemical modeling provides a useful tool to understand how large shifts in the chlorine partitioning can evolve and be maintained in the polar environment (Jones et al., 1990). The approach we choose to present here consists of taking individual trajectories to examine specific chemical signatures generated over short time periods (≤ 10 days). In a second step (section 7.1), a more general view will be obtained by

examining the photochemical evolution of the vortex over its lifetime using idealized trajectories. The ER-2 observations of HCl, ClO, NO, OH, HO₂ along with their associated quantities ClONO₂^{*}, HOCl^{*}, Cl₂O₂^{*}, provide strict constraints, and a direct comparison with model results will help us elucidate the mechanisms governing the evolution of reactive species in the polar lower stratosphere. Furthermore, it will allow us to estimate the rates of ozone loss occurring during the polar winter and spring (see section 7.2 and 7.3).

In this section, we examine whether the model simulations can account for the observed amounts of HCl lost, and ClO produced, as a result of a PSC encounter. In particular, we pose the question of whether different aerosol surfaces and temperature histories leave specific fingerprints on the partitioning of chlorine species, and other reactive species. To that end, we focus on a detailed analysis of two ER-2 flights made on July 28, 1994, and August 6, 1994. During this period of austral winter, temperatures were very cold throughout the vortex, and intense heterogeneous processing had been taking place since early June (Waters et al., 1993; Santee et al., 1994).

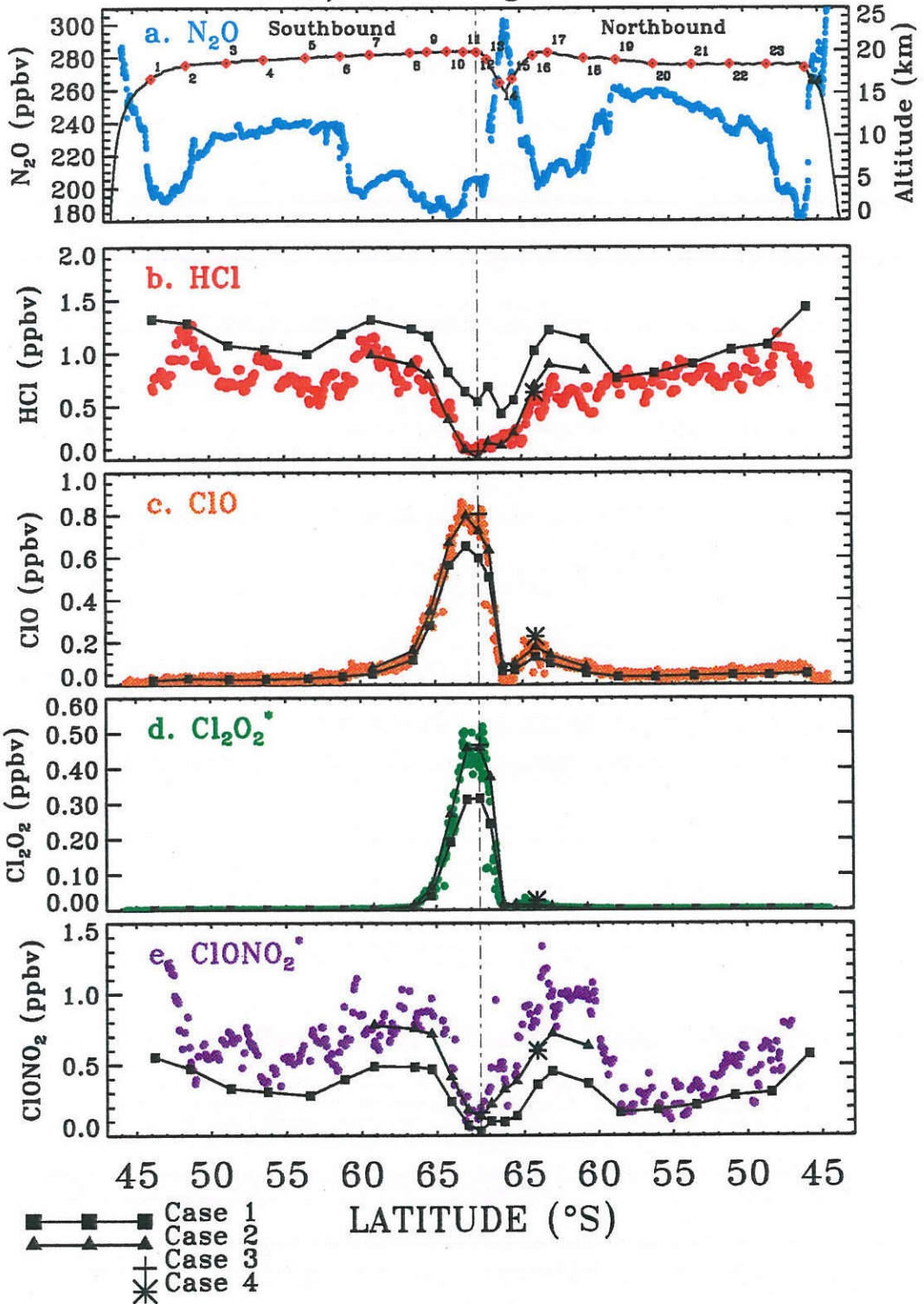
6.1 On-going heterogeneous processing: July 28, 1994

Observations obtained during the flight of July 28, 1994, are shown in Fig. 8a and 8b, as a function of latitude. During this flight, temperatures as cold as 190 K were measured southward of 60°S (top panel in figure 8b) and the ER-2 flew through a polar stratospheric cloud between 65.5 and 67.5°S. Ten-day backtrajectories show that the air had been rapidly cooling over the 12 hours prior to being sampled by the ER-2 (Fig. 9a). Inside the vortex (the maximum horizontal wind was observed at 64°S), ClO mixing ratios reached a maximum of 0.85 ppbv, while HCl levels decreased down to values lower than 0.2 ppbv (Fig. 8a), close to the detection limit of the instrument.

In a first step, we assume in our calculations that the aerosols are in the liquid phase and that they grow by condensation of HNO₃ and H₂O to form supercooled ternary solutions (STS) at low temperatures. The levels of HCl, ClO, Cl₂O₂^{*}, HOCl^{*} and

Figure 8a: Flight of July 28, 1994. Comparison between observations and results from ten-day photochemical trajectory calculation for chlorine species, (b) HCl, (c) ClO, (d) Cl₂O₂^{*}, (e) ClONO₂^{*}. All species with stars are calculated from observations assuming steady-state (see text). N₂O and altitude are represented on the upper panel, as well as the specific air parcel locations used in the analysis. The model results assume heterogeneous reactions on background sulfate aerosols, and growth of supercooled ternary solutions (STS) particles as a function of temperature (see Fig. 7). The full squares connected with lines (case 1) represent model calculations assuming no previous processing of chlorine, while the triangles (case 2) show the model results assuming an initialization with 0.35 ppbv of HCl having been heterogeneously processed previously. The plus at 67°S (case 3) and the star at 64°S (case 4) correspond to model cases assuming respectively, formation of Type I and II PSCs, and frozen SAT particles (see text). The vertical line going through all the panels indicates the southern most latitude reached (~ 67.5°S).

ASHOE/MAESA flight : 940728



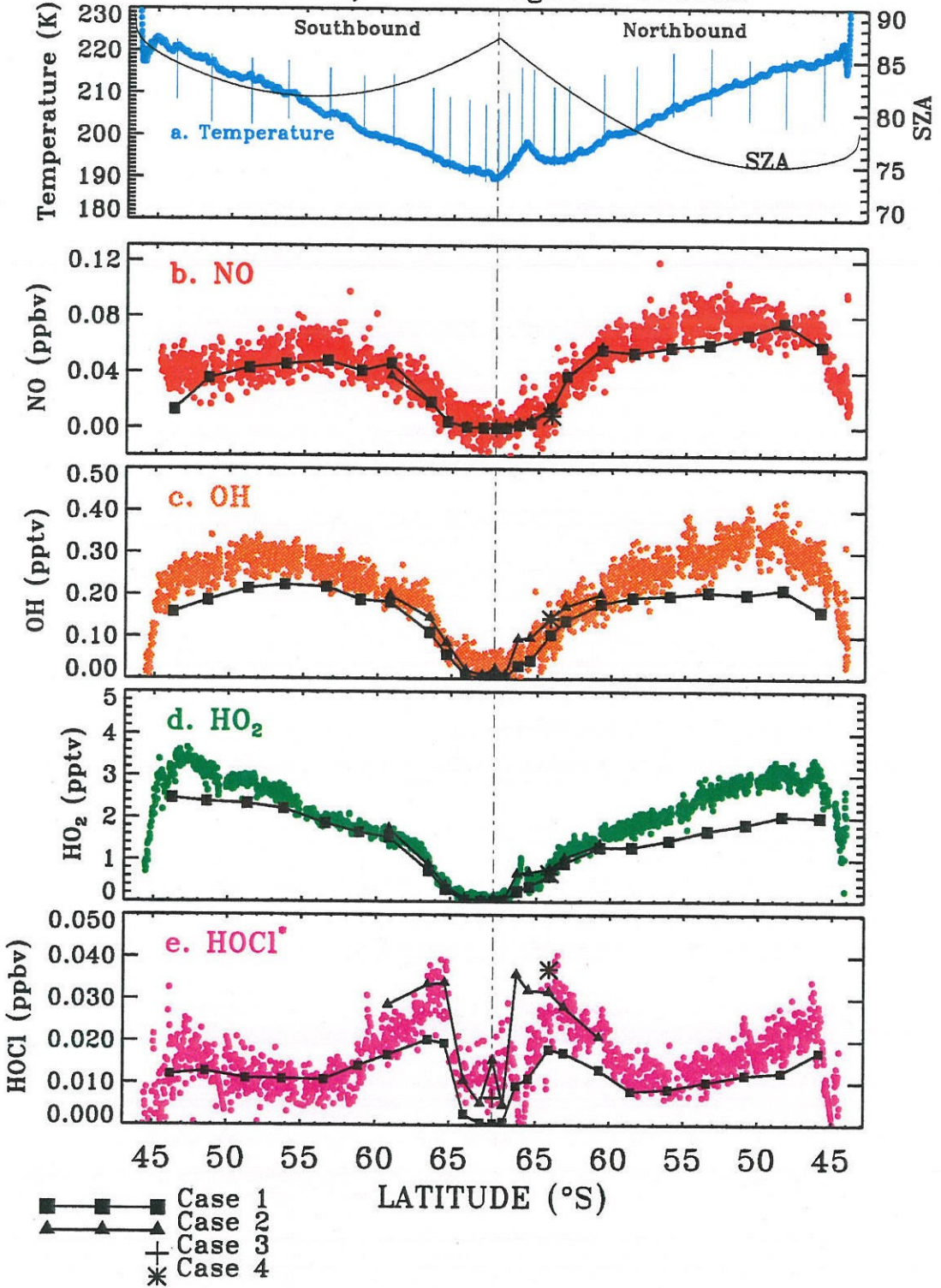
ClONO_2^* are compared to the backtrajectory calculations in Fig. 8a, as a function of latitude. Two different sets of model initializations are considered. In case 1 (squares), we assume no pre-processing of the chlorine reservoirs: HCl and ClONO_2 are initialized from their empirical relations with CFC-11 in the fall (see section 3.1). In the second case (case 2 - triangles) we assume that poleward of 61°S (a) 0.35 ppbv of HCl (~25 % of HCl) had previously undergone heterogeneous processing and that (b) ClONO_2 has had time to recover such that ClO levels were back to low values, consistent with observations in early June (Fig. 4a) and our stoichiometry analysis in section 4. As shown in Fig. 8a, the first case clearly overestimates HCl poleward of 66°S and underestimates ClO, suggesting that HCl had indeed been processed earlier than ten days before. If we assume no previous processing, then the maximum amount of active chlorine liberated is limited by the smallest reservoir, which is ClONO_2 in case 1. Previous processing of HCl followed by conversion of ClO into ClONO_2 (case 2) results in higher predicted levels of ClO, and an extremely well reproduced sharp latitudinal gradient in ClO (Fig. 8a, panel c).

The NO mixing ratios (Fig. 8b) are decreasing southward of 57°S due to the slow photolysis of HNO_3 at higher latitudes combined with heterogeneous conversion of N_2O_5 on sulfate aerosols (Fahey et al., 1993). South of 66°S extremely low levels of NO are observed: heterogeneous reactions [1]-[2] produce increasing amounts of HNO_3 and high levels of ClO convert NO_x to ClONO_2 . The latitudinal gradient in NO is well reproduced, in particular the near zero values inside the vortex. Because it accounts for temperature and latitude variations in the recent history of an air parcel, the Lagrangian calculation reflects much better the NO_x partitioning in the context of varying temperature history than a photochemical steady-state model (Kawa et al., 1993; Gao et al., 1995).

Odd-hydrogen (HO_x) mixing ratios predicted by the model follow the shape of OH and HO_2 *in situ* observations as a function of latitude (Fig. 8b). However, the model

Figure 8b: Same as for 8a, but for (d) NO, (c) OH, (d) HO₂, and (e) HOCl*. Temperature and solar zenith angle along the ER-2 flight track are presented on the upper panel. The vertical bars show the range of temperatures encountered in the previous ten days, as obtained from backtrajectory calculations.

ASHOE/MAESA flight : 940728



tends to underpredict OH and HO₂ by 10-30% outside the vortex. Our calculation includes BrONO₂ hydrolysis with a sticking coefficient of 0.5 (Hanson and Ravishankara, 1995). As discussed by Hanson and Ravishankara (1995) and Lary et al. (1995), BrONO₂ hydrolysis on sulfate aerosols leads to increased HOBr levels, which, via photolysis, produces higher levels of HO_x in particular close to sunrise. The reasons for this systematic underprediction of HO_x by models at mid-latitudes are yet unclear (Wennberg et al., 1994; Salawitch et al., 1994; Michelsen et al., 1994).

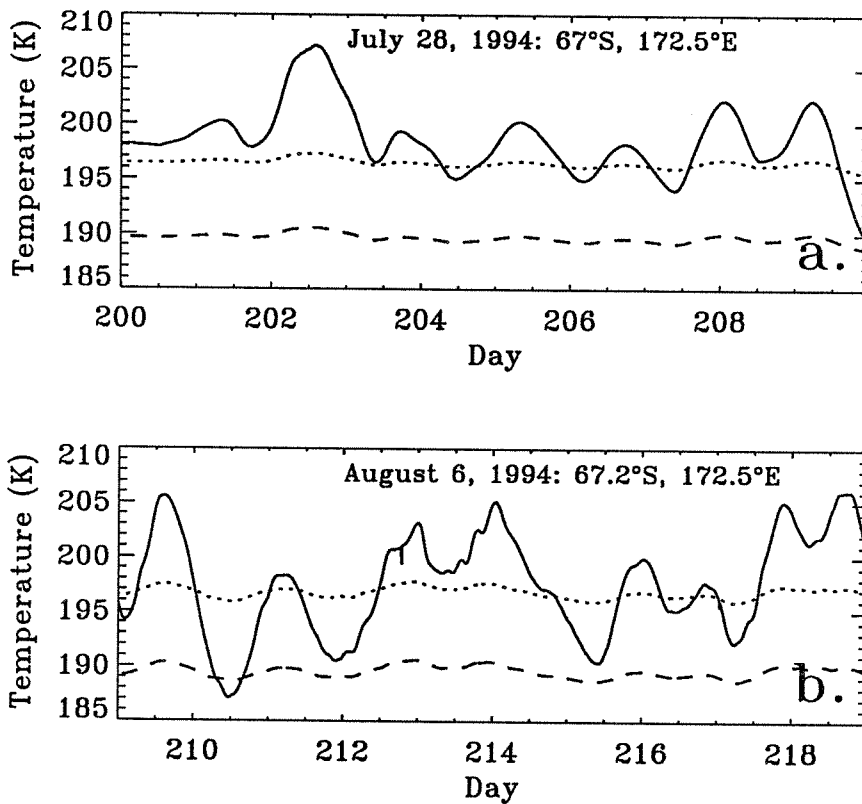
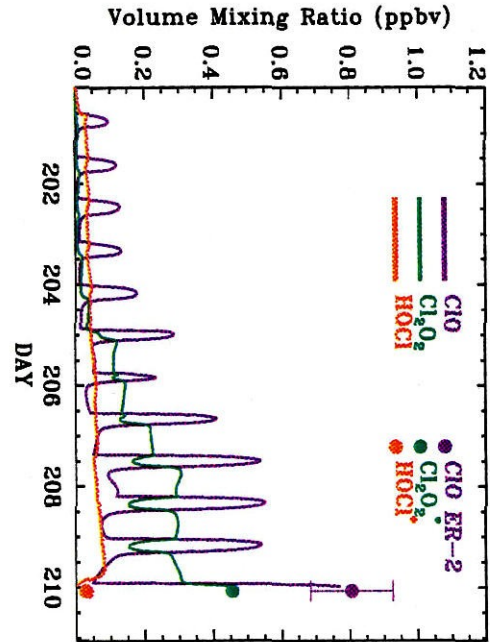
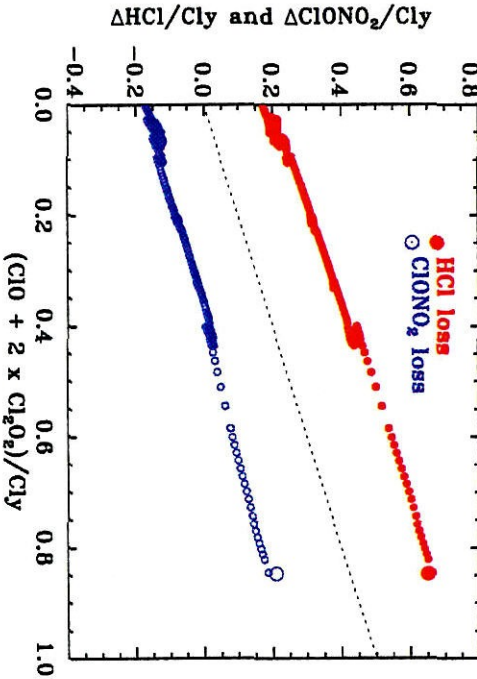
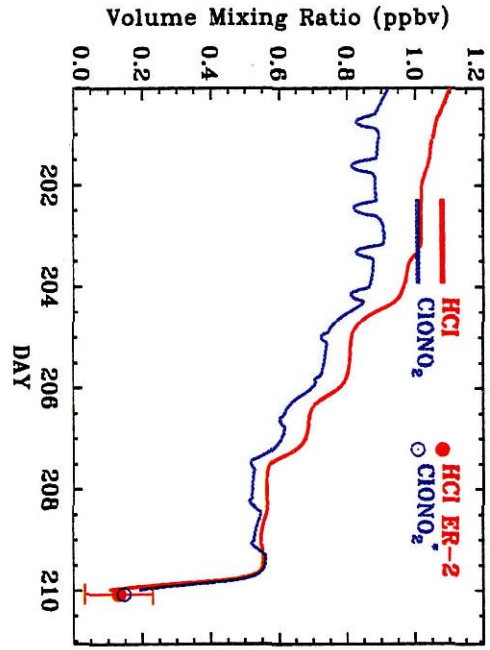
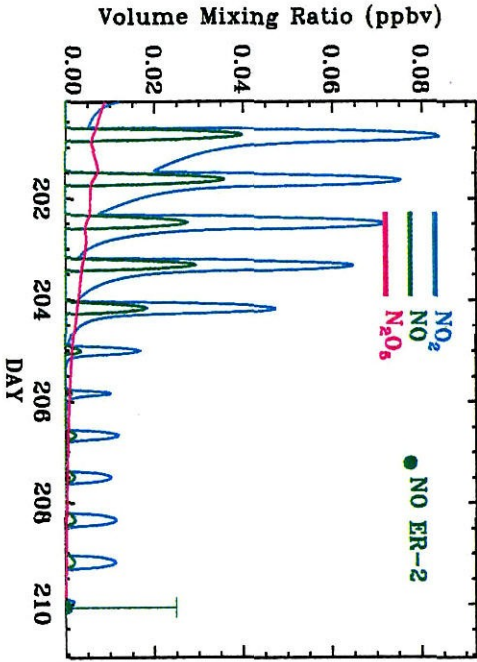


Figure 9: Backtrajectory temperatures for end points on (a) July 28, 1994, at 67°S, 172.5°E (parcel 11 in Fig. 8a); and (b) August 6, 1994, at 67.2°S, 172.5°E. The dotted lines show the NAT formation temperatures, T_{NAT} (Hanson and Mauersberger, 1988), for respectively (a) 7.2 ppbv HNO₃ and 4.8 ppmv H₂O; (b) 10.3 ppbv HNO₃ and 5 ppmv H₂O. The dashed line corresponds to the ice formation temperature, T_{ICE} . The variations in both T_{NAT} and T_{ICE} reflect the changes in pressure along the trajectories.

If we now study parcel 11 of Fig. 8a, with a temperature history shown in Fig. 9, we obtain model calculations for the evolution of individual species during the ten days prior to the ER-2 measurement, as shown in Fig. 10. These results correspond to the initialization in case 2, assuming pre-processing of HCl. When the temperature decreases below 196 K (on days 204, 206 and 207), the reaction of HCl and ClONO₂ on STS becomes fast enough to deplete both chlorine reservoirs and increase Cl_x. The reactivity of reaction [1] for these temperatures is close to 0.01 (Fig. 6). Thus, over the course of the nine and a half first days of the trajectory, 50% of HCl is processed, and ClO increases from 0.1 ppbv to 0.55 ppbv. Note the strong diurnal variation of ClO which is due to the photolysis of Cl₂O₂ during the day. At night, the ClO dimer is the dominant Cl_x species. These high levels of ClO suppress NO_x via reaction of ClO and NO₂ to form ClONO₂ (bottom left panel in Fig. 10).

Figure 10. Evolution of model calculations along a trajectory starting on July 18 (day 200) and ending on July 28, 1994 (67°S, 172.5°E, at 22:34 GMT). Parcel 11 in Fig. 8a. Values of the species as observed by the ER-2 are represented by the symbols with error bars at the end of the trajectory. Temperatures along the trajectory are shown in Fig. 9a.



The precipitous drop in temperatures for the last 12 hours of the trajectory causes the reactivity of [1] to increase by an order of magnitude, while at the same time the uptake of HNO_3 generates the growth of aerosols (Fig. 7) to form supercooled ternary solutions. As a consequence of high reactivity and increased surface area, HCl and ClONO_2 are rapidly converted to Cl_2 which itself is transformed to ClO and Cl_2O_2 . Heterogeneous reaction of HCl with HOCl (reaction [3]) causes HCl to decrease slightly more rapidly than ClONO_2 . In our calculations, the rate of [3] is a fifth of that of [1]. On the other hand, reaction [2] proceeds at a rate which is more than ten times slower than [1]. Model calculated HCl , ClONO_2 , ClO , Cl_2O_2 compare very well with the observed and derived quantities at the intercept with the ER-2 flight-track. The NO levels are below the detection limit of the instrument.

The analysis we presented in section 4 showed that the stoichiometry of the reaction converting HCl and ClONO_2 to active chlorine is 1/2, suggesting a dominant role for $\text{ClONO}_2 + \text{HCl} \rightarrow \text{Cl}_2 + \text{HNO}_3$. In our model simulations, where heterogeneous reactions with laboratory measured reactions rates are included, we see the same behavior as illustrated in the bottom right panel of Fig. 10, where we plot the loss in HCl as a function of model produced active chlorine over the course of the ten-day trajectory. Thus, as expected, the overall stoichiometry of the heterogeneous reactions listed in Table 2 is close to that of reaction [1]. Note that the contribution of [3] creates a slope slightly smaller than 1:2 for ΔClONO_2 over the last 12 hours of the calculation.

The bottom right panel on Figure 10 illustrates the evolution of reservoir losses and active chlorine production for a given air parcel as a function of time rather than an instantaneous snapshot for many air parcels as in Fig. 4 and 5. The similarity of the two pictures comes from the fact that these slopes develop as a result of different integrated amounts of time spent at cold temperatures, for multiple air parcels, or for one single parcel as it circulates around the vortex.

The role of the heterogeneous reaction $\text{HOCl} + \text{HCl} \rightarrow \text{Cl}_2 + \text{H}_2\text{O}$

Once temperatures reach levels below 198 K, reaction [3] begins to be important and HOCl rapidly reacts with HCl to produce Cl_2 (see Fig. 6). HOCl itself is mainly formed by the reaction $\text{ClO} + \text{HO}_2 \rightarrow \text{HOCl} + \text{O}_2$, as well as heterogeneously via [2]. In this manner, as pointed out by Prather (1992) and Crutzen et al. (1992), reaction [3] acts as an effective sink for HO_x in the polar stratosphere. For the first time, we have direct observational evidence for reaction [3]: the panels c and d in figure 8b illustrate how levels of OH and HO_2 are indeed suppressed inside the vortex, with mixing ratios of ~ 0.05 pptv and 0.15 pptv respectively. The trajectory model results are consistent with this effect, predicting HO_x values slightly lower than observed. If we compare these mixing ratios with a model calculation in which we did not include reaction [3], HOCl would be a factor of 10 higher (~ 0.1 ppbv), and predicted OH and HO_2 levels would be 0.15 pptv and 0.5 pptv respectively. Such a strong signal, particularly for HO_2 , is well above the detection limit and would have been seen if reaction [3] had not been occurring. Table 3 summarizes the model calculated HO_x production rates for these two cases.

Table 3 - Chemical loss and production rates for OH and HO_2 inside the vortex on July 28, 1994, at 66°S , 172.5°E (20 km).

	Observations	Model with HOCl + HCl	Model without HOCl + HCl
OH and HO_2 (pptv)	0.05 ± 0.02 ; 0.15 ± 0.05	0.02; 0.07	0.15; 0.5
	24-hr production rates	in molecules/cm ³ /s	
$\text{O}(^1\text{D}) + \text{H}_2\text{O}$		34	31
$\text{HNO}_3 + h\nu$		300	280
CH_4 oxidation		260	330
$\text{HOCl} + h\nu$		4600	6910
$\text{HOCl} + \text{HCl}$		1575	0
$\text{ClONO}_2 + \text{H}_2\text{O}$		1000	470
HOCl (ppbv)		0.01	0.1

The role of aerosol surface type

In all of the above we have assumed that aerosols were present in the form of supercooled ternary solutions $\text{H}_2\text{SO}_4/\text{HNO}_3/\text{H}_2\text{O}$ which grow in volume as HNO_3 and H_2O condense at temperatures below ~ 193 K (Fig. 7). Observations of total nitrogen for this flight indeed show the presence of HNO_3 in the aerosols phase (Del Negro et al., 1995). In *situ* observations of the particle composition and phase suggest a much more complex picture during this flight. In particular, aerosol samples collected at 67°S - inside the PSC - show the presence of Type I and Type II PSCs with an effective radius of $7 \mu\text{m}$ (Goodman et al., 1995). These crystals seem to most likely originate from higher altitudes and were falling through the air sampled by the ER-2. Because of their low observed concentrations, the contribution of Type I and II PSCs to the total surface area is small (less than 5%, Goodman et al., 1995).

Our calculations show an additional increase in chlorine activation of less than 2% if we include both Type I and II aerosols (at a surface area of $0.2 \mu\text{m}^2/\text{cm}^3$ for the last 12 hours of the trajectory, corresponding the observations by Goodman et al.) in addition to supercooled aerosols. This particular model calculation is illustrated by the plus symbol in Fig. 8 (case 3). Furthermore, wire impactor measurements during this flight show that up to 30% of the sulfate aerosols were frozen at 64°S on the northbound leg of the flight (Goodman et al., 1995). If we assume that frozen sulfate aerosols were present with a surface area of $0.8 \mu\text{m}^2/\text{cm}^3$, in addition to background aerosols, we obtain 0.07 ppbv more ClO produced (star symbol in Fig. 8a, case 4).

Thus, for the ER-2 flight of July 28, the high ClO levels seem to have been mainly caused by heterogeneous reactions [1] and [3] on supercooled sulfate aerosols surfaces. Because of their low concentrations, Type I and II PSCs did not contribute much to chlorine activation. When present, frozen aerosols have the potential of increasing chlorine activation, but under the conditions studied here, their role was comparable to

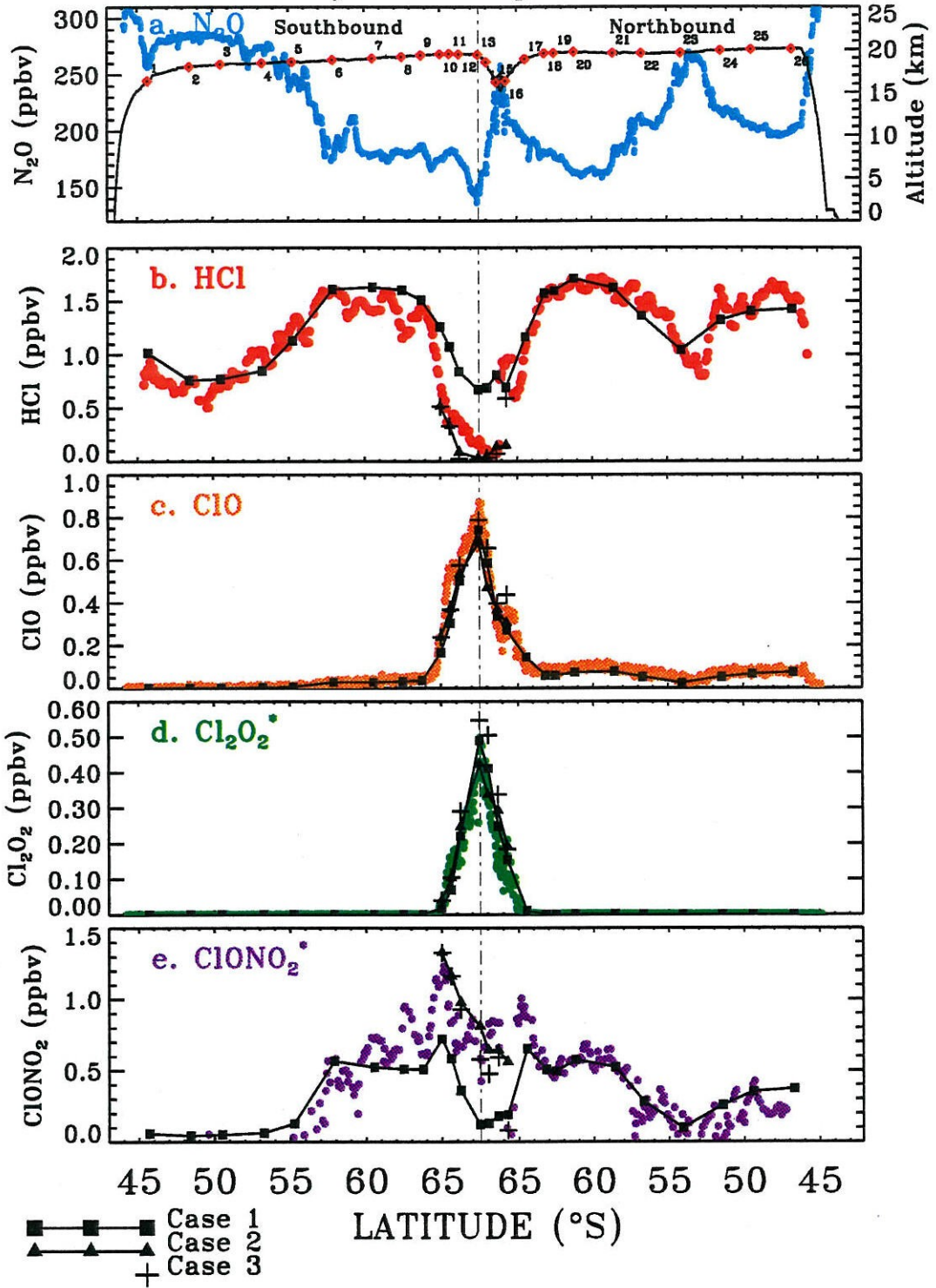
sulfate aerosols. Here, for the first time, we have observational evidence for reaction [3] as provided by suppressed levels of *in situ* OH and HO₂.

6.2 Recent heterogeneous processing: August 6, 1994

Observations during the flight of August 6, 1994, are summarized in Fig. 11a and 11b. The temperatures measured aboard the ER-2 were on average 10 K warmer than on July 28, 1994. The lowest temperatures reached were close to 200 K (top of panel 11b). Backtrajectories show that, southward of 64°S, this air was repeatedly exposed to temperatures well below NAT formation temperatures (Fig. 9b), and had been warming on the last few days before being sampled by the instruments aboard the ER-2. HCl levels outside the vortex (equatorward of 64°S as defined by the polar jet maximum) are higher than for July 28 because the air sampled contained more Cl_y, as indicated by the lower N₂O values measured.

Figure 11a: *Flight of August 6, 1994. Same as 8a. The full squares connected with lines (case 1) represent model calculations assuming no previous processing of chlorine, while the triangles (case 2) show the model results assuming that 0.35 ppbv of HCl have been heterogeneously processed. Both cases assume heterogeneous reactions on sulfate aerosols and STS. The plus symbols (case 3) show model results assuming pre-processing and formation of NAT and ice PSCs.*

ASHOE/MAESA flight : 940806



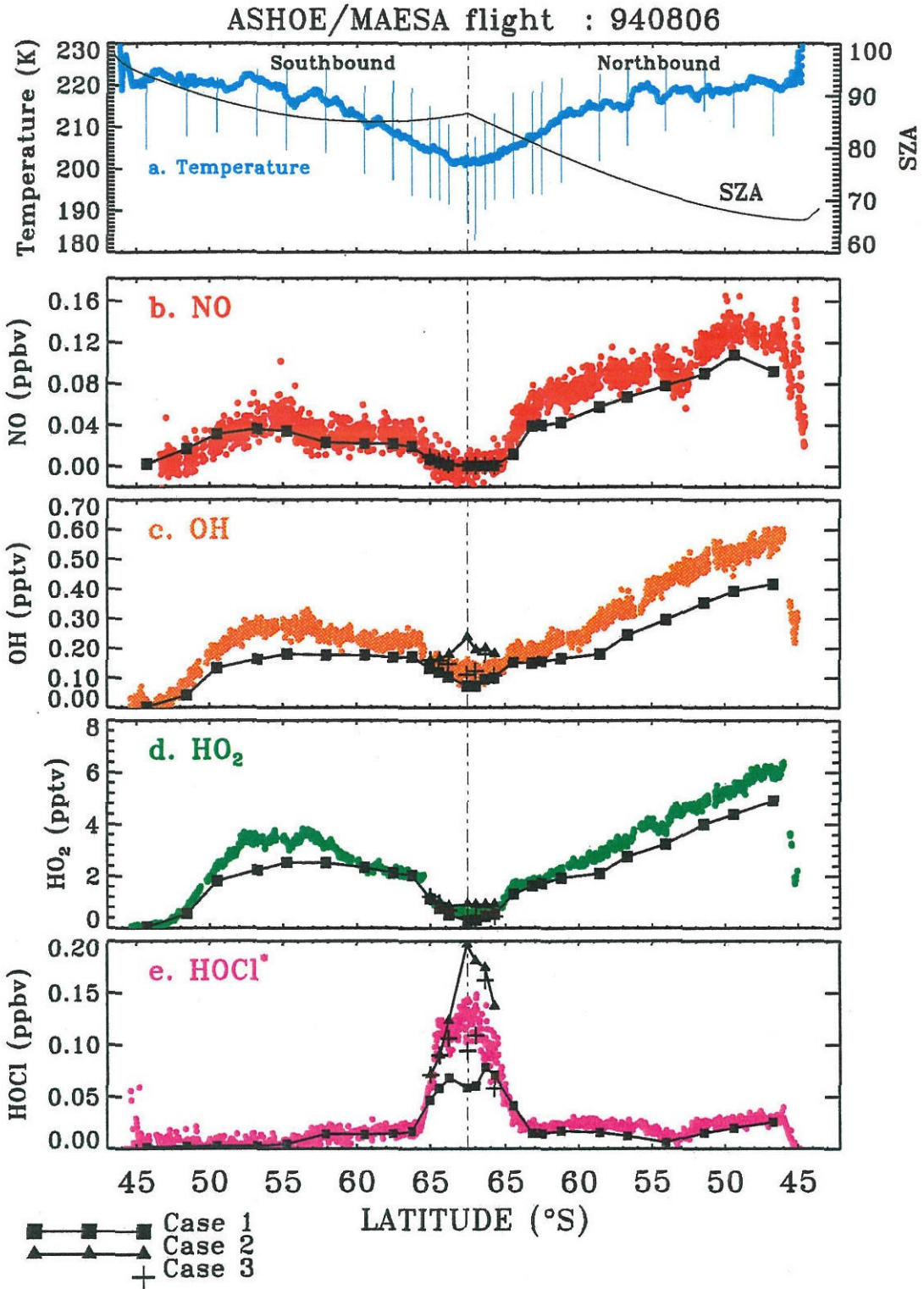


Figure 11b: Flight of August 6, 1994. Same as 11a, but for (d) NO, (c) OH, (d) HO₂, and (e) HOCl*.

As in section 6.1, we first assume that the aerosols are in the liquid phase and that they incorporate HNO_3 to form STS at low temperatures. Model calculations along trajectories are compared to the observations in Fig. 11. The latitudinal extent of enhanced ClO and Cl_2O_2^* is well reproduced by the model. If we assume no previous processing event, modeled HCl levels poleward of 65°S are much too high: over the ten days of the calculation, most of ClONO_2 has been consumed, and HCl lacks a partner to be further depleted. When the chlorine reservoirs are initialized assuming that 35% of Cl_y has been processed (case 2, triangles) - as suggested by observations on July 28, 1994 - then all of HCl is depleted south of 64°S . Model results for ClONO_2 are in better agreement with the calculated budget residual ClONO_2^* . The total depletion of HCl , however, generates levels of OH and HO_2 inside the vortex that are too high compared to observations (Fig. 11b). This reflects the accumulation of HOCl which can no longer react with HCl via [3], and as a consequence acts as a source of HO_x . We thus need to reconcile our model calculations with the observations of HO_x at the inner vortex edge, and discuss this below.

As the temperature is oscillating well below 195 K for air parcels inside the vortex, we might expect the phase of the aerosols to be NAT, water ice and/or frozen particles, depending on the temperature thresholds reached. We next examine the sensitivity of our model calculations to the assumed aerosol composition, which has an impact on both the surface reactivities and growth properties of the particles.

Model sensitivity to aerosol composition

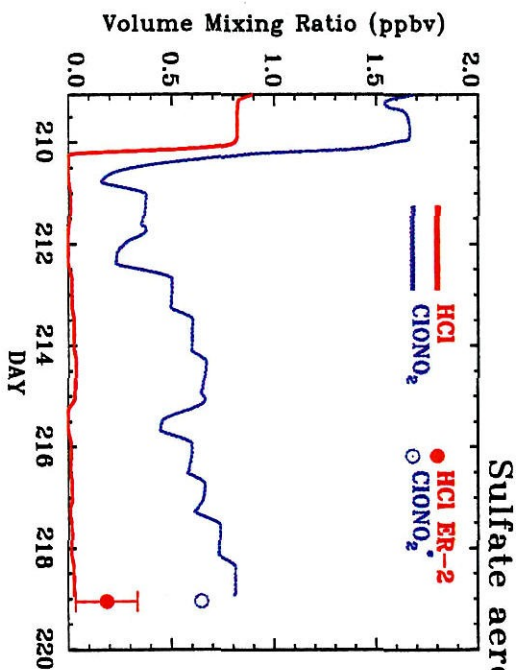
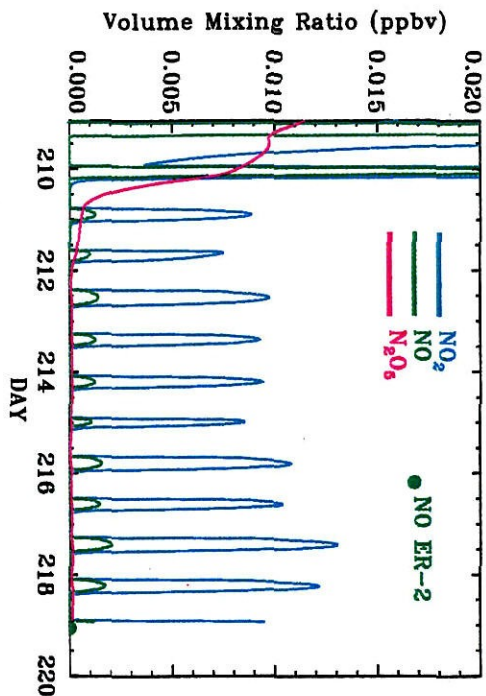
For the August 6, 1994, flight, no continuous aerosol measurements are available. However, the samples collected by the Ames wire impactor experiment (Pueschel et al., 1989) show a relatively low amount of background aerosols ($\sim 1 \mu\text{m}^2/\text{cm}^3$) - all in the liquid phase. This is consistent with volume observations obtained a few days later on August 8 and 10, 1994, with the continuous aerosol measurements, which are a factor of two lower than on July 28 and 30, 1994 ($\sim 2\text{-}3 \mu\text{m}^2/\text{cm}^3$ outside of the PSC). One

possible explanation for this phenomenon could be the growth and subsequent sedimentation of large aerosols ($>1 \mu\text{m}$) when cold temperatures are repeatedly reached during the 8-10 day period separating the flights.

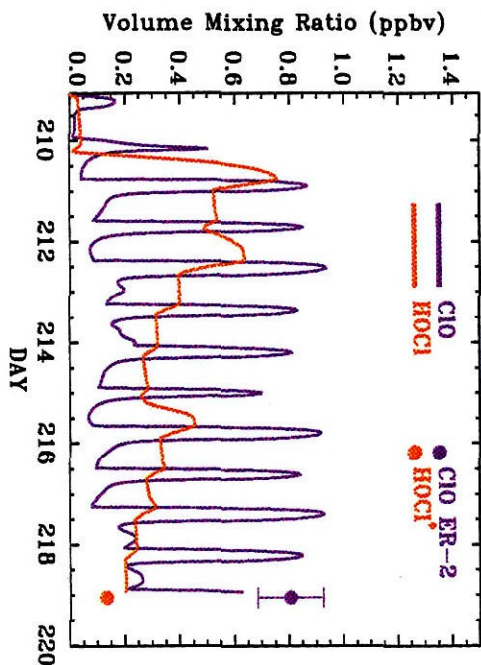
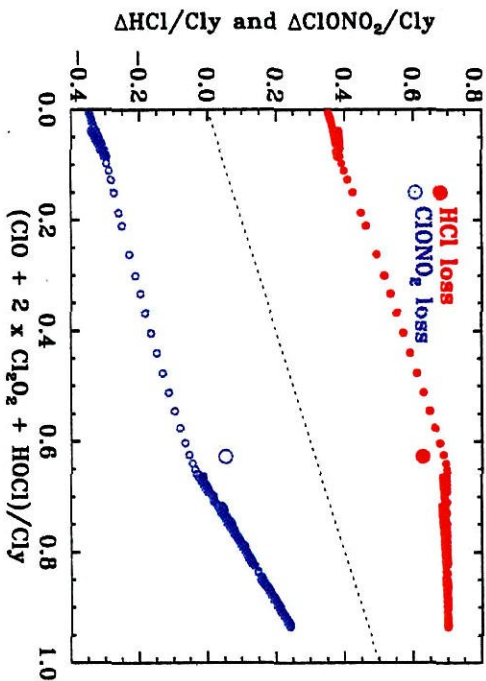
The stratospheric temperature at which NAT particles are formed is not clearly known and seems to depend on the state of background particles (Rosen et al., 1993) as well as on the amount of condensing vapors (Hanson and Mauersberger, 1988). Observations seem to imply a barrier to the thermodynamic formation of NAT, which tends to form 3 K below T_{NAT} (Fahey et al., 1989). It is possible that surfaces need some 'accommodation' before NAT readily forms (Zhang et al., 1995). Or, in a more complex manner, cooling and warming cycles could cause selective formation of different surface types (Tabazadeh and Toon, 1995).

We can construct the following scenario. During the first cooling cycle NAT forms on background liquid aerosols at 3 K supersaturation ($T_{\text{NAT}} - 3\text{K}$). Once $T > T_{\text{NAT}}$, NAT evaporates and leaves behind liquid aerosols. The next formation cycle may take place at 0 K supersaturation, due to preactivation of the background surfaces (Zhang et al., 1995). When temperatures decrease below the ice formation temperature, we assume formation of Type II PSCs with a surface area of $10 \mu\text{m}^2/\text{cm}^3$. In these calculations, we do not include the effects of aerosol sedimentation out of the considered air parcel or originating from air masses above. This phenomenon was observed in the redistribution of H_2O and NO_y observations during the ER-2 dive ($\sim 16 \text{ km}$) during this flight (Tuck et al., 1995a), but not elsewhere.

Figure 12: Inside the vortex: evolution of model calculations along a trajectory starting on July 26 (day 209) and ending on August 6, 1994 (67.2°S , 172.5°E , at 22:45 GMT). Parcel 11 in Fig. 11a. Temperature history in Fig. 9b. The initialization assumes pre-processing of the reservoirs. We assume formation of STS on background sulfate aerosols.



Sulfate aerosols and STS



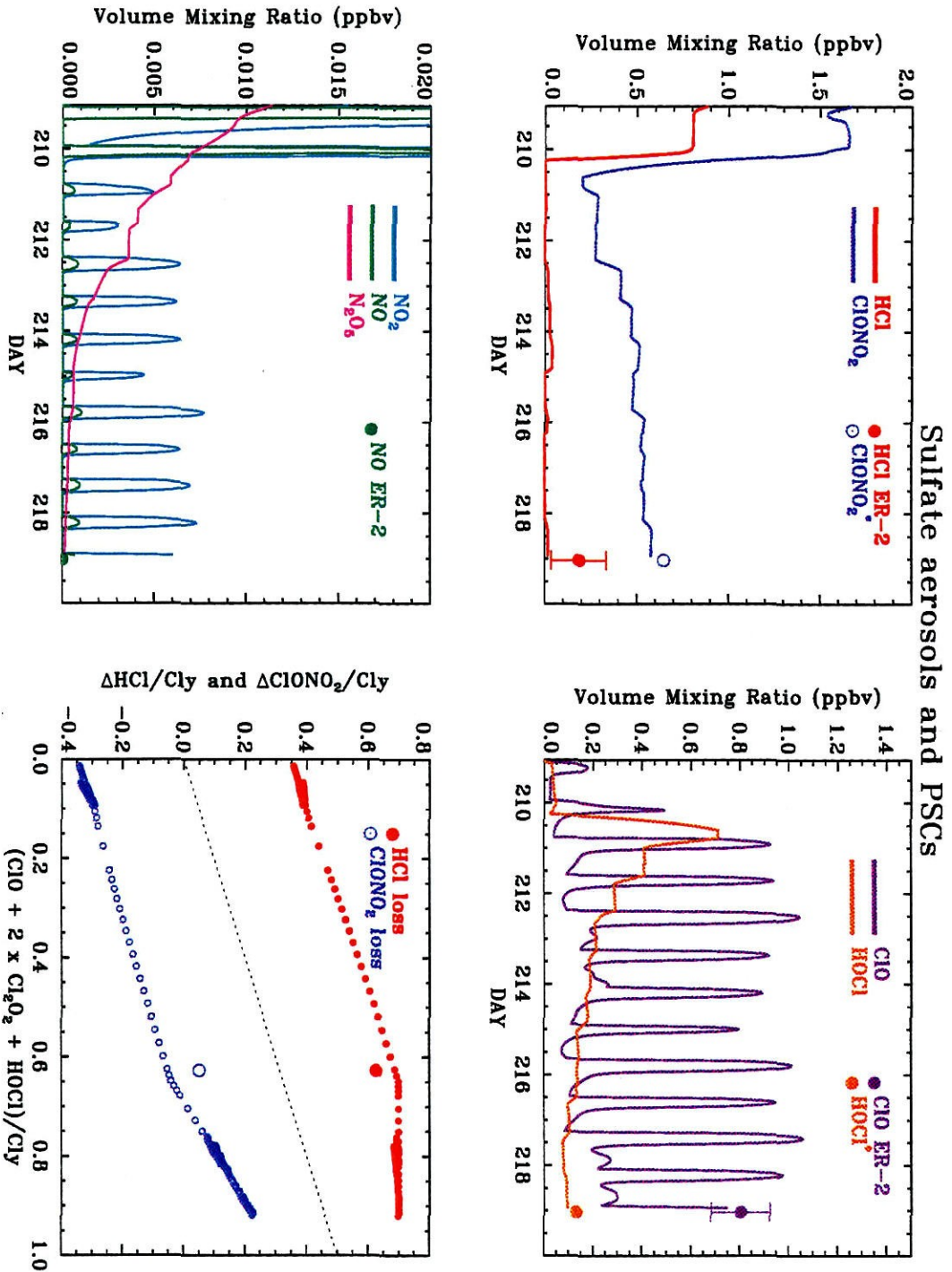


Figure 13. Inside the vortex: Same as Fig. 12, assuming NAT and ice PSC formation.

In figures 12 and 13 we compare the different behavior of reactive species for the STS case and for the described PSC scenario, with sulfate aerosols acting as the background surfaces. These Lagrangian calculations correspond to the temperature history shown in figure 9b (parcel 12), and assumes previous processing of HCl as discussed above. For the STS case, in Fig. 12, ClONO₂ and HCl are rapidly lost via reaction [1]. Once all of HCl has been consumed on day 210, the heterogeneous processing of ClONO₂ continues through [2] and generates very high levels of HOCl (~0.7 ppbv). As illustrated in Fig. 6, the hydrolysis of ClONO₂ on sulfate aerosols proceeds more rapidly if there is no competition from its reaction with HCl. Small excursions of the air parcel to lower latitudes (up to 58°S) allow ClONO₂ to reform by reaction of ClO with NO₂ resulting from the photochemical conversion of HNO₃ (on days 212 and 216). Repeated exposures to cold temperatures continue the processing of ClONO₂ via [2] and maintains high ClO and HOCl levels. For the PSC scenario in figure 13, further depletion of ClONO₂ after day 210 takes place through hydrolysis of ClONO₂ on ice (which forms in the model between the times 210.1 and 210.5, when temperatures decrease below T_{ice} = 188 K). Hydrolysis of ClONO₂ on NAT surfaces is much slower than on ice or sulfate aerosols; therefore, the high levels of HOCl first produced on day 210 cannot be maintained through [2] on NAT, and slowly decrease via photolysis, and heterogeneous reaction with both HCl and HBr. As a consequence of these lower HOCl mixing ratios, the resulting OH and HO₂ are in better agreement with observations for the PSC case (case 3 in Fig. 11b) rather than for the STS case (case 2). We have used a sticking coefficient of 0.001 for [2] on NAT as recommended by DeMore et al. (1994). However, laboratory results range between 1e-6 and 0.02 (Leu et al. 1991; Moore et al., 1990). If we use a value of 0.01, our calculations yield slightly larger HOCl levels, and further improvement in the agreement with the HO_x observations.

Thus, compared to the July 28 flight, during August 6 relatively high levels of OH and HO₂ were measured inside the vortex: 0.15 and 1 pptv respectively as opposed to 0.05

and 0.2 pptv for July 28 (for similar solar zenith angles). This source of HO_x is supplied by high HOCl mixing ratios on August 6 (Fig 11b). In this case, the sustained near zero HCl mixing ratios contribute to turning off the main sink for HOCl, reaction [3]. Comparison between model calculations and observations support the laboratory measured small reactivity of [2] on NAT surfaces, as opposed to the faster rates for the same reaction on sulfate aerosols and Type II PSCs.

The bottom right panels of Fig. 12 and 13 show the two types of slopes obtained for ΔHCl and ΔClONO_2 which were discussed in section 4 for case 4: as reaction [1] proceeds the 1:2 slope is developed, but when all of HCl is depleted, ClONO_2 continues to produce active chlorine through [2] on sulfate aerosols or Type II PSCs, forming the 1:1 slope. The different PSC composition assumed for these two cases do not have a large effect on active chlorine and HCl levels, and therefore there is not much difference in the patterns on these two bottom plots.

The wire impactor measurements on July 28, 1994, have clearly shown that SAT could be present in the polar environment. Thus we have conducted a test case where we have assumed the background aerosols to be all frozen, and that NAT forms on these surfaces. The results obtained are very similar to those shown in Fig. 13, due to heterogeneous reactivities for SAT that are comparable to those on sulfate aerosols.

From our photochemical analysis of the ER-2 observations, we deduce that the amount of chlorine activation is fairly independent on the composition of PSCs (STS, NAT, Ice), due to the very similar reactivity of [1] on all these surfaces (Fig. 6). Thus on the basis of ClO and HCl observations alone, no differentiation is possible. On the other hand, reaction [2] has very different rates for these surfaces, and its impact on HO_x levels has been used to deduce the likely formation of Type I and Type II PSCs. In this manner, OH and HO_2 can be very sensitive indicators of the degree of processing of HCl and exhibit different signatures depending on the type of heterogeneous surfaces that affected chlorine activation.

7. Implications

In the previous section, we have shown that our Lagrangian model using 10-day trajectories quantitatively reproduces the partitioning of reactive species observed aboard the ER-2. We will now extend this analysis to examine the chemical evolution of the Antarctic vortex throughout the polar winter, focusing on the particular conditions existing at the edge of the vortex. In this region, both excursions in and out of sunlight and mixing with unprocessed air (Prather and Jaffe, 1990) are thought to play important roles for chlorine activation and the accompanying ozone-loss rates.

7.1 Chemical Evolution during the Antarctic winter

We consider the chemical evolution associated with an idealized air parcel between April and November, as it circulates in the edge region of the vortex ($\sim 62\text{--}66^\circ\text{S}$). To represent both the temperature and latitude variability of the air parcel, the temperature over this time period was specified from climatological means on which we superposed 5-10 K fluctuations, and the latitude was assumed to be centered around 64°S , with excursions to lower and higher latitudes (Fig. 14). The model was initialized with the chlorine partitioning observed during ER-2 flights in April, prior to any processing. We assume formation of NAT and water ice PSCs on background sulfate aerosols, when temperatures reach T_{NAT} and T_{ICE} respectively. Because of the temperature fluctuations in the model, PSCs periodically form and evaporate between June and September, and the condensed gases return to the gas phase. We do not consider the effects of denitrification in this study, because it was generally not observed for the air masses sampled during ASHOE/MAESA (Fahey et al., 1995).

The effects of excursions in and out of sunlight

The evolution of model calculated chlorine partitioning is compared to observations in Fig. 15. In order to assess the effects of latitudinal excursions, we consider two model cases: in the first case the latitude of the idealized air parcel is kept fixed at 69°S (case A),

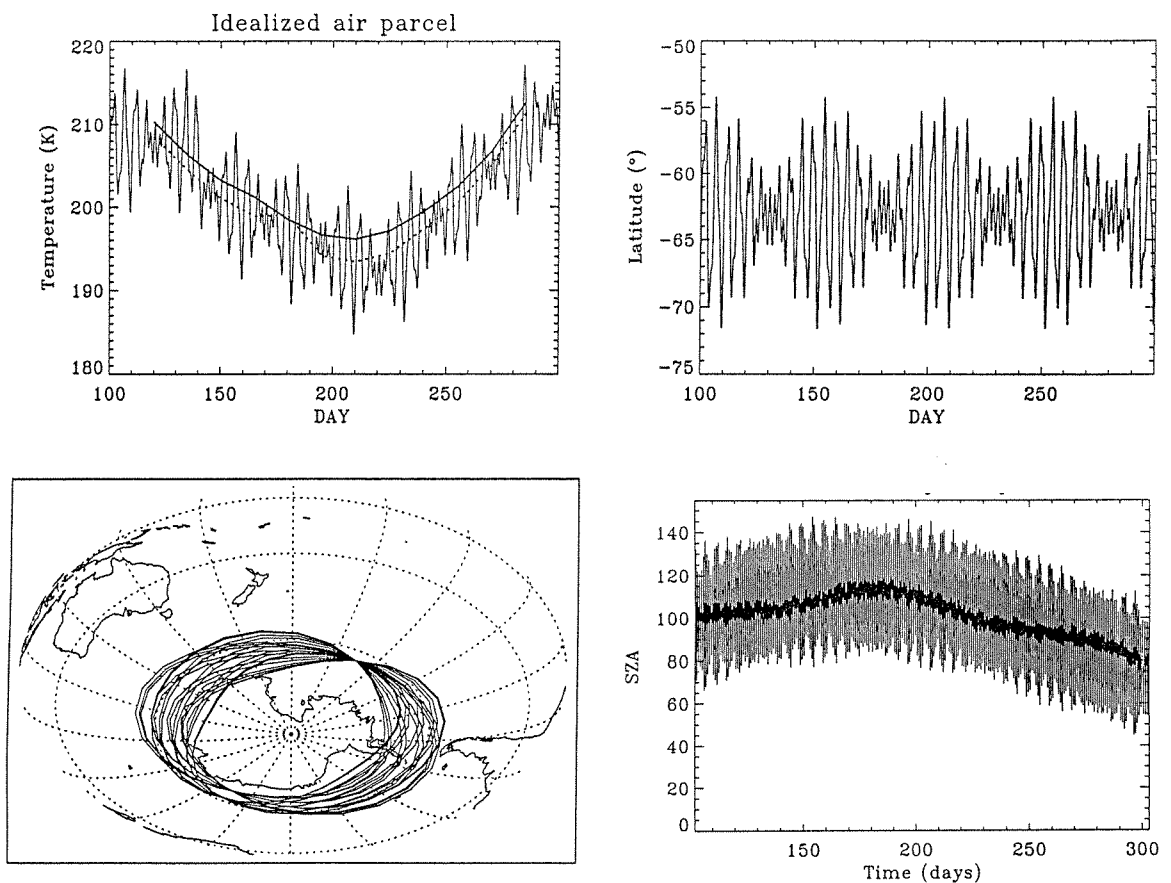


Figure 14: Evolution of an idealized air parcel inside the vortex at 20 km (55 mbar) between April and November 1994. (a) Temperature, (b) latitude, (d) solar zenith angle, and (e) parcel location versus time for the model period.

while in the second case (case B), the latitude varies according to Fig. 14. For both cases, chlorine activation begins in early June, when temperatures are cold enough for rapid heterogeneous reactions on background sulfate aerosols. Fast destruction of HCl proceeds until mid-June, due to reaction [1], in agreement with observations of HCl and ClO.

Once all of ClONO₂ has been consumed, HCl processing stops in case A, while in case B, excursions to lower latitudes provide enough sunlight to produce HO_x and NO_x which combine with ClO (via ClO + HO₂ and ClO + NO₂, respectively) to produce small

amounts of HOCl and ClONO₂. Subsequently, as the parcel returns to higher latitudes and colder temperatures, heterogeneous reactions of HCl with both reservoirs via [1] and [3] continue to deplete HCl. Under these conditions, where ClONO₂ and HOCl are present in similar amounts, reaction [3] contributes to 90% of the HCl loss, and [1] to only 10%. Total HCl loss is predicted by early July.

In this manner reaction [1] is responsible for the rapid early winter loss of HCl, until all of ClONO₂ has been consumed. Reaction [3] and [1] then combine to continue this process, at a slower rate, limited by excursions into sunlight. As a result, 90% of the chlorine is activated by early August (case B), compared to 60% for case A. Thus, the near total removal of HCl that was observed in this study, as well as in airborne (Toon et al., 1989) column measurements, can take place from excursion in and out of sunlight, with resupply of HOCl and ClONO₂ which provide oxidation partners for HCl. Deeper inside the vortex, HO_x and NO_x production by galactic cosmic rays could replace the role of these excursions in generating total loss of HCl (Liu et al., 1992) via [3] and [1] (Müller and Crutzen, 1993).

By late August, sunlight levels at 69°S become sufficient to form HOCl and ClONO₂, and the remaining HCl in case A is rapidly processed because the temperatures in the model are still cold enough for PSC formation. The very rapid recovery of HCl seen for both cases A and B is a consequence of the depleted O₃ levels reached at the end of the polar night. Normally, the chlorine atoms, Cl, are rapidly combining with O₃ to form ClO; however, when all of the O₃ has been depleted, the dominant pathway for Cl loss is by reaction with CH₄ forming high levels of HCl (Prather and Jaffe, 1990; Douglass et al., 1995; Santee et al., 1996). This recovery process was directly observed during ASHOE/MAESA with the *in situ* instruments aboard the ER-2 in mid-October (Webster et al., 1995b; Wamsley et al., 1995).

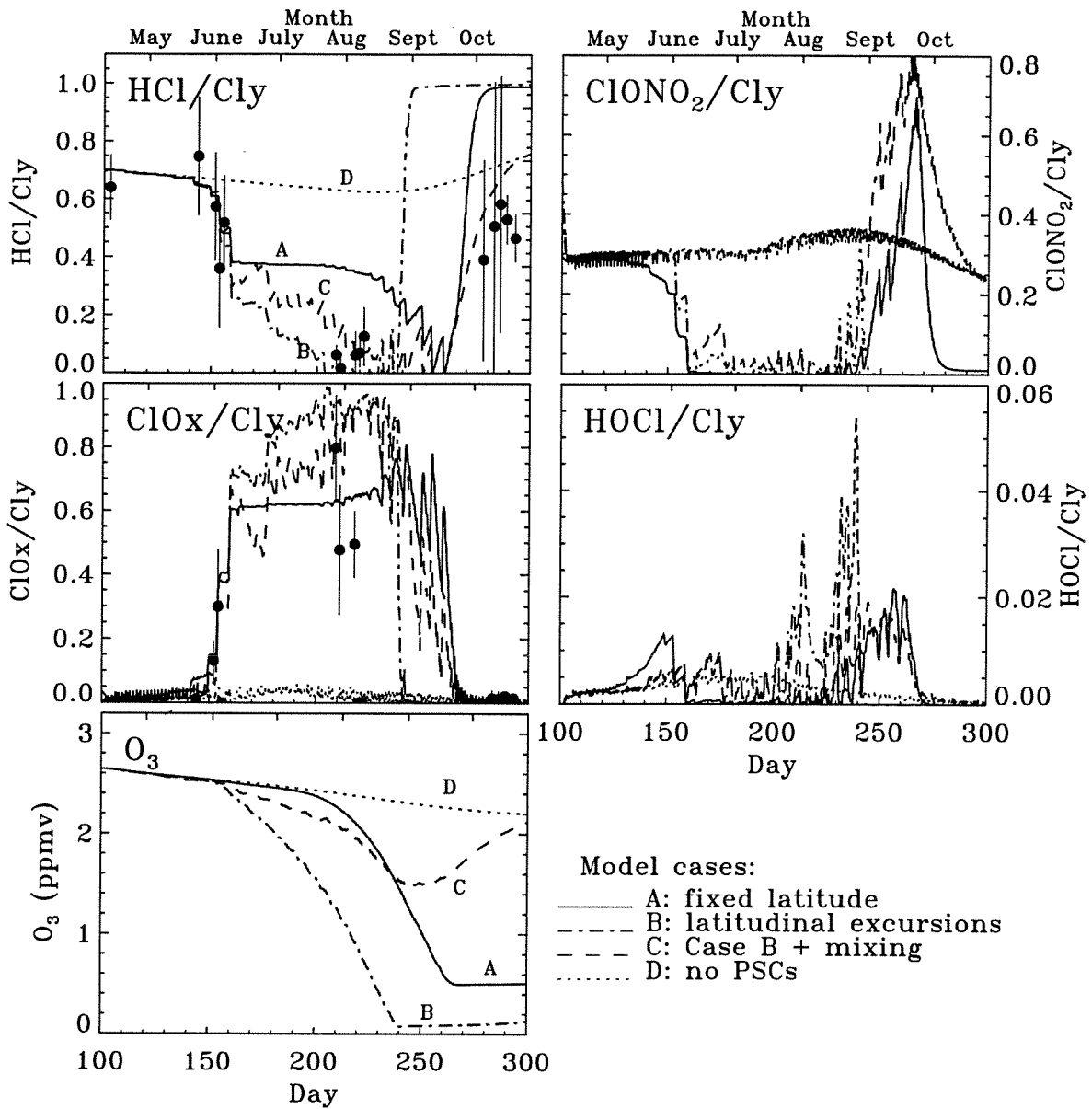


Figure 15: Mixing ratios of HCl/Cl_y, ClONO₂/Cl_y, HOCl/Cl_y, Cl_x/Cl_y, and O₃ between May and November 1994: comparison between observations aboard the ER-2 (see Fig. 3) and calculations for an idealized air parcel. Four model cases are shown. For case A, the latitude was kept fixed at 69°S and the temperature evolution is the same as on Fig. 14. For case B, the temperature and latitude are those shown on Fig. 15. Case C includes mixing, with the same meteorological conditions as case B. Finally, case D has a fixed temperature of 205K and the same latitudinal variations as on Fig. 14.

For case B it is probably unrealistic to assume that an air parcel which undergoes latitudinal excursions and comes in contact with unprocessed air would remain isolated. In the following, we consider the effects of mixing and how it interacts with the photochemistry of air parcels having undergone heterogeneous processing.

Mixing at the edge of the vortex

Analysis of previous observations near the vortex edge have shown that mixing occurs in a region extending up to 5° of latitude on both sides of the edge (Murphy et al., 1989; Pierce et al., 1994; Tao and Tuck, 1994). Furthermore, on the basis of horizontal and vertical gradients of *in situ* observations of CH₄, HCl, NO_y and H₂O during ASHOE/MAESA, Tuck et al. (1995b) find evidence for mixing between inner and outer vortex air. The mechanisms for this mixing process are not clear, but possibilities include inertial gravity waves (Danielsen et al., 1991; Pierce et al., 1994); diabatic cooling; or random differential advection (Reid et al., 1993). Erosion at the vortex edge could take place via filamentation (Waugh, 1993).

Mixing in the stratosphere is probably a combination of a number of these processes. We have implemented a very simple mixing scheme into the trajectory model, by assuming a diffusive type process between the Lagrangian air parcel and the unprocessed air (from outside of the vortex). Thus, at each time step, in addition to the photochemical loss and production of a species A, we have a mixing term which can be written as follows:

$$(\delta[A]/\delta t)_{\text{mixing}} = (1 - V) \times [A]_t + V \times [A]_{\text{out}} \quad [11]$$

where V is the amount of mixing taking place at each time step of the calculation, and $[A]_{\text{out}}$ is the concentration of the species A outside of the vortex. This formulation is not meant to be a description of the mixing processes, but rather to illustrate the potential impact of mixing on the photochemistry of a perturbed air parcel.

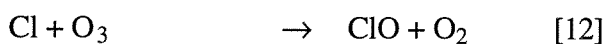
The interaction between mixing and photochemistry can be seen for case C on Fig. 15, for which we have assumed mixing with unprocessed air to take place at a rate $V=2e-7 \text{ s}^{-1}$, which yields air composed of 75% inner vortex air and 15% outer vortex air after ten days. In this model case, the air parcel follows the temperature and latitude shown on Fig. 14. HCl loss during the winter takes place more slowly than in case 2 due to mixing in of outer vortex HCl, but faster than for case A. By late August, there is enough sunlight for more permanent formation of NO_x via decomposition of HNO_3 . The NO_x then combines with ClO (through reaction [4]) to rapidly replenish ClONO_2 which reaches a maximum in mid-September. Production of HCl begins later, and by mid-October HCl has almost entirely recovered to its normal levels, as shown by both model and observations.

By comparison, if the temperature is kept fixed at 205 K (case D) to inhibit heterogeneous reactions on sulfate aerosols and PSC particles, ClO levels remain below 5% of Cl_y , while HCl and ClONO_2 stay fairly constant throughout the winter.

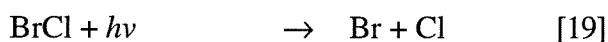
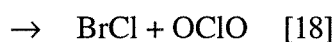
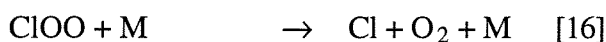
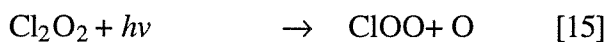
7.2 Ozone loss calculations

For this same period, our calculations predicts different scenarios for ozone loss depending on model case considered. Case D ($T=205 \text{ K}$) illustrates the relaxation of O_3 to its photochemical equilibrium in the polar environment, without enhanced active chlorine levels: Over the 200 days of the simulation ozone decreases by 15% at a rate of about 0.002 ppmv/day.

For case A (isolated air parcel at 69°S), ozone begins to rapidly decrease in August (bottom panel in Fig. 15), continuing until the springtime when higher sun levels fuel the chemical cycles involving halogens (destruction rate of 0.045 ppmv/day). These cycles account for 95% of the photochemical loss of O_3 and cause destruction of O_3 via



ClO and BrO are converted back to Cl and Br mainly through the following two pathways (Molina and Molina, 1987; McElroy et al., 1986):



In case B, excursions in and out of sunlight (centered around 64°S) allow these cycles to take place during the winter, starting as early as mid-June, when high ClO and BrO levels are present. As a result of these excursions and the generally higher latitude, O₃ loss occurs earlier than in case A and near complete destruction of ozone is reached (97%) in mid-August.

When mixing occurs (case C), resupply of O₃ rich air partially counteracts the effects of the halogen cycles, and ozone reaches a minimum of 1.5 ppmv in early September. After this point, active chlorine decreases, due to formation of ClONO₂, and mixing contributes to increasing the O₃ levels.

In situ O₃ observations during ASHOE/MAESA show that 25% of O₃ has been depleted by early August (Proffitt et al., 1995; Tuck et al., 1995a). Case C shows good agreement with these observations. Furthermore, while air with extremely depleted O₃ levels (99%) was sampled by the ER-2 on two occasions in mid-October (as predicted by case B), in general, observations at this time show ozone losses in excess of 75% at the highest latitudes (Proffitt et al., 1995), closer to case A. These different amounts of ozone loss observed thus reflect separate regimes of chlorine recovery.

Thus, while excursions into sunlight enhance ozone depletion, they can be counteracted by the mixing processes that would accompany such excursions.

8. Summary and conclusions

Measurements of HCl and ClO during the Antarctic winter of 1994 indicate chemical processing of the chlorine reservoir HCl to active chlorine via the heterogeneous reaction $\text{HCl} + \text{ClONO}_2 \rightarrow \text{Cl}_2 + \text{HNO}_3$. This processing is diagnosed by large losses in HCl, increases in ClO, and a slope of 1:2 for ΔHCl versus $\text{ClO} + 2 \text{Cl}_2\text{O}_2$ - consistent with the stoichiometry of the above reaction. The consistency between model calculations and observations strengthens our confidence in the current understanding of stratospheric gas phase and heterogeneous polar chemistry. Examination of two separate ER-2 flights with a box model along trajectories has confirmed the dominant role of reaction [1] in generating the observed HCl loss and ClO production. Evidence of the reaction $\text{HCl} + \text{HOCl}$ on sulfate aerosols was found by its impact on HO_x levels. Furthermore, in this environment, the exact physical and chemical state of the surfaces providing sites for heterogeneous reactions does not significantly change the amount of chlorine activation generated. It is shown that while [1] dominates early loss of HCl, reaction [3] contributes to subsequent total removal of HCl, in the context of excursions in and out of sunlight. Such excursions generate very rapid ozone loss which can be slowed down when mixing between processed and non-processed air occurs. Together, these findings quantitatively confirm the central role of heterogeneous chemistry on sulfate aerosols and PSCs in the Antarctic stratosphere, and point to the importance of latitudinal excursions and mixing in the edge region of the vortex.

Acknowledgements. The authors would like to thank Hari Nair for providing the original modifications to the photochemical Lagrangian code. Kenneth Carslaw made available his code for ternary solution growth. Additional field operations support of

ALIAS was provided by Matt Tuchscherer and Greg Flesch. Part of the research described in this paper was carried out by the Jet Propulsion Laboratory, California Institute of Technology, under contract with the National Aeronautics and Space Administration (NASA). This research is also supported in part by NASA grant NAGW-413 to the California Institute of Technology.

REFERENCES

- Abbatt, J.P.D., Heterogeneous reaction of HOBr and HCl on ice surfaces at 228 K, *Geophys. Res. Lett.*, 21, 665-668, 1994.
- Abbatt, J.P.D. and M.J. Molina, The heterogeneous reaction of HOCl + HCl \rightarrow Cl₂ + H₂O on ice and nitric acid trihydrate: reaction probabilities and stratospheric implications, *Geophys. Res. Lett.*, 19, 461-464, 1992.
- Anderson, J.G. and O.B. Toon, Airborne Arctic Stratospheric Expedition II: An overview, *Geophys. Res. Lett.*, 20, 2499-2502, 1993.
- Anderson, J.G., D.W. Toohey, and W.H. Brune, Free radicals within the Antarctic vortex: the role of CFCs in Antarctic Ozone loss, *Science*, 251, 39-46, 1991.
- Austin, J., R.L. Jones, D.S. McKenna, A.T. Buckland, J.G. Anderson, D.W. Fahey, C.B. Farmer, L.E. Heidt, M.H. Proffitt, A.F. Tuck, and J.F. Vedder, Lagrangian photochemical modeling studies of the 1987 Antarctic Spring vortex 2. Seasonal trends in ozone, *J. Geophys. Res.*, 94, 16717-16735, 1989.
- Baumgardner, D., J.E. Dye, B.W. Gandrud, and R.G. Knollenberg, Interpretation of measurements made by the forward scattering spectrometer probe (FSSP-300) during the airborne arctic stratospheric expedition, *J. Geophys. Res.*, 97, 8035-8046, 1992.
- Brune, W.H., J.G. Anderson, and K.R. Chan, *In situ* observations of ClO in the Antarctic: ER-2 aircraft results from 54°S to 72°S latitude, *J. Geophys. Res.*, 94, 16649-16663, 1989.
- Burkholder, B., Ultraviolet-absorption cross-sections of Cl₂O₂ between 210 and 410 nm., *J. Phys. Chem.*, 94, 687-695, 1990.
- Carslaw, K.S., B.P. Luo, and T. Peter, An analytic expression for the composition of aqueous HNO₃-H₂SO₄ stratospheric aerosols including gas phase removal of HNO₃, *Geophys. Res. Lett.*, 22, 1877-1880, 1995.

Carslaw, K.S., B.P. Luo, S.L. Clegg, T. Peter, P. Brimblecombe, and P.J. Crutzen, Stratospheric aerosol growth and HNO₃ gas phase depletion from coupled HNO₃ and water uptake by liquid particles, *Geophys. Res. Lett.*, 21, 2479-2482, 1994.

Chipperfield, M.P., J.A. Pyle, C.E. Blom, N. Glatthor, M. Hopfner, T. Gulde, C. Piesch, and P. Simon, The variability of ClONO₂ and HNO₃ in the Arctic polar vortex: comparison of Transall Michelsen interferometer for passive atmospheric sounding measurements and three-dimensional model results, *J. Geophys. Res.*, 100, 9115-9129, 1995.

Crutzen, P.J. and F. Arnold, Nitric acid cloud formation in the cold Antarctic stratosphere: a major cause for the springtime "ozone hole", *Nature*, 324, 651-655, 1986.

Crutzen, P.J., R. Müller, Ch. Brühl, and Th. Peter, On the potential importance of the gas phase reaction CH₃O₂ + ClO → ClOO + CH₃O and the heterogeneous reaction HOCl + HCl → H₂O + Cl₂ in "ozone hole" chemistry, *Geophys. Res. Lett.*, 19, 1113-1116, 1992.

Danielsen, E.F., R.S. Hipskind, W.L. Starr, J.F. Vedder, S.E. Gaines, D. Kley and K.K. Kelly, Irreversible transport in the stratosphere by internal waves of short vertical wavelength, *J. Geophys. Res.*, 17433-17452, 1991.

Del Negro, L.A., D.W. Fahey et al., in preparation for *J. Geophys. Res.* (ASHOE/MAESA special issue), 1995.

DeMore, W.B., S.P. Sander, D.M. Golden, R.F. Hampson, M.J. Kurylo, C.J. Howard, A.R. Ravishankara, C.E. Kolb, and M.J. Molina, Chemical Kinetics and Photochemical Data for Use in Stratospheric Modeling: Evaluation Number 10, *JPL Publication* 94-26, 1994.

Douglass, A.R., M.R. Schoeberl, R.S. Stolarski, J.W. Waters, J.M. Russell, A.E. Roche, and S.T. Massie, Interhemispheric differences in springtime production of HCl and ClONO₂ in the polar vortices, *J. Geophys. Res.*, 100, 13967-13978, 1995.

Elkins, J.W., D.W. Fahey, J.M. Gilligan, G.S. Sutton, T.J. Baring, C.M. Volk, R.E. Dunn, R.C. Myers, S.A. Montzka, P.R. Wamsley, A.H. Hayden, J.H. Butler, T.M. Thompson, T.H. Swanson, E.J. Dlugokencky, P.C. Novelli, D.F. Hurst, J.M. Lobert, S.J. Ciciora, R.J. McLaughlin, T.L. Thompson, R.H. Winkler, P.J. Fraser, L.P. Steele, and M.P. Lucarelli, Airborne gas chromatograph for the *in situ* measurements of long-lived species in the upper troposphere and lower stratosphere, submitted to *Geophys. Res. Lett.*, 1995.

Fahey, D.W. et al., in preparation for *J. Geophys. Res. (ASHOE/MAESA special issue)*, 1995.

Fahey, D.W., S.R. Kawa, E.L. Woodbridge, P. Tin, J.C. Wilson, H.H. Jonsson, J.E. Dye, D. Baumgardner, S. Borrmann, D.W. Toohey, L.M. Avallone, M.H. Proffitt, J. Margitan, M. Loewenstein, J.R. Podolske, R.J. Salawitch, S.C. Wofsy, M.K.W. Ko, D.E. Anderson, M.R. Schoeberl, and K.R. Chan, *In situ* measurements constraining the role of sulfate aerosols in mid-latitude ozone depletion, *Nature*, 363, 509-514, 1993.

Fahey, D. W., K. K. Kelly, S. R. Kawa, A. F. Tuck, M. Loewenstein, K. R. Chan, and L. E. Heidt, Observations of denitrification and dehydration in the winter polar stratospheres, *Nature*, 344, 321-324, 1990.

Fahey, D. W., K. K. Kelly, G. V. Ferry, L. R. Poole, J. C. Wilson, D. M. Murphy, M. Loewenstein, and K. R. Chan, *In situ* measurements of reactive nitrogen, total water, and aerosol in a polar stratospheric cloud in the antarctic, *J. Geophys. Res.*, 94, 11299-11315, 1989.

Farman, J.C., G.C. Gardiner, J.D. Shanklin, Large losses of total ozone in Antarctica reveal seasonal ClO_x/NO_x interaction, *Nature*, 315, 207-210, 1985.

Farmer, C. B., G.C. Toon, P.W. Schaper, J.-F. Blavier, and L.L. Lowes, Stratospheric trace gases in the spring 1986 Antarctic atmosphere, *Nature*, 329, 126-130, 1987.

Gao, R.S., D.W. Fahey, R.J. Salawitch, S.A. Lloyd, D.E. Anderson, R. DeMajistre, C.T. MeElroy, E.L. Woodbridge, R.C. Wamsley, S.G. Donnelly, L.A. Del Negro, M.H.

Proffitt, R.M. Stimpfle, D.W. Kohn, P.A. Newman, M. Lowenstein, J.R. Podolske, J.E. Dye, J.C. Wilson, and K.R. Chan, Partitioning of reactive nitrogen reservoir in the lower stratosphere of the southern hemisphere: observations and modeling, submitted to *J. Geophys. Res. (ASHOE/MAESA special issue)*, 1995.

Goodman, J., S. Verma, R.F. Pueschel, P. Hamill, G.V. Ferry, and D. Webster, Collection of Type I and Type II polar stratospheric cloud particles in the Antarctic Stratosphere, submitted to *J. Geophys. Res. (ASHOE/MAESA special issue)*, 1995.

Hanson, D.R., and A.R. Ravishankara, Heterogeneous chemistry of bromine species in sulfuric-acid under stratospheric conditions, *Geophys. Res. Lett.*, 22, 385-388, 1995.

Hanson, D.R., A.R. Ravishankara, and S. Solomon, Heterogeneous reactions in sulfuric acid aerosols: a framework for model calculations, *J. Geophys. Res.*, 99, 3615-3630, 1994a.

Hanson, D.R., and A.R. Ravishankara, Reactive uptake of ClONO_2 onto sulfuric-acid due to reaction with HCl and H_2O , *J. Phys. Chem.*, 98, 5728-5735, 1994b.

Hanson, D.R. and A.R. Ravishankara, Reaction of ClONO_2 with HCl on NAT, NAD, frozen sulfuric acid and hydrolysis of N_2O_5 and ClONO_2 on frozen sulfuric acid, *Geophys. Res.*, 98, 22931-22936, 1993.

Hanson, D. and K. Mauersberger, Laboratory studies of the nitric acid trihydrate: implications for the south polar stratosphere, *Geophys. Res. Lett.*, 15, 855-858, 1988.

Herman, R.L., H. Hu, C.R. Webster, R.D. May, and D.C. Scott, in preparation for *J. Geophys. Res.*, 1995.

Hofmann, S.J. Oltmans, J.A. Lathrop, J.M. Harris, and H. Vömel, Record low ozone at the South Pole in the spring of 1993, *Geophys. Res. Lett.*, 21, 421-424, 1994.

Huder, K.J., and W.B. DeMore, Absorption cross sections of the ClO dimer, *J. Phys. Chem.*, 99, 3905-3908, 1995.

Jones, R.L., J. Austin, D.S. McKenna, J.G. Anderson, D.W. Fahey, C.B. Farmer, L.E. Heidt, K.K. Kelly, D.M. Murphy, M.H. Proffitt, A.F. Tuck, and J.F. Vedder, Lagrangian

photochemical modeling studies of the 1987 Antarctic spring vortex, 1. Comparison with AAOE observations, *J. Geophys. Res.*, 94, 11,529-11,558, 1989.

Jonsson, H.H., J.C. Wilson, C.A. Brock, R.G. Knollenberg, R. Newton, J.E. Dye, D. Baumgardner, S. Borrmann, G.V. Ferry, R. Pueschel, D.C. Woods, and M.C. Pitts, Performance of a focused cavity aerosol spectrometer for measurements in the stratosphere of particle size in the 0.06-2.0 μm - diameter range, *J. Atmos. Ocean. Technol.*, 12, 115-129, 1995.

Kawa, S.R., D.W. Fahey, J.C. Wilson, M.R. Schoeberl, A.R. Douglass, R.S. Stolarski, E.L. Woodbridge, H.H. Jonsson, L.R. Lait, P.A. Newman, M.H. Proffitt, D.E. Anderson, M. Lowenstein, K.R. Chan, C.R. Webster, R.D. May, and K.K. Kelly, Interpretation of NO_x/NO_y observations from AASE-II using a model of chemistry along trajectories, *Geophys. Res. Lett.*, 20, 2507-2510, 1993.

Kawa, S.R., D.W. Fahey, L.E. Heidt, W.H. Pollock, S. Solomon, D.E. Anderson, M. Loewenstein, M.H. Proffitt, J.J. Margitan, and K. R. Chan, Photochemical partitioning of the reactive nitrogen and chlorine reservoirs in the high-latitude stratosphere, *J. Geophys. Res.*, 97, 7905-7923, 1992.

Kelly, K.K., A.F. Tuck, D.M. Murphy, M.H. Proffitt, D.W. Fahey, R.L. Jones, D.S. McKenna, M. Lowenstein, J.R. Podolske, S.E. Strahan, G.V. Ferry, K.R. Chan, J.F. Vedder, G.L. Gregory, W.D. Hypes, M.P. McCormick, E.V. Browell, and L.E. Heidt, Dehydration in the lower Antarctic stratosphere during late winter and early spring, 1987, *J. Geophys. Res.*, 94, 11,317-11357, 1989.

Kohn, D. and R. Stimpfle, submitted to *J. Geophys. Res.* (ASHOE/MAESA special issue), 1995.

Lary, D.J, M.P. Chipperfield, and R. Toumi, Atmospheric heterogeneous bromine chemistry, submitted to *J. Geophys. Res.*, 1995.

Lefèvre, F., G.P. Brasseur, I. Folkins, A.K. Smith, and P. Simon, Chemistry of the 1991-1992 stratospheric winter - three-dimensional model simulations, *J. Geophys. Res.*, 99, 8183-8195, 1994.

Leu, M.T., S.B. Moore, and L.F. Keyser, Heterogeneous reactions of chlorine nitrate and hydrogen chloride on type I polar stratospheric clouds, *J. Phys. Chem.*, 95, 7763-7771, 1991.

Leu, M.T., Laboratory studies of sticking coefficients and heterogeneous reactions important in the Antarctic stratosphere, *Geophys. Res. Lett.*, 15, 17-20, 1988.

Liu, X., R.D. Blatherwick, F.J. Mucray, J.G. Keys, and S. Solomon, Measurements and model calculations of HCl column amounts and related parameters over McMurdo during the Austral spring in 1989, *J. Geophys. Res.*, 97, 29795-20804, 1992.

Lutman, E.R., J.A. Pyle, R.L. Jones, D.J. Lary, A.R. McKenzie, I. Kilbane-Dawe, N. Larsen, and B. Knudsen, Trajectory model studies of Cl_x activation during the 1991/92 northern hemispheric winter, *Geophys. Res. Lett.*, 21, 1419-1422, 1994a.

Lutman, E.R., R. Toumi, R.L. Jones, D.J. Lary, and J.A. Pyle, Box model studies of Cl_x deactivation and ozone loss during the 1991/92 northern hemispheric winter, *Geophys. Res. Lett.*, 21, 1415-1418, 1994b.

Manney, G.L. and R.W. Zurek, Interhemispheric comparison of the development of the stratospheric polar vortex during fall: a three-dimensional perspective for 1991-1992, *Geophys. Res. Lett.*, 20, 1275-1278, 1993.

McCormick, M.P., H.M. Steele, P. Hamill, W.P. Chu, and T.J. Swissler, Polar stratospheric cloud sightings by SAM II, *J. Atmos. Sci.*, 39, 1387-1397, 1982.

McElroy, M.B., R.J. Salawitch, S.C. Wofsy, and J.A. Logan, Reductions of antarctic ozone due to synergistic interactions of chlorine and bromine, *Nature*, 321, 759-762, 1986.

Michelsen, H.A., R.J. Salawitch, P.O. Wennberg, and J.G. Anderson, Production of O(¹D) from photolysis of O₃, *Geophys. Res. Lett.*, 21, 2227-2230, 1994.

Molina, M.J., R. Zhang, P.J. Wooldridge, J.R. McMahon, J.E. Kim, H.Y. Chang, and K. Beyer, Physical chemistry of the $\text{H}_2\text{SO}_4/\text{HNO}_3/\text{H}_2\text{O}$ system: implications for the formation of polar stratospheric clouds and heterogeneous chemistry, *Science*, 216, 1418-1423, 1993.

Molina, L.T. and M.J. Molina, Production of Cl_2O_2 from the self-reaction of the ClO radical, *J. Phys. Chem.*, 91, 433-436, 1987.

Moore, S.B., L.F. Keyser, M.T. Leu, R.P. Turco, and R.H. Smith, Heterogeneous reactions on nitric acid trihydrate, *Nature*, 345, 333-335, 1990.

Müller R. and P.J. Crutzen, A possible role of galactic cosmic-rays in chlorine activation during polar night, *J. Geophys. Res.*, 98, 20483-20490, 1993.

Murphy, D.M., A.F. Tuck, K.K. Kelly, K.R. Chan, M. Loewenstein, J.R. Podolske, M.H. Proffitt, and S.E. Strahan, Indicators of transport and vertical motion from correlations between *in situ* measurements in the Airborne Antarctic Ozone Experiment, *J. Geophys. Res.*, 94, 11669-11685, 1989.

Nair, H., Thesis, California Institute of Technology, 1996.

Oelhaf, H., T. von Clarmann, H. Fischer, F. Friedlvalon, C. Fritzsche, A. Linden, C. Piesch, M. Seefeldner, and W. Volker, Stratospheric ClONO₂, HNO₃ and O₃ profiles inside the Arctic vortex from MIPAS-B limb emission spectra obtained during EASOE, *Geophys. Res. Lett.*, 21, 1263-1266, 1994.

Pierce, R.B., T.D. Fairlie, W.L. Grose, R. Swinbank, and A. O'Neill, Mixing processes within the polar night jet, *J. Atmos. Sci.*, 51, 2957-2972, 1994.

Prather, M.J., More rapid ozone depletion through the reaction of HOCl with HCl on polar stratospheric clouds, *Nature*, 355, 534-537, 1992.

Prather, M.J. and A.H. Jaffe, Global impact of the antarctic ozone hole: chemical propagation, *J. Geophys. Res.*, 95, 3473-3492, 1990.

Proffitt, M.H. et al., in preparation for *J. Geophys. Res. (ASHOE/MAESA special issue)*, 1995.

Proffitt, M.H., M.J. Steinkamp, J.A. Powell, R.J. McLaughlin, O.A. Mills, A.L. Schmeltekopf, T.L. Thompson, A.F. Tuck, T. Tyler, R.H. Winkler, and K.R. Chan, *In situ* ozone measurements within the 1987 Antarctic ozone hole from a high-altitude ER-2 aircraft, *J. Geophys. Res.*, 94, 16547-16556, 1989.

Pueschel, R.F., K.G. Snetsinger, J.K. Goodman, O.B. Toon, G.V. Ferry, V.R. Oberbeck, J.M. Livingston, S. Verma, W. Fong, W.L. Starr, and K.R. Chan, Condensed nitrate, sulfate, and chloride in Antarctic stratospheric aerosols, *J. Geophys. Res.*, 94, 11,271-11,284, 1989.

Pyle, J.A., N.R.P. Harris, J.C. Farman, F. Arnold, G. Braathen, R.A. Cox, P. Faucon, R.L. Jones, G. Megie, A. O'Neill, U. Platt, J.-P. Pommeraeau, U. Schmidt, and F. Stordal, An overview of the EASOE campaign, *Geophys. Res. Lett.*, 21, 1191-1194, 1994.

Reid, S.J., G. Vaughan, and E. Kyro, Occurrence of ozone laminae near the boundary of the stratospheric polar vortex, *J. Geophys. Res.*, 98, 8883-8890, 1993.

Roche, A.E., J.B. Kumer, J.L. Mergenthaler, R.W. Nightingale, W.G. Uplinger, G.A. Ely, J.F. Potter, D.J. Wuebbles, P.S. Connell, and D.E. Kinnison, Observations of lower-stratospheric ClONO_2 , HNO_3 , and aerosol by the UARS CLAES experiment between January 1992 and April 1993, *J. Atmos. Sci.*, 51, 2877-2902, 1994.

Roche, A.E., J.B. Kumer, and J.L. Mergenthaler, CLAES observations of ClONO_2 and HNO_3 in the Antarctic stratosphere, between June 15 and September 17, 1992, *Geophys. Res. Lett.*, 20, 1223-1226, 1993.

Rodriguez, J.M., Probing stratospheric ozone, *Science*, 261, 1128-1129, 1993.

Rodriguez, J.M., M.K.W. Ko, and N.D. Sze, Role of heterogeneous conversion of N_2O_5 on sulphate aerosols in global ozone losses, *Nature*, 352, 134-137, 1991.

Rosen, J.M., N.T. Kjome, and S.J. Oltmans, Simultaneous ozone and polar stratospheric cloud observations at South Pole Station during winter and spring 1991, *J. Geophys. Res.*, 98, 12,741-12,751, 1993.

Salawitch, R.J., S.C. Wofsy, P.O. Wennberg, R.C. Cohen, J.G. Anderson, D.W. Fahey, R.S. Gao, E.R. Keim, E.L. Woodbridge, R.M. Stimpfle, J.P. Koplw, D.W. Kohn, C.R. Webster, R.D. May, L. Pfister, E.W. Gottlieb, H.A. Michelsen, G.K. Yue, M.J. Prather, J.C. Wilson, C.A. Brock, H.H. Jonsson, J.E. Dye, D. Baumgardner, M.H. Proffitt, M. Loewenstein, J.R. Podolske, J.W. Elkins, G.S. Dutton, E.J. Hints, A.E. Dessler, E.M. Weinstock, K.K. Kelly, K.A. Boering, B.C. Daube, K.R. Chan, and S.W. Bowen, Implications for the heterogeneous production of HNO_2 , *Geophys. Res. Lett.*, 21, 2551-2554, 1994.

Salawitch, R.J., S.C. Wofsy, E.W. Gottlieb, L.R. Lait, P.A. Newman, M.R. Schoeberl, M. Loewenstein, J.R. Podolske, S.E. Strahan, M.H. Proffitt, C.R. Webster, R.D. May, D.W. Fahey, D. Baumgardner, J.E. Dye, J.C. Wilson, K.K. Kelly, J.W. Elkins, K.R. Chan, and J.G. Anderson, Chemical loss of ozone in the Arctic polar vortex in the winter of 1991-1992, *Science*, 261, 1146-1149, 1993.

Salawitch, R. J., S. C. Wofsy, and M. B. McElroy, Influence of polar stratospheric clouds on the depletion of Antarctic ozone, *Geophys. Res. Lett.*, 15, 871-874, 1988.

Sander, S.P., R.R. Friedl, and Y.L. Yung, Rate of formation of the ClO dimer in the polar stratosphere: implications for ozone loss, *Science*, 245, 1095-1098, 1989.

Santee, M.L., J.W. Waters, and L. Froidevaux, in preparation, 1995.

Santee, M.L., W.G. Read, J.W. Waters, L. Froidevaux, G.L. Manney, D.A. Flower, R.F. Jarnot, R.S. Harwood, and G.E. Peckham, Interhemispheric differences in polar stratospheric HNO_3 , H_2O , ClO and O_3 from UARS MLS, *Science*, 267, 849-852, 1994.

Schoeberl, M.R., A.R. Douglass, R.S. Stolarski, P.A. Newman, L.R. Lait, D.W. Toohey, L.M. Avallone, J.G. Anderson, W.H. Brune, D.W. Fahey, and K.K. Kelly, The evolution of ClO and NO along air parcel trajectories, *Geophys. Res. Lett.*, 20, 2511-2514, 1993.

Schoeberl, M.R., L.R. Lait, P.A. Newman, and J.E. Rosenfeld, The structure of the polar vortex, *J. Geophys. Res.*, 97, 7859-7882, 1992.

Schoeberl, M.R. and D.L. Hatmann, The dynamics of the stratospheric polar vortex and its relation to springtime ozone depletion, *Science*, 251, 46-52, 1991.

Scott, S. G., T.P. Bui, K.R. Chan, and S.W. Bowen, The meteorological measurement system on the NASA ER-2 aircraft, *J. Atm. Ocean. Tech.*, 7, 525-540, 1990.

Solomon, S., Progress towards a quantitative understanding of antarctic ozone depletion, *Nature*, 347, 347-354, 1990.

Solomon, S., R.R. Garcia, F.S. Rowland, and D.J. Wuebbles, On the depletion of antarctic ozone, *Nature*, 321, 755-758, 1986.

Steele, H.M., P. Hamill, M.P. McCormick, and T.J. Swissler, The formation of polar stratospheric clouds, *J. Atmos. Sci.*, 40, 2055-2067, 1983.

Tabazadeh, A. and O.B. Toon, Freezing behavior of stratospheric sulfate aerosols inferred from trajectory studies, *Geophys. Res. Lett.*, 22, 1725-1728, 1995.

Tabazadeh, A., R.P. Turco, and M.Z. Jacobson, A model for studying the composition and chemical effects of stratospheric aerosols, *J. Geophys. Res.*, 99, 12897-12914, 1994.

Tao, X. and A.F. Tuck, On the distribution of cold air near the vortex edge in the lower stratosphere, *J. Geophys. Res.*, 99, 3431-3450, 1994.

Tolbert, M.A., M.J. Rossi, R. Malhotra, and D.M. Golden, Reaction of chlorine nitrate with hydrogen chloride and water at Antarctic stratospheric temperatures, *Science*, 238, 1258-1260, 1987.

Toohey, D.W., L.M. Avallone, L.R. Lait, P.A. Newman, M.R. Schoeberl, D.W. Fahey, E.L. Woodbridge, and J.G. Anderson, The seasonal evolution of reactive chlorine in the northern hemisphere stratosphere, *Science*, 261, 1134-1136, 1993.

Toon, G.C., J.-F. Blavier, and J.T. Szeto, Latitude variations of stratospheric trace gases, *Geophys. Res. Lett.*, 23, 2599-2602, 1994.

Toon, G.C., C.B. Farmer, L.L. Lowes, P.W. Schaper, J.-F. Blavier, and R.H. Norton, Infrared aircraft measurements of stratospheric composition over Antarctica during September 1987, *J. Geophys. Res.*, 94, 7939-7962, 1989.

Toon, O.B., P. Hamill, R.P. Turco, and J. Pinto, Condensation of HNO_3 and HCl in the winter polar stratospheres, *Geophys. Res. Lett.*, 13, 1284-1287, 1986.

Tuck, A.F., C.R. Webster, R.D. May, D.C. Scott, S.J. Hovde, J.W. Elkins, and K.R. Chan, Time and temperature dependences of fractional HCl abundances from airborne data in the Southern Hemisphere during 1994, in press *Faraday Discuss.*, 1995a.

Tuck, A.F., K.K. Kelly, C.R. Webster, M. Lowenstein, R.M. Stimpfle, M.H. Proffitt, and K.R. Chan, Airborne chemistry and dynamics at the edge of the 1994 Antarctic vortex, *J. Chem. Soc. Farad. Trans.*, 91, 3063-3071, 1995b.

Tuck, A.F., T. Davies, S.J. Hovde, M. Nogueralba, D.W. Fahey, S.R. Kawa, K.K. Kelly, D.M. Murphy, M.H. Proffitt, J.J. Margitan, M. Lowenstein, J.R. Podolske, S.E. Strahan, and K.R. Chan, Polar stratospheric cloud processed air and potential vorticity in the Northern Hemisphere lower stratosphere at mid-latitudes during winter, *J. Geophys. Res.*, 97, 7883-7904, 1992.

Tuck, A.F., R.T. Watson, E.P. Condon, J.J. Margitan, and O.B. Toon, The planning and execution of ER-2 and DC-8 aircraft flights over Antarctica, August and September 1987, *J. Geophys. Res.*, 94, 11,181-11,222, 1989.

von Clarmann, T., H. Fischer, F. Friedlvalon, A. Linden, H. Oelhaf, C. Piesch, and M. Seefeldner, Retrieval of stratospheric O_3 , HNO_3 , and ClONO_2 profiles from 1992 MIPAS-B limb emission spectra: method, results, and error analysis, *J. Geophys. Res.*, 98, 20495-20506, 1993.

Wamsley, R., D.W. Fahey, et al., in preparation for *J. Geophys. Res.* (ASHOE/MAESA special issue), 1995.

Waters, J.W., L. Froidevaux, G.L. Manney, W.G. Read, and L.S. Elson, Stratospheric ClO and O_3 from the Microwave Limb Sounder on the Upper Atmospheric Research Satellite, *Nature*, 362, 597-602, 1993.

Waugh, J.W., Contour advection surgery simulations of a forced polar vortex, *J. Atmos. Sci.*, 50, 714-730, 1993.

Webster, C.R., et al., Interhemispheric asymmetry in the stratospheric HCl concentrations, in preparation for *J. Geophys. Res. (ASHOE/MAESA special issue)*, 1995a.

Webster, C.R., et al., Total conversion of inorganic chlorine to HCl observed at 15 km in polar air severely depleted in ozone, in preparation for *J. Geophys. Res. (ASHOE/MAESA special issue)*, 1995b.

Webster, C.R., R.D. May, C.A. Trimble, R.G. Chave, and J. Kendall, Aircraft (ER-2) Laser Infrared Absorption Spectrometer (ALIAS) for *in situ* stratospheric measurements of HCl, N₂O, CH₄, NO₂, and HNO₃, *Applied Optics*, 33, 454-472, 1994.

Webster, C.R., R.D. May, D.W. Toohey, L.M. Avallone, J.G. Anderson, P. Newman, L. Lait, M.R. Schoeberl, J.W. Elkins, and K.R. Chan, Chlorine chemistry on polar stratospheric cloud particles in the Arctic vortex, *Science*, 261, 1130-1134, 1993.

Wennberg, P.O., R.C. Cohen, N.L. Hazen, L.B. Lapson, N.T. Allen, T.F. Hanisco, J.F. Oliver, N.W. Lanham, J.N. Demusz, and J.G. Anderson, Aircraft-borne laser-induced fluorescence instrument for the *in situ* detection of hydroxyl and hydroperoxyl radicals, *Rev. Sci. Instrum.*, 65, 1858-1876, 1994.

Wennberg, P.O., R.C. Cohen, R.M. Stimpfle, J.P. Koplow, J.G. Anderson, R.J. Salawitch, D.W. Fahey, E.L. Woodbridge, E.R. Keim, R. Gao, C.R. Webster, R.D. May, D.W. Toohey, L.M. Avallone, M.H. Proffitt, M. Loewenstein, J.R. Podolske, K.R. Chan, and S.C. Wofsy, The removal of stratospheric O₃ by radicals: *In situ* measurements of OH, HO₂, NO, NO₂, ClO, and BrO, *Science*, 266, 389-404, 1994.

World Meteorological Organization, *Scientific Assessment of Ozone Depletion: 1994*, Global Ozone Research and Monitoring Project - Report No. 37, World Meteorological Organization, Geneva, 1995.

Wornop, D.R., L.E. Fox, M.S. Zahniser, and S.C. Wofsy, Vapor pressures of solid hydrates of nitric acid: implications for polar stratospheric clouds, *Science*, 259, 71-74, 1993.

Zhang, R., M.-T. Leu, and M.J. Molina, Formation of stratospheric clouds on preactivated background aerosols, Submitted to *Nature*, 1995.

Zhang, R., P.J. Wooldridge, J.P.D. Abbatt, and M.J. Molina, Physical chemistry of the H₂SO₄/H₂O binary system at low temperatures: stratospheric implications, *J. Phys. Chem.*, 97, 7351-7358, 1993.